

**Melanin in the human pathogenic fungus *Aspergillus fumigatus*:
Discovery of a novel melanin in the fungus and the use of conidial
melanin as a target for camelid *heavy-chain* antibodies**

Dissertation

zur Erlangung des akademischen Grades doctor rerum naturalium
(Dr. rer. nat.)

vorgelegt dem Rat der Biologisch-Pharmazeutischen Fakultät der
Friedrich-Schiller-Universität Jena

von

Dipl.-Apothekerin Jeannette Christina Schmalzer-Ripcke

geboren am 23.11.1979 in Hoyerswerda

2009

1. Gutachter: Prof. Axel A. Brakhage, Jena
2. Gutachter: Prof. Bernhard Hube, Jena
3. Gutachter: Prof. Gerhard Braus, Göttingen

Datum der öffentlichen Verteidigung: 1. Dezember 2009

ABSTRACT

The most important air-borne fungal pathogen, *Aspergillus fumigatus*, is the causative agent of invasive aspergillosis. This disease is often fatal for immunocompromised patients due to the difficult diagnosis and limited therapy. The biosynthesis of the pigment dihydroxynaphthalene (DHN)-melanin is an important virulence determinant of this fungus. DHN-melanin is predominantly present in conidia, and it may be produced during infection to protect the fungus from the host immune system.

This work aimed at: (i) studying the role of melanisation as pathogenicity mechanism and (ii) detecting the fungus with the help of a melanin specific antibody. For this purpose, an *in vitro* method for the selection of recombinant antibodies against conidial structures was developed and techniques for the characterisation and application were established. Conidia were chosen as antigen presenting structure since they expose DHN-melanin in its natural conformation. A competitive selection with conidia of the DHN-melanin lacking *pksP* mutant strain was performed to minimise the selection against other surface structures. A recombinant library of camelid VHH domains served as an antibody pool for the selection via phage-display.

A camelid antibody domain was successfully selected against melanised conidia applying a newly developed filtration approach. Its recombinant production in *Escherichia coli* by high cell density fermentation provided a pure antibody and its fusion to alkaline phosphatase re-established the bivalency of natural camelid heavy-chain antibodies. The purified antibody bound with high affinity to melanised conidia of different *Aspergillus* species. A less stringent binding to synthetic DOPA-melanin and *Sepia*-melanin was observed in ELISA studies. Furthermore, the biotinylated antibody demonstrated melanisation of conidia and hyphae by an immunofluorescent staining approach. Pigmentless hyphae from *in vitro*-grown cultures did not show an immunofluorescent signal for melanin. Thus, the potential of the established filtration method for the selection and characterisation of recombinant antibodies against conidial structures was shown by the successful generation of a camelid domain antibody against conidial melanin.

Furthermore, melanisation of *A. fumigatus* was studied by means of deletion mutants of genes coding for key enzymes of the DHN-melanin and pyomelanin pathway. The loss of a functional Arp2 enzyme, a reductase involved in the DHN-melanin biosynthesis, did not result in a distinct phenotype from wild type despite the colour change of the conidia from grey-green to pinkish. The sensitivity to reactive oxygen intermediates (ROI), the growth rate, the conidial surface morphology and the virulence in a low dose mouse infection model

resembled the wild-type characteristics. Hence, the modified DHN-melanin is as protective as the grey-green wild-type pigment and it allows the exposition of hydrophobins on the conidial surface contrary to the *pksP* mutant strain.

To investigate the biological role of the pyomelanin, an alternative melanin produced by a different pathway starting from L-tyrosine, the genes encoding homogentisate dioxygenase (HmgA) and 4-hydroxyphenylpyruvate dioxygenase (HppD) were deleted. Comparable FTIR spectroscopy of synthetic pyomelanin and pigment extracted from *A. fumigatus* cultures confirmed the identity of the observed pigment as pyomelanin. In the *hmgA* deletion strain, HmgA activity was abolished and the accumulation of homogentisic acid triggered an increased pigment formation. However, a pigment deposition did neither alter the surface structure of hyphae nor of conidia. By contrast, homogentisic acid and pyomelanin were not present in culture supernatants of an *hppD* deletion mutant which was confirmed by HPLC and spectroscopic analysis. Germlings of the *hppD* deletion mutant showed an increased sensitivity to ROI in two independent assays. The transcription of both studied genes was induced by L-tyrosine in liquid cultures. The fusion of the *hppD*-promotor to *gfp* revealed the transcriptional activation of *hppD* in conidia, germlings, hyphae and conidiophores. Despite activation of the genes during infiltrational growth in the mouse lung and the increased sensitivity of the Δ *hppD* strain to ROI, the mutant was not attenuated in its virulence in the mouse infection model. The loss of both melanins in a double deletion mutant revealed phenotypical characteristics similar to each single deletion mutant.

In the present study the occurrence of a second type of melanin in *A. fumigatus* was demonstrated. Homogentisic acid was shown to be the major intermediate in the L-tyrosine degradation pathway which yields in the formation of pyomelanin. No clear evidence could be provided for the involvement of pyomelanin in the pathogenicity of *A. fumigatus*.

KURZZUSAMMENFASSUNG

Aspergillus fumigatus ist der bedeutendste, über die Luft verbreitete, opportunistisch pathogene Pilz und verursacht die invasive Aspergillose. Die schwierige Diagnose und die limitierte Therapie tragen bei immunsupprimierten Patienten zu einer hohen Letalität bei. Die Biosynthese von Dihydroxynaphthalen (DHN) -Melanin ist ein wichtiger Virulenzfaktor dieses Erregers. DHN-Melanin ist vorwiegend in den Konidien vorhanden und wird wahrscheinlich während der Infektion zum Schutz des Erregers vor dem Immunsystem des Wirtes gebildet.

Die vorliegende Arbeit verfolgte zwei Hauptziele: (i) die Aufklärung der Bedeutung der Melanisierung für die Virulenz und (ii) die Detektion des Pilzes mittels eines melaninspezifischen Antikörpers. Für das letztere Ziel wurden Methoden für die Selektion eines rekombinanten Antikörpers gegen Oberflächenstrukturen von Konidien und für dessen Charakterisierung und Anwendung entwickelt. Konidien dienten zur Antigenpräsentation, da sie Melanin in seiner natürlichen Konformation exponieren. Die kompetitive Selektion mit Konidien der *pksP* Mutante, die kein DHN-Melanin synthetisiert, verfolgte den Ausschluss der Selektion gegen andere Oberflächenstrukturen. Die Präsentation des Antikörperpools, bestehend aus einer rekombinanten Bibliothek von VHH-Regionen der *heavy-chain* Antikörper der *Camelidae*, erfolgte über *phage display*.

Ein Kamelantikörperfragment wurde erfolgreich mit Hilfe einer neu entwickelten Filtrationsmethode gegen melanierte Konidien selektiert und durch die rekombinante Produktion in *Escherichia coli* und Hochzelllichtfermentation in reiner Form dargestellt. Die Fusion mit der alkalischen Phosphatase bildete die natürliche Bivalenz der *heavy-chain* Antikörper nach. Der gereinigte Antikörper zeigte eine hohe Affinität zu melanierten Konidien verschiedener Aspergillen. Ferner demonstrierte der biotinylierte Antikörper die Melanisierung von Hyphen und Konidien mit Hilfe der Immunfluoreszenz wohingegen melaninfreie Hyphen nicht detektiert wurden. Demzufolge konnte das Potenzial der entwickelten Selektions- und Charakterisierungsmethode durch die erfolgreiche Generierung eines gegen Melanin gerichteten Kamelantikörpers gezeigt werden.

Weiterhin wurden zentrale Enzyme der DHN- und Pyomelaninbiosynthese zur Charakterisierung der Melanisierung von *A. fumigatus* deletiert. Der Verlust der Arp2 Reduktase der DHN-Melaninbiosynthese verursachte einen dem Wildtyp ähnlichen Phänotyp. Bis auf die pinke Konidienfarbe, entsprachen die Empfindlichkeit gegenüber reaktiven Sauerstoffintermediaten (ROI), die Wachstumsrate, die Oberflächenstruktur der

Konidien und die Virulenz im Mausinfektionsmodell dem Wildtypphänotyp. Folglich weist das modifizierte Pigment eine ebenso protektive Wirkung wie das Wildtyppigment auf.

Um die Rolle des, von der Anwesenheit von Tyrosin abhängigen, Pigments zu untersuchen, wurden Deletionsmutanten der *p*-Hydroxyphenylpyruvatdioxigenase (*HppD*) und der Homogentisatdioxigenase (*HmgA*) generiert. In der *hmgA* Deletionsmutante bewirkte die Akkumulation von Homogentisinsäure eine verstärkte Pigmentbildung, jedoch verursachte die Pigmentablagerung weder bei den Konidien noch bei den Hyphen eine Veränderung der Oberflächenstruktur. Der Vergleich der FTIR-Spektren von synthetischem Pyomelanin mit dem aus *A. fumigatus* Kulturen extrahierten Pigment ermöglichte die Identifizierung des in den Pilzkulturen angereicherten Pigments als Pyomelanin. Hingegen zeigten HPLC und spektroskopische Analyse die Abwesenheit von Homogentisinsäure und Pyomelanin im Kulturüberstand der *hppD* Deletionsmutante. Die semiquantitative Transkriptanalyse mit Hilfe der *reverse transcription*-PCR und eine *hppD*-Promotorfusion mit *gfp* bestätigten die Aktivierung beider Gene durch Tyrosin in Konidien, Keimlingen, Hyphen und Konidiophoren. Obwohl auch beide Gene während des infiltrativen Wachstums in der Mauslunge aktiviert waren, und die *hppD* Deletionsmutante eine höhere Empfindlichkeit gegenüber ROI zeigte, konnte keine Attenuierung im Mausinfektionsmodell nachgewiesen werden. Eine Mutante, die weder DHN-Melanin noch Pyomelanin synthetisierte, zeigte phänotypische Charakteristika, die den einzelnen Deletionsmutanten entsprachen.

In der vorliegenden Arbeit wurde die Synthese von Pyomelanin in *A. fumigatus* aufgedeckt. Dabei konnte die Akkumulation von Homogentisinsäure, einem Intermediat des Tyrosinkatabolismus, als essenzielle Voraussetzung für die Pyomelaninbildung identifiziert werden. Die Studie liefert keinen klaren Beweis für eine Bedeutung des Pyomelaninbiosynthesewegs für die Pathogenität von *A. fumigatus*.

TABLE OF CONTENTS

ABSTRACT	I
KURZZUSAMMENFASSUNG	III
TABLE OF CONTENTS	V
A INTRODUCTION	1
1 The opportunistic human pathogen <i>Aspergillus fumigatus</i>	1
1.1 Biology and genetics of <i>A. fumigatus</i>	1
1.2 Clinical relevance of the fungus.....	1
1.3 Diagnostics of <i>A. fumigatus</i> infections	2
2 Melanin in <i>A. fumigatus</i>	4
2.1 The involvement of melanin in virulence.....	4
2.2 Dihydroxynaphthalene melanin	5
2.3 Pyomelanin	7
3 Camelid antibodies	9
3.1 Characteristics of camelid antibodies.....	9
3.2 Camelid antibodies in biotechnology.....	11
3.3 Phage display as a principle for antibody selection.....	12
4 Aims of the work	13
B MATERIAL AND METHODS	15
1 Strains, plasmids, oligonucleotides and media	15
1.1 Table 2. <i>Escherichia coli</i> strains and phages used.....	15
1.2 Table 3. Fungal strains used	15
1.3 Table 3. Plasmids used.....	16
1.4 Table 4. Oligonucleotides used.....	17
1.5 Standard media and supplements.....	17
2 Standard molecular biological, microbiological and biochemical methods	18
2.1 DNA extraction, modification and cloning.....	18

2.2	Southern blot analysis.....	19
2.3	Transformation of <i>A. fumigatus</i>	19
2.4	SDS polyacrylamide gel electrophoresis	20
2.5	Detection of proteins after SDS-PAGE	20
3	Pigment extraction, synthesis and analysis.....	21
3.1	Pigment extraction from <i>A. fumigatus</i> cultures	21
3.2	Production of synthetic pyomelanin	21
3.3	FTIR analysis of natural and synthetic melanin	21
3.4	Preparation of melanin ghosts.....	21
4	Characterisation of <i>A. fumigatus</i> mutant strains <i>in vitro</i>	22
4.1	Determination of colony radial growth.....	22
4.2	Inhibition zone plate assay.....	22
4.3	XTT-assay for the susceptibility testing to H ₂ O ₂	23
4.4	Homogenisate dioxygenase assay	23
4.5	Melanin formation and analysis of <i>A. fumigatus</i> culture supernatants	24
4.6	Transcript analysis in liquid cultures	24
4.7	Expression analysis of <i>hppD</i> via an eGFP-fusion.....	25
5	<i>In vivo</i> characterisation of <i>A. fumigatus</i> strains	25
5.1	Animal infection model.....	25
5.2	Preparation of stained lung sections.....	26
5.3	Transcript analysis in infected lung tissue	26
6	Methods for antibody selection.....	27
6.1	General buffers and material for antibody experiments	27
6.2	Selection of VHH domains against <i>A. fumigatus</i> conidia	28
6.3	Transfection of <i>E. coli</i> , determination of phage concentration, phage amplification and phage recoverage	29
6.4	Purification of phages.....	30
7	Methods for antibody production and characterisation.....	31
7.1	Phage ELISA.....	31
7.2	Antibody ELISA.....	31
7.3	Fermentation of the antibody	32
7.4	Purification of the antibody	32
7.5	Biotinylation of the antibody.....	33
7.6	Simultaneous competition antibody ELISA.....	33
7.7	Immunofluorescence studies	34

7.8	2-D gel electrophoresis and Western blotting of conidia extracts	35
8	Microscopy	36
8.1	Electron microscopy	36
8.2	Light and fluorescence microscopy	37
9	Databases and bioinformatics	37
C	RESULTS	38
1	A camelid antibody domain against fungal melanin.....	38
1.1	Selection and synthesis of the antibody	38
1.1.1	Design of a panning method against conidia.....	38
1.1.2	Design of phage and antibody ELISA.....	39
1.1.3	Sequence analysis of selected VHH domains	40
1.1.4	Antibody synthesis.....	41
1.1.5	Optimisation of antibody synthesis	41
1.1.6	High-cell-density fermentation and purification of the antibody.....	43
1.2	Characterisation of the antibody	44
1.2.1	Displacement of the antibody in the competition ELISA.....	45
1.2.2	Binding of the antibody to conidia and melanin particles in the ELISA.....	45
1.2.3	Detection of melanin by MelPhoA applying immunofluorescence	48
1.2.4	MelPhoA in Western blot analysis of conidia extracts	50
2	The DHN-melanin mutant strain $\Delta arp2$	51
2.1	Arp2 and DHN-melanin biosynthesis - database search and literature study.....	51
2.2	Generation of the <i>arp2</i> deletion strain and reintegration of the gene	53
2.3	Characterisation of growth and surface of the <i>arp2</i> mutant strain.....	54
2.4	Susceptibility of the <i>arp2</i> mutant strains to ROI.....	56
2.5	Contribution to virulence in a murine model of invasive aspergillosis	57
3	Pyomelanin in <i>A. fumigatus</i>	58
3.1	Organisation of the genes in the L-tyrosine degradation cluster	58
3.2	Generation of $\Delta hmgA$, $\Delta hppD$ and <i>pksP</i> $\Delta hppD$ mutant strains.....	59
3.3	Complementation of $\Delta hmgA$, $\Delta hppD$ and <i>pksP</i> $\Delta hppD$ mutant strains.....	60
3.4	Pigment production and growth of pyomelanin mutant strains.....	62
3.4.1	Pigmentation of mycelia, conidia and media.....	62
3.4.2	Pigmentation dependent on the nature of the inducer molecule.....	64
3.4.3	The influence of pyomelanin on the surface structure of conidia and hyphae ..	65

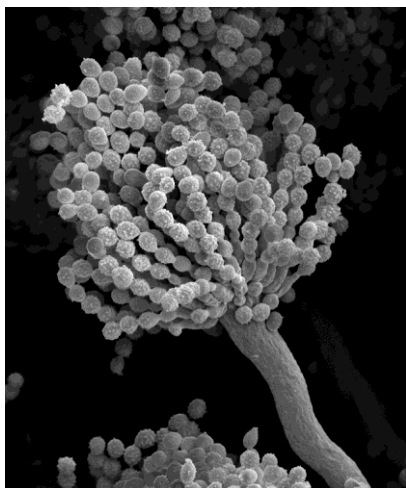
3.4.4	Radial growth of pyomelanin mutant strains	66
3.5	Characterisation of the pigment triggered by tyrosine addition.....	67
3.5.1	FTIR analysis of natural and synthetic melanin.....	67
3.5.2	Pigment accumulation, tyrosine consumption and HGA synthesis	68
3.5.3	Binding of the anti-melanin antibody to mycelia	70
3.6	Regulation of the cluster	70
3.6.1	Transcription of <i>hppD</i> and <i>hmgA</i> dependent on the addition of tyrosine	70
3.6.2	HmgA activity dependent on the addition of tyrosine	72
3.6.3	Transcript analysis in the infected mouse lung	72
3.6.4	Activation of <i>hppD</i> in different developmental stages	73
3.7	Susceptibility of pyomelanin mutant strains to ROI.....	76
3.8	Pyomelanin mutant strains in the murine model of invasive aspergillosis.....	79
D	DISCUSSION	82
1	A camelid domain antibody directed against fungal melanin.....	82
1.1	The challenging generation of an anti-melanin antibody.....	82
1.2	An elegant antibody engineering.....	84
1.3	Uncovering targets of the selected camelid domain.....	86
1.4	Elucidating the specificity of the VHH-domain antibody.....	88
2	DHN-melanin and pyomelanin in <i>A. fumigatus</i>.....	90
2.1	Pink versus grey-green – does the colour make the difference?	90
2.2	Pyomelanin – a novel melanin produced by <i>A. fumigatus</i>	93
2.3	Pyomelanin – a novel virulence determinant of <i>A. fumigatus</i> ?	96
2.4	Two types of melanin in <i>A. fumigatus</i> – a benefit for the fungus?.....	98
E	REFERENCES	101
	ABBREVIATIONS.....	A1
	FIGURES.....	A3
	TABLES.....	A4
	PUBLIKATIONSLISTE	
	DANKSAGUNGEN	

A INTRODUCTION

1 The opportunistic human pathogen *Aspergillus fumigatus*

1.1 Biology and genetics of *A. fumigatus*

The saprophytic fungus *Aspergillus fumigatus* is one of the most common inhabitants of the air-borne fungal flora (Zielinska-Jankiewicz *et al.*, 2008) and plays an important role in recycling carbon and nitrogen sources (Tekaiia & Latgé, 2005). *A. fumigatus* is a member of the Ascomycota and is mainly distributed by asexual, haploid, uninucleate conidia. These grey-green conidia are produced in chains by phialides and represent the uniseriate conidiophores (reviewed in Brakhage & Langfelder, 2002). Parasexual recombination and the application of selectable markers allow the genetic manipulation of the strains. The deletion of the *akuB^{KU80}* gene reduces non-homologous end-joining events. Therefore, homologous recombination is favoured and the establishment of specific mutations is facilitated (da Silva Ferreira *et al.*, 2006). Additionally, the clinical isolate Af293 and the CEA17 derivative A1163 have been sequenced in 2005 and 2008, respectively and nearly 10,000 genes have been predicted for both strains (Fedorova *et al.*, 2008; Nierman *et al.*, 2005). The recent discovery of the teleomorph of *A. fumigatus*, designated as *Neosartorya*



fumigata, might offer further potential for genetic manipulation. In the presence of two opposite mating types, sexual reproduction can occur under specific growth conditions leading to the production of yellowish-white to greenish-white ascospores in cleistothecia (O'Gorman *et al.*, 2009). Furthermore, the pathogenicity of the fungus is a polygenetic trait; it cannot be ascribed to the presence of a single virulence gene. Therefore, the possibility of sexual recombination in this heterothallic fungus might accelerate the detection of virulence determinants shortly.

Fig. 1. Electron micrograph of *A. fumigatus* conidiophores. Conidiophores depict the typical columnar, uniseriate conidial head. Phialids are the conidiogenous cells which produce long chains of conidia in basipetal succession (micrograph was taken within this work).

1.2 Clinical relevance of the fungus

The infectious agents of *A. fumigatus* are its conidia which are abundantly released into the atmosphere. Due to their size, 2-3 μm in diameter, they are small enough to reach the

lung alveoli after inhalation and to bypass mucociliary clearance. Indeed, studies have demonstrated that humans inhale several hundreds of these air-borne conidia every day (Chazalet *et al.*, 1998; Leenders *et al.*, 1999).

Diseases following inhalation can be assigned to one of three main categories: (i) Systemic infections of *A. fumigatus* represent a major cause of mortality in immunocompromised patients, e.g., hematopoietic stem cell transplant recipients, patients with acute leukaemia and liver transplantation (reviewed in Brakhage, 2005; Maschmeyer *et al.*, 2007). In fact, invasive aspergillosis (IA) is the most commonly identified invasive fungal infection among hematopoietic stem cell transplant recipients with an incidence of approximately 10 % (Marr *et al.*, 2002). Despite improving rates of survival, 6-week mortality rates remain as high as 21 % (Neofytos *et al.*, 2009). Other recent studies even reported mortality rates up to 72 % (Pagano *et al.*, 2007). (ii) In immunocompetent persons inhalation of conidia rarely causes adverse effects due to sufficient elimination by innate immune mechanisms. Still, *A. fumigatus* possesses potential to colonise the lung or the sinuses with restricted invasiveness and causes diseases like aspergilloma, also called fungal ball, or chronic pulmonary aspergillosis (Ellis, 1999). (iii) Additionally, air-borne conidia are also allergens associated with asthma, allergic sinusitis and bronchoalveolitis. Such allergic bronchopulmonary aspergillosis reduces pulmonary function in asthmatic and cystic fibrosis patients (Al-Alawi *et al.*, 2005).

1.3 Diagnostics of *A. fumigatus* infections

A favourable outcome of an invasive *Aspergillus* infection demands specific and early diagnosis which is, however, hampered by several issues (Subirà *et al.*, 2003). Firstly, clinical signs of invasive *Aspergillus* infections are very unspecific and clinical manifestation occurs late. Secondly, there is no universally applicable test with satisfying specificity and sensitivity available. The differentiation from other mycoses, manifesting in similar clinical symptoms, is demanding. Thirdly, *Aspergillus* spp. are widespread and false positive tests can be due to contaminations. Finally, a very inhomogeneous patient group has a high risk of an *Aspergillus* infection.

The combination of histological and culture methods allows speciation in many cases and susceptibility testing in parallel. Speciation is particularly important due to the emergence of non-*fumigatus* species as *A. terreus* and *A. nidulans* which are resistant to Amphotericin B, a widely used drug in the treatment of *A. fumigatus* infections. However, disadvantages include the requirement for specialised expertise for species determination, the long duration to obtain cultures and the low culture yield from tissue (30-52 %)

(Tarrand *et al.*, 2003), expectorated sputum and broncho-alveolar lavage (0-89 %) (Reichenberger *et al.*, 1999). Cultures from broncho-alveolar lavage are often negative (57 %) despite a histological proof of IA in lung tissue (Reichenberger *et al.*, 1999). Additionally, different *Aspergillus* spp. and *Fusarium*, *Scedosporium* and *Acremonium* spp. have histopathological features indistinguishable from each other (Hayden *et al.*, 2003). Aspergillosis caused by *A. fumigatus* is rarely diagnosed by blood culture and false positives often represent contaminations. This is in contrast to the comparably convenient detection of *Aspergillus terreus* and other angioinvasive fungi (e.g. *Fusarium* spp., *Scedosporium proliferans*) in blood samples due to their ability to sporulate in tissue and blood (Kontoyiannis *et al.*, 2000).

Despite the lack of specificity, high resolution computed tomography can detect lesions indicative of pulmonary aspergillosis in an early stage of IA and improve the outcome of patients with IA (Yeghen *et al.*, 2000). PCR and real-time PCR technology for the detection of *Aspergillus* spp. DNA in blood, sputum and broncho-alveolar lavage samples are promising approaches in early diagnosis (Bretagne, 2003). However, these methods are not established in routine diagnostics due to the absence of standardised and commercially available tests.

The detection of galactomannan, a cell-wall polysaccharide of *Aspergillus* and *Penicillium* spp. that is released during fungal growth, is of diagnostic relevance. Advantages are the correlation between the level of galactomannan and fungal burden in tissue (Marr *et al.*, 2004), the availability of two commercial tests (Platelia Aspergillus EIA and Pastorex™ Aspergillus, both Biorad, Germany), the non-invasiveness of the method and the possibility to detect the infection at an early stage. However, there are some disadvantages of this method comprising transient positivity, false-positive results which demand for repetition of that rather expensive test and inhomogeneous sensitivity (29-100 %) caused by numerous variables that affect the performance (Mennink-Kersten *et al.*, 2004). Another unspecific, serological test is based on the detection of 1,3- β -D-glucan (Fungitell® Assay, Associates of Cape Cod, Inc., USA) a cell wall component of most fungi, except of *Cryptococcus* spp. and the Zygomycetes.

The detection of serum antibodies against *Aspergillus* antigens does not provide a reliable method for acute IA in contrast to its importance in the diagnosis of chronic pulmonary aspergillosis. Antibodies can only be detected in about one-third of patients with acute IA due to the depleted immune response in most patients (Chan *et al.*, 2002).

Other methods are under investigation, including assays based on fungal metabolites as diagnostic markers, such as gliotoxin (Kupfahl, 2008; Lewis *et al.*, 2005), or *in situ*

hybridisation of RNA in tissue samples with labelled oligonucleotide probes (Hayden *et al.*, 2003). Novel immunolabeling approaches to positron emission tomography are also methods with potential in future diagnostics (Lionakis *et al.*, 2005). Such assays as well as *in situ* diagnostics in tissue samples demand for high specific antibodies against *Aspergillus* spp.

2 Melanin in *A. fumigatus*

2.1 The involvement of melanin in virulence

Aspergilli have adapted to overcome various chemical, physical, and biological stresses found in their heterogeneous environments. The production of melanin is one feature of *A. fumigatus* which contributes to its adaptation and to its pathogenicity (Hohl & Feldmesser, 2007). The term “melanin” originates from *melanos* – a Greek word for black. However, not all melanins are black, the denotation of a compound as melanin is rather based on the presence of the following properties: the hydrophobic pigment is a negatively charged, stable free radical of high molecular mass, formed after oxidative polymerisation of phenolic and/or indolic compounds, it is insoluble in aqueous and organic fluids, resistant to concentrated acids and susceptible to bleaching by oxidising agents (Riley, 1997).

Further properties of the polymer are attributed to survival advantage and pathogenicity. This comprises free radical-generating and -scavenging activity, protection against oxidants, extreme temperatures, heavy metals and lysing enzymes, the ability to confer radioprotection (Dadachova *et al.*, 2008) as well as to protect against UV and solar radiation (for an overview see Jacobson, 2000; Langfelder *et al.*, 2003; Nosanchuk & Casadevall, 2003). Additionally, melanin has an essential role in the formation of functional appressoria in the plant pathogenic fungus *Magnaporthe grisea* (Howard & Ferrari, 1989). Besides, the involvement of melanin in the pathogenicity of several human pathogenic fungi has been suggested, respectively proven (Table 1).

Dihydroxyphenylalanine (DOPA) -melanin is the type of melanin also present in humans. The black DOPA-melanin lacks thiol groups and is often referred to eumelanin, whereas pheomelanin is the designation for the brown pigment which contains thiols. Precursors are synthesised from L-tyrosine by tyrosinases or laccases. Tyrosinases catalyse the oxidation of L-tyrosine or L-DOPA to dopaquinone. Alternatively, the latter conversion can be catalysed by a laccase. The highly reactive dopaquinone is further converted to leucodopachrome and

subsequently oxidised to dopachrome. Additional oxidation and polymerisation steps result in the black or brown pigment (reviewed in Langfelder *et al.*, 2003).

Melanins are distinguished between two further types, pyomelanin, a polymerised tyrosine degradation product and dihydroxynaphthalene (DHN) -melanin, a polyketide based pigment.

Table 1. Examples of human pathogenic fungi with a virulence associated to melanin.

Fungus	Type of melanin	Selected references
<i>Cryptococcus neoformans</i>	DOPA-melanin	Deletion of a laccase essential for melanin formation reduced the virulence in the mouse infection model (Salas <i>et al.</i> , 1996). Melanin gives resistance to ionic oxidants and inhibits phagocytosis by macrophages (Wang <i>et al.</i> , 1995).
<i>Aspergillus fumigatus</i>	DHN-melanin	The melanin deficient mutant, <i>pksP</i> , is attenuated in a mouse infection model (Jahn <i>et al.</i> , 1997; Langfelder <i>et al.</i> , 1998; Tsai <i>et al.</i> , 1998). The hypermelanised mutant Δ <i>ags3</i> exhibits increased virulence (Maubon <i>et al.</i> , 2006).
<i>Paracoccidioides brasiliensis</i>	^a DOPA-melanin ^b Pyomelanin	Melanisation increases resistance against phagocytosis by macrophages (da Silva <i>et al.</i> , 2006). Conidia and yeast cells produce melanin during infection (Gomez <i>et al.</i> , 2001). Data for virulence of a melanin deficient mutant in the animal model are lacking.
<i>Wangiella (Exophiala) dermatitidis</i>	DHN-melanin	Disruption of a DHN-melanin pathway leads to reduced virulence and killing by neutrophils (Dixon <i>et al.</i> , 1992; Feng <i>et al.</i> , 2001).
<i>Sporothrix schenckii</i>	DHN-melanin	Melanised conidia are more resistant to phagocytosis and killing by human monocytes and murine macrophages, melanised yeast cells interfere as well (Romero-Martinez <i>et al.</i> , 2000).
<i>Histoplasma capsulatum</i>	^a DOPA-melanin	Yeast cells are melanised in infected tissue (Nosanchuk <i>et al.</i> , 2002). Data for virulence of a melanin deficient mutant in the animal model are lacking.

^a The fungus produces melanin after addition of DOPA to the media suggesting the production of DOPA-melanin.

^b Genes of tyrosine degradation are highly expressed during yeast mycelium transition which might correlate with pyomelanin production (Nunes *et al.*, 2005).

2.2 Dihydroxynaphthalene melanin

The pigment present in the grey-green conidia of *A. fumigatus* is DHN-melanin, the polymerisation product of 1,8-DHN (Langfelder *et al.*, 1998; Tsai *et al.*, 1998). Its biosynthesis pathway is displayed in Fig. 2. The best studied enzyme of that pathway is the polyketide synthase PksP (Alb1). The complete loss of melanin pigment after the deletion of that key enzyme results in white conidia with a smooth surface. These conidia revealed an elevated susceptibility to reactive oxygen intermediates (ROI) which derived from hydrogen peroxide and sodium hypochlorite as well as from host immune effector cells (Jahn *et al.*, 2000; Jahn *et al.*, 1997). Besides, a PksP-GFP fusion proved the transcription of that gene in

hyphae of germinating conidia isolated from lungs of infected, immunosuppressed mice (Langfelder *et al.*, 2001). PksP is also involved in the inhibition of phagosome-lysosome fusion and thereby in the killing of *A. fumigatus* conidia (Jahn *et al.*, 2002). On the contrary, DHN-melanin did not protect *W. dermatitidis* against hydrogen peroxide but against permanganate and hypochlorite in a study of Jacobson *et al.* (1995).

Disruption of the gene encoding the reductase Arp1 yielded in the production of reddish pink conidia which showed an enhanced C3 deposition on their surface (Tsai *et al.*, 1997). The C3 fragment of the complement system affects the virulence by facilitating opsonisation, phagocytosis and killing by polymorphnuclear cells. *Arp1* transcripts were only detectable after induction of conidiation. Studies of the *abr2* deletion strain revealed a colour change of the conidia from wild-type bluish-green to brown. Still, no influence in virulence and ROI scavenging activity was observable. Furthermore, *abr2* was only expressed during conidiation (Sugareva *et al.*, 2006).

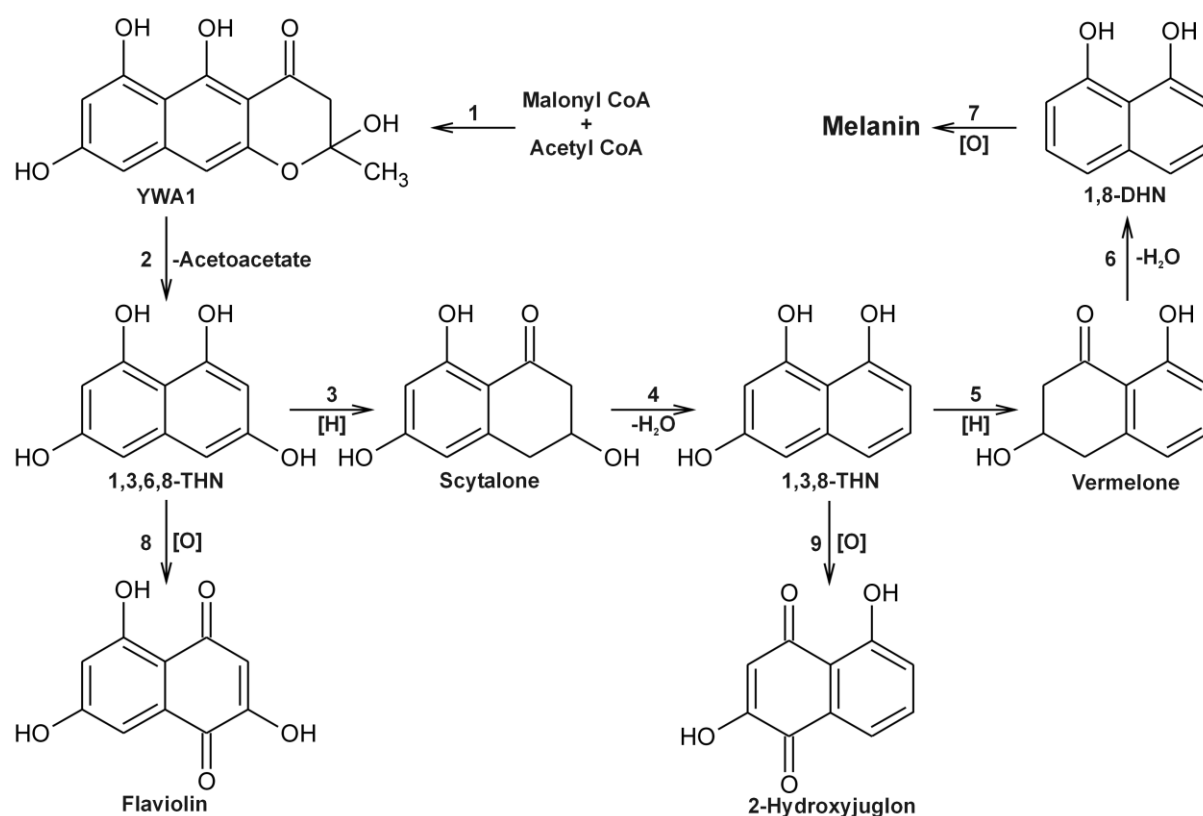


Fig. 2. Biosynthesis of DHN-melanin in *A. fumigatus* (adapted from Langfelder *et al.*, 2003; Tsai *et al.*, 2001). The polyketide synthase PksP catalyses the synthesis of the heptaketide YWA1 in step 1. After the chain-length shortening of the precursor by Ayg1 in step 2 the reduction [H] of 1,3,6,8-tetrahydroxynaphthalene (THN) by Arp2 follows in step 3. Step 4 is the dehydration of scytalone to 1,3,8-THN by Arp1. After formation of vermelone by reduction in step 5 and a further dehydration in step 6 1,8-DHN is synthesised. Finally, the laccase Abr2 polymerises the monomer 1,8-DHN in step 7 to DHN-melanin. Flaviolin and 2-hydroxyjuglon are auto-oxidation products which especially accumulate after blockage of the reduction reactions (Tsai *et al.*, 1999).

Three further sparsely studied genes participate in the DHN-melanin biosynthesis cluster. The *abr1* gene codes for a multicopper oxidase, however the catalysed reaction during DHN-melanin synthesis remains unidentified. Disruption of *arp2*, *ayg1* and *abr1* led to reddish-pink, yellowish green and brown conidia, respectively, and transcript analysis revealed an association in conidiation for all genes (Sugareva, 2006; Tsai *et al.*, 1999). However, investigations about their involvement in virulence of *A. fumigatus* are pending. Summing up, the DHN-melanin biosynthesis pathway contributes in a complex manner to the pathogenicity of *A. fumigatus*. Still, the role of specific pathway intermediates has not been fully elucidated.

2.3 Pyomelanin

In addition to DOPA- and DHN-melanin, a third type of melanin is distinguishable. Pyomelanin is a brown pigment produced from L-tyrosine via a pathway involving the accumulation and auto-oxidation of intermediates of the tyrosine catabolism as shown in Fig. 3 (Carreira *et al.*, 2001; Coon *et al.*, 1994; Kotob *et al.*, 1995). The term pyomelanin is particularly used to describe this pigment in microbes and was first introduced by Yabuuchi *et al.* for a water soluble brown pigment produced by the sanious bacterium *Pseudomonas aeruginosa* (Yabuuchi & Ohyama, 1972). Alkaptomelanin is a second designation for the same compound but often referred to the pigment formed in humans. Here, the tyrosine degradation pathway has been subject to numerous investigations as many severe metabolic disorders, e.g., phenylketonuria, alcaptonuria, tyrosinaemia, and Hawkinsinuria, are associated with enzymatic defects in the catabolism of phenylalanine and tyrosine (Fernández-Cañón & Peñalva, 1998; Moran, 2005; Peñalva, 2001).

Beside *P. aeruginosa*, pyomelanin production has been postulated in a broad range of bacteria. *Burkholderia cenocepacia*, a gram-negative opportunistic pathogen in patients suffering from cystic fibrosis, is apparently protected by pyomelanin from *in vitro* and *in vivo* sources of oxidative stress (Keith *et al.*, 2007). Hypervirulent *Vibrio cholera* strains also seem to produce pyomelanin in response to stress confrontation, e.g., elevated temperatures (Kotob *et al.*, 1995). Further prokaryotes with pyomelanin synthesis are *Shewanella colwelliana* (Coon *et al.*, 1994) and *Legionella pneumophila* (Steinert *et al.*, 2001). The yeast *Yarrowia lipolytica* also possesses a potential to produce pyomelanin (Carreira *et al.*, 2001).

Little is known about the tyrosine degradation pathway via homogentisic acid (HGA) in clinically important fungi. The only study relating a human pathogenic fungus to pyomelanin production concerns *C. neoformans*. The fungus exhibits a pyomelanin formation after HGA addition dependent on the presence of a laccase. In connection with pyomelanin production

appears a reduced susceptibility to UV radiation and reduced phagocytosis by macrophages compared to non-melanised cells (Frases *et al.*, 2007). Additionally, the non-pathogenic fungus *Aspergillus nidulans* served as model organism to elucidate the genetic and biochemical basis of the inherited disorders in human phenylalanine catabolism (Fernández-Cañón & Peñalva, 1995b; Peñalva, 2001). Besides, these studies provided evidence for the pharmacological mode of action of Orfadin® (NTBC, 2-[2-nitro-4-(trifluoromethyl)benzoyl]cyclohexane-1,3-dione, Nitisinone) in the treatment of hereditary tyrosinaemia type 1 (HT-1) with a deficiency in the activity of FahA enzyme. The mode of action of this orphan drug is the inhibition of 4-hydroxyphenylpyruvate dioxygenase (HppD). HppD deficiency, type III tyrosinaemia, only causes mild symptoms compared to Hawkinsinuria (mutated HppD), alkaptonuria (lack of active HmgA) and HT-1, which might extend the range of indications for Orfadin® (Scott, 2006).

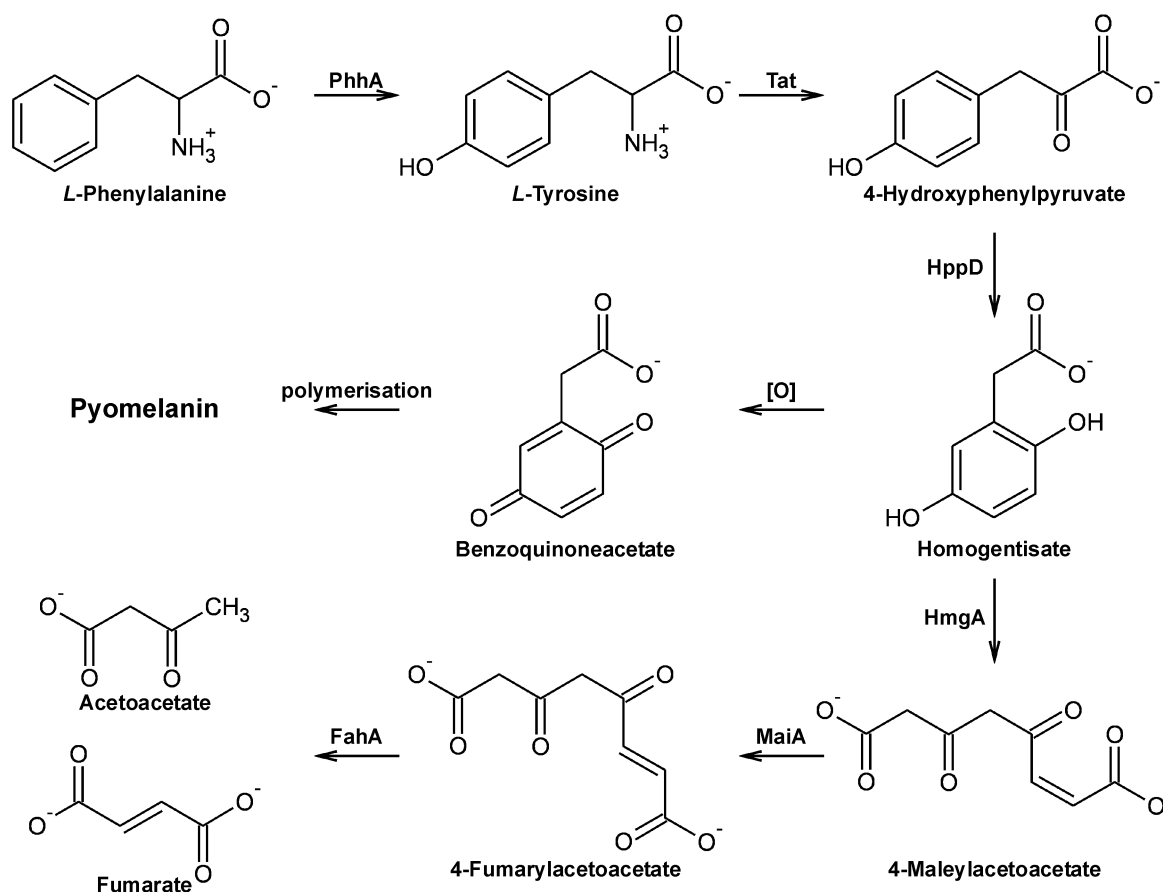


Fig. 3. L-tyrosine degradation pathway via homogentisate (adapted from Moran, 2005). Phenylalanine hydroxylase (PhhA) catalyses the para-hydroxylation of L-phenylalanine to gain L-tyrosine. The following reaction is a desamination by the tyrosine aminotransferase (Tat) to form *p*-hydroxyphenylpyruvate. Homogentisate, the pathway characteristic compound, is consecutively synthesised by the 4-hydroxyphenylpyruvate dioxygenase (HppD) and can lead to pyomelanin after oxidation [O] to benzoquinoneacetate and following polymerisation. Moreover, the degradation of homogentisate by the homogentisate dioxygenase (HmgA) to 4-maleylacetoacetate by oxidative ring cleavage is possible to bypass pigment formation. The conversion of this compound by maleylacetoacetate isomerase (MaiA) to 4-fumarylacetoacetate follows. Finally, fumarylacetoacetate hydrolase (FahA) forms the end products acetoacetate and fumarate.

Interestingly, NTBC is of agricultural significance as well. HppD inhibitors are applicable as herbicide due to their efficient prevention of plant growth. In plants, the enzyme is essential for the anabolic production of plastoquinone and tocopherol from homogentisate, indispensable for photosynthesis (reviewed in Moran, 2005). Furthermore, studies in *Paracoccidioides brasiliensis* revealed the overexpression of *hppD* in the mycelium-yeast transition. The inhibition of the gene resulted in a reduced growth and an arrest of *P. brasiliensis* in the mycelium form suggesting a potential of NTBC in the treatment of paracoccidioidomycosis (Nunes *et al.*, 2005).

Thus, the tyrosine degradation pathway with homogentisate as central compound plays a major role in animals, fungi as well as in plants. Especially the melanisation, based on the accumulation of pathway intermediates, seems to contribute to the virulence in some organisms.

3 Camelid antibodies

3.1 Characteristics of camelid antibodies

Sera of all species of the Camelidae feature conventional IgG antibodies as well as the structurally reduced heavy-chain antibodies (HCAb). Beside their abundance in the Camelidae, HCABs have only been described in particular cartilaginous fish, e.g., nurse shark (Roux *et al.*, 1998), a primitive vertebrate lineage. The only occurrence of HCABs in mammals other than the Camelidae is in heavy chain diseases. Here, B-cells produce truncated monoclonal HCABs without light chains and CH1 domains (Wahner-Roedler & Kyle, 2005).

Although native antibody production in the bacterial host system has been established nearly 20 years ago (Plückthun, 1990), the *E. coli* expression system is particularly suited for the direct production of small antibody fragments (Skerra & Plückthun, 1988). To fully understand the advantages of HCABs for the recombinant production in *E. coli*, firstly, the biotechnologically applied antibody structures have to be summarised. Conventional IgG antibodies provided the basis for the design and development of smaller recombinant antibody structures as depicted in Fig. 4. For instance, the removal of the Fc region (CH2 and CH3 domain of the heavy chain), which is only essential for antibody dependent cellular toxicity and Fc receptor binding, is possible to minimise the size of antibodies. This structural reduction avoids glycosylation between CH2 domains, and thus, it facilitates the production in *E. coli*. The paired N-terminal regions of the variable VH and VL domains still

retain sufficient antigen binding qualities. Such fragments can be produced after proteolysis or cloning as Fab monovalent antibodies or as Fv structure, a non-covalent association of VH and VL fragments. To avoid dissociation, these Fv fragments have to be further stabilised by a synthetic peptide linker yielding the scFv antibody (single chain Fv). The smallest known fragment from conventional antibodies with antigen affinity is the VH domain. However, such VH domains have to be further engineered for an application as the hydrophobicity of such domains causes their aggregation and sticky character which hampers their production in a soluble form (Muyldermans, 2001).

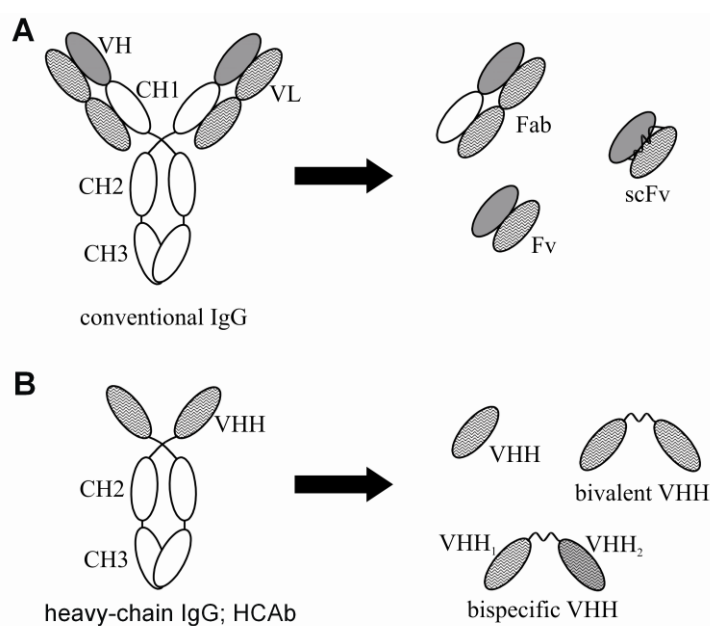


Fig. 4. Schematic presentation of conventional (A) and heavy-chain (B) antibodies and antigen binding fragments thereof (adapted from Harmsen & De Haard, 2007; Hamers-Casterman *et al.*, 1993). Heavy chains are drawn in white and light chains are filled with curved lines. The entire light chain and the CH1 domain are absent in HcAbs. Fab, the domain obtained after proteolysis, Fv, the variable domains of non-covalently linked heavy and light chains, and the scFv, which is a stabilised Fv by a synthetic linker, derive from conventional IgGs. VHH, the variable domain of a HcAb, which can be obtained after cloning, and its bivalent and bispecific derivatives are presented as examples for reduced structures of HcAbs.

In contrast, camelid HcAbs are devoid of light chains. Therefore, the diversity due to random pairing of heavy and light chains is lost. Additionally, their heavy chains lack the first constant domain (CH1) and thus, possess a lower molecular mass (approximately 100 kDa) compared to conventional heavy chains (150 kDa) (Hamers-Casterman *et al.*, 1993). Even though the separation of conventional IgGs into heavy and light chains decreases their antigen binding activity (Ward *et al.*, 1989), HcAbs are still capable of binding to antigens with high affinity (Ghahroudi *et al.*, 1997). The smallest fully active antigen binding domain of such HcAbs is even smaller. The variable domain of the heavy immunoglobulin chain, comprising 15 kDa, is the smallest intact antigen-binding fragment derived from

immunoglobulins. It is referred to as VHH or Nanobody[®] to distinguish it from VH domains of conventional IgGs. Despite the structural reduction of VHH domains, these antibodies exhibit an increased variability of their antigen binding sites. As VH domains, Nanobodies comprise four highly conserved framework regions (FR), which code for the core structure of the antibody, and in between three complementary-determining regions (CDRs). These CDRs are highly variable and involved in antigen binding. At least four different subclasses of VHH domains were isolated from different species of the Camelidae (Harmsen *et al.*, 2000). Still, the extensive antigen binding repertoire of most HCAs can be explained by few characteristic features. These include an increased surface area and a high rate of paratope shaping due to the introduction of interloop disulfide bridges (Desmyter *et al.*, 1996) and due to an extended CDR3 (Muyldermans *et al.*, 1994). Additionally, an extra hypervariable region upstream of CDR1 also contributes to the occurrence of novel paratopes compared to conventional VH domains (Nguyen *et al.*, 2000).

3.2 Camelid antibodies in biotechnology

The field of research and development of recombinant antibodies has rapidly progressed in the last decades. The main focus is especially put on the selection of antibodies against targets of human therapeutic, diagnostic and research agent applications. Indeed, 419 biopharmaceuticals, including 162 antibodies, are passing through clinical phase I, II or III in 2008. Hence, the focus lies on the development of innovative biopharmaceutical drugs. Additionally, approved drugs made of biopharmaceuticals already account for 16 % of the German drug market in 2008. In 2007, ten out of 40 newly approved drugs in Germany were biopharmaceuticals. Tocilizumab, Ustekinumab and Catumaxomab are three recombinant antibody drugs recently approved (Michl & Heinemann, 2009).

The structural properties of the VHH domains provide a device with high potential in antibody technology. HCAs and their VHH domains have an increased solubility compared to conventional antibody fragments due to the exchange of some hydrophobic amino acids in FR2. In conventional antibodies, this hydrophobic region is essential for the interdomain interactions between the VH domain and the VL chain, but this region is dispensable in single domain antibodies. Additional disulfide bonds, the increased hydrophilicity and the single domain nature of the VHHs contribute to a superior heat stability (van der Linden *et al.*, 1999), an increased resistance against denaturation as well as to an efficient folding and refolding (Ewert *et al.*, 2002).

For therapeutic applications, the low immunogenicity due to the stable structure and the high sequence homology to VH domains is advantageous (Coppieters *et al.*, 2006; Hermeling

et al., 2004). Additionally, the small size allows access to recessed antigenic sites. These characteristics allow the genetic fusion of single domains with further domains to enhance the avidity and also the synthesis of bispecific antibodies for targeted therapy, in short, this permits a plug-and-play approach. The way of their synthesis is flexible as well. A variety of organisms is qualified to produce VHH-domain antibodies. Because of the absence of the constant region and consequently the lack of glycosylation sites, the production is not restricted to mammalian cells. VHH domains have been generated in *E. coli* and there are also examples for their production in filamentous fungi and in yeast, such as *Pichia pastoris* (reviewed in Harmsen & De Haard, 2007).

A variety of VHH domains has been tested in preclinical studies of major disease areas, such as inflammation, thrombosis, oncology and Alzheimer's disease. One VHH-domain antibody, a novel anti-thrombotic, has already entered a multi-dose Phase 1b study in patients in May 2008 (<http://www.ablynx.com/home/index.php>).

3.3 Phage display as a principle for antibody selection

The *in vitro* selection of antibodies is based on recombinant DNA libraries which encode for the diverse antibody variants. To select specific antibodies encoded by such libraries against specific targets, the protein produced by a library clone has to be physically linked to its corresponding genotype. The following five selection methods fulfill this condition: phage display, cell surface display (on bacterial, yeast or mammalian cells), ribosome display, mRNA display and covalent DNA display (reviewed in Sergeeva *et al.*, 2006).

Phage display is a well established method with its origin in 1985 (Smith, 1985). A randomised peptide, encoded by the phage ssDNA is fused to a capsid protein of a filamentous phage and displayed on the surface. The primarily used filamentous Ff class bacteriophage M13 consists of a single stranded covalently closed DNA which is mainly surrounded by the major capsid protein pVIII. One end of the particle contains about five copies of the minor coat proteins pIII and the same number of protein pVI which are essential for bacterial infection and the termination of phage assembly. The other side of the flexible cylinder features the packaging signal and bears approximately five complexes of the capsid proteins pVII and pIX. Both proteins are required for initiation and maintenance of the phage assembly in the host bacteria (Marvin, 1998).

In most applications, pIII is used as a display vehicle for polypeptides. However, the fusion of proteins to pIII might reduce the infectivity of phages (Smith, 1985). This problem can be circumvented by the display of proteins on smaller filamentous particles, on phagemids (Bass *et al.*, 1990; Breitling *et al.*, 1991), with the help of *E. coli* and helper

phages. Here, the pIII polypeptide fusion is encoded in a phagemid DNA which also contains a phage origin of replication and a resistance marker. All the other proteins are encoded in the genome of the helper phage. A defective packaging signal in the helper phage allows the primary production of hybrid particles after superinfection of *E. coli* with phagemid and helper phage. Such hybrid particles expose pIII and pIII fusions and contain the phagemid DNA.

A main advantage of this method is the rapid, robust and simple procedure to enrich binding phages in three to five panning rounds. In a panning step, a phage library is incubated with a target followed by the removal of the non-reacting phages. Also the propagation of phage particles in a bacterial host and the final sequence identification of the selected binders are rapidly done. The anti-TNF immunoglobulin Adalimumab (Humira®) proves the potential of the phage display approach. This biopharmaceutical drug against rheumatoid arthritis provides an example of an approved therapeutic antibody developed with the assistance of the phage display method.

4 Aims of the work

A. fumigatus is the most important air-borne fungal pathogen in immunocompromised patients. Its pathogenicity mechanisms are still not fully understood, but the DHN-melanin biosynthesis is a known virulence determinant. The diagnosis of invasive aspergillosis and its treatment demand improvements to achieve a reduction of mortality rates. It was therefore the objective of this work to further elucidate the role of melanins in the pathogenicity of the fungus.

Antibodies are excellent tools for basic research as well as for diagnostics. However, specific antibodies against melanin are not available. A specific antibody against DHN-melanin might help to study the production of melanin in different developmental stages. Furthermore, such an antibody might allow the detection of the fungus as the presence of DHN-melanin is restricted to the fungal kingdom. This type of melanin is absent in mammals. Thus, the work aimed at developing a method to generate a melanin specific antibody, to characterise the produced antibody and to employ the antibody for the detection of melanin and the fungus.

The biosynthesis of DHN-melanin contributes to the virulence of *A. fumigatus* in an unidentified way. The reductase Arp2 is involved in its biosynthesis. The deletion of this gene may allow answering the question whether modified pigments are as effective as wild-

type DHN-melanin in the protection of the fungus. Additionally, this mutant could help to assign the pathogenicity to a pigment or another product of that pathway.

The addition of L-tyrosine to *A. fumigatus* cultures induces the synthesis of a brown pigment. Recently the nature of the pigment has been suggested to represent pyomelanin. Its definite identification, its biosynthesis pathway, the involvement in the protection of the fungus and its role in the pathogenicity still have to be elucidated. The deletion of the central enzymes of the tyrosine degradation pathway, HmgA and HppD, and the study of the deletion mutants should give insights into the production of pyomelanin and into a possible association to the virulence of the fungus. Finally, a double mutant lacking both DHN- and pyomelanin may reveal whether the pigments complement one another with regard to different developmental stages.

B MATERIAL AND METHODS

1 Strains, plasmids, oligonucleotides and media

1.1 Table 2. *Escherichia coli* strains and phages used

Strain	Genotype	Reference
K12-TG1	<i>supE thi-1</i> $\Delta(lac-proAB)\Delta(mcrB-hsdSM)5(r_K^- m_K^-)$ [F' <i>traD36 proAB lacI^q\Delta</i> M15]	Stratagene
K12-RV308	<i>lac74-galSII::OP308-strA</i>	ATCC 31608
K12-XL1-Blue	<i>endA1 gyrA96(nal^R) thi-1 recA1 relA1 lac glnV44 F'[::Tn10</i> <i>proAB⁺ lacI^q \Delta(lacZ)M15] hsdR17(r_K^- m_K^+)</i> , Tet ^R	Stratagene
α -Select Chemically Competent Cells	F- <i>deoR endA1 recA1 relA1 gyrA96 hsdR17(r_K^- m_K^+) supE44</i> <i>thi-1 phoA \Delta(lacZYA argF)U169 \Phi80lacZ\Delta</i> M15 λ^-	Bioline
VCSM13	Helper Phage, derived from M13 K07 mutant, Kan ^R	Stratagene

1.2 Table 3. Fungal strains used

Strain	Description	Reference
<i>Aspergillus fumigatus</i> strains		
<i>pksP</i> mutant	contains a non-functional <i>pksP</i> gene which impairs DHN-melanin biosynthesis, derived from ATCC46645	Langfelder <i>et al.</i> , 1998
ATCC46645	wild type	ATCC
CEA17 Δ <i>akuB^{KU80}</i>	<i>akuB^{KU80}::pyrG</i> ; PyrG ⁺	da Silva Ferreira <i>et al.</i> , 2006
Δ <i>abr2</i>	<i>abr2\Delta::hph</i> , Hyg ^R , derived from ATCC46645	Sugareva <i>et al.</i> , 2006
Δ <i>arp2</i>	<i>arp2\Delta::hph</i> , Hyg ^R , derived from ATCC46645	this study
<i>arp2^c</i>	<i>arp2\Delta::arp2</i> , Hyg ^R , PtrA ^R , derived from ATCC46645	this study
Δ <i>hppD</i>	<i>akuB^{KU80}\Delta</i> ; <i>hppD::ptrA</i> ; PtrA ^R	this study
<i>hppD^c</i>	<i>akuB^{KU80}\Delta</i> ; <i>hppD\Delta::hppD</i>	this study
Δ <i>hmgA</i>	<i>akuB^{KU80}\Delta</i> ; <i>hmgA::ptrA</i> ; PtrA ^R	this study
<i>hmgA^c</i>	<i>akuB^{KU80}\Delta</i> ; <i>hmgA\Delta::hmgA</i>	this study
<i>pksP\Delta</i> <i>hppD</i>	<i>hppD::ptrA</i> ; PtrA ^R , derived from <i>pksP</i> mutant strain	this study
<i>pksP hppD^c</i>	<i>hppD\Delta::hppD</i> , derived from <i>pksP</i> mutant strain	this study
<i>hppDp-eGFP</i>	<i>hppDp(598 bp)-eGFP</i> , <i>ptrA</i> , PtrA ^R , derived from <i>pksPp(l)-red</i> mutant strain	this study
<i>pksPp(l)-red</i>	<i>pyrG1</i> , <i>pksPp(1300 bp)-DsRed2</i> , PyrG ⁺	Behnsen, 2005

Strain	Description	Reference
Other fungal strains		
<i>A. niger</i>	FSU-871	M. Brock, Jena
<i>A. nidulans</i>	SCF5; <i>veA1</i> , derived from RMS011×A26	C. Fleck, Jena
<i>A. nidulans</i>	RMS011; <i>pabaA1, yA2; ΔargB::trpCΔB, trpC801; veA1</i>	Brock, 2005
<i>A. terreus</i>	i402	HKI strain collection

1.3 Table 3. Plasmids used

Name	Relevant phenotype	Reference
pAK200	<i>phagemid</i> for fusion of heterologous genes with gene III for presentation on M13 surface, Cm ^R	Krebber <i>et al.</i> , 1997
pAKMel	selected <i>phagemid</i> from library after panning, Cm ^R	this study
pTetA6H	for expression of VHH domains with PelB signal sequence and as PhoA fusion, Cm ^R , Tet ^R	G. Habicht, Jena
pTetA6H_Mel	Plasmid for the production of MelPhoA, Cm ^R , Tet ^R	this study
pTetpA6H_Mel*	Plasmid for the production of melanin antibody (without amber codon) as PhoA fusion and with PelB signal sequence (MelPhoA), Cm ^R , Tet ^R	this study
pCR2.1 <i>arp2</i>	<i>arp2</i> , Amp ^R , Kan ^R	this study
pCR2.1 <i>arp2^C</i>	<i>arp2, ptrA</i> ; Amp ^R , Kan ^R , PtrA ^R ; complementation construct	this study
pUC18 <i>arp2</i>	<i>arp2</i> ; Amp ^R	this study
pUC18 Δ <i>arp2</i>	Δ <i>arp2</i> ; Amp ^R ;	this study
pUC18 Δ <i>arp2hph</i>	Δ <i>arp2, gpdAp-hph</i> ; Amp ^R , Hyg ^R ; deletion construct	this study
<i>coat_hph_pCR2.1</i>	<i>gpdAp-hph</i> ; Amp ^R , Kan ^R	C. Fleck, Jena
pCR2.1 <i>hppDp-egfp</i>	<i>hppDp-egfp</i> , Amp ^R , Kan ^R	this study
p123	<i>otefp-egfp</i> ; Amp ^R	Spellig <i>et al.</i> , 1996
pSK- <i>hppDp-egfp</i>	<i>hppDp-egfp</i> , Amp ^R , PtrA ^R	this study
pSK275	Amp ^R , PtrA ^R	S. Krappmann, Würzburg
pCR2.1	Amp ^R , Kan ^R	Invitrogen, Germany
pCR2.1 <i>hmgA</i>	<i>hmgA</i> ; Amp ^R , Kan ^R	this study
pUC18 <i>hmgA</i>	<i>hmgA</i> ; Amp ^R	this study
pUC Δ <i>hmgA</i>	Δ <i>hmgA</i> ; Amp ^R ; deletion construct	this study
pUC18 Δ <i>hmgAptrA</i>	Δ <i>hmgA, Amp^R, PtrA^R</i> ; deletion construct	this study
pUC <i>hmgA^C</i>	<i>hmgA^C</i> ; Amp ^R , complementation construct	this study
pCR2.1 <i>hppD</i>	<i>hppD</i> ; Amp ^R , Kan ^R	this study
pCR2.1 Δ <i>hppDptrA</i>	Δ <i>hppD, Amp^R, Kan^R, PtrA^R</i> ; deletion construct	this study
pCR2.1 <i>hppD^C</i>	<i>hppD^C</i> ; Amp ^R , Kan ^R ; complementation construct	this study

1.4 Table 4. Oligonucleotides used

Oligonucleotide	Sequence 5' → 3'
HmgAXbaI_for	ACCAGTCATTCATCTAGACGACGCC
HmgAXbaI_rev	CATCCGTGACTCTAGAGCATCATCC
HmgASfiI_up	AGGCCTGAGTGGCCGGCATGACGTCGAATATCTGC
HmgASfiI_down	AGGCCATCTAGGCCCAACAAGGCCCTAGTAGGAAG
HppD_for	CATCTCCTCCAGTTGATCGG
HppD_rev	TTCTCTCAACATGACTGTCACC
HppD_Sfi_up	AGGCCTGAGTGGCCATAAGAGCTGTCAGAGAGGC
HppD_Sfi1_down	AGGCCATCTAGGCCCTTGTATAGGACTTCGGTGC
hmgA_FspI_for	CACAACGTCATGAGTGGCGCATGGTCCCGAC
hmgA_FspI_rev	GTCGGGACCATGGCACTCATGACGTTGTG
HppD*_C_for	CCTCAAGGCTCGAGGTGTTGAG
HppD*_C_rev	CTCAACACCTCGAGCCTTGAGG
AfCitAcode_up	GCAAGGTCATCGGCGAGG
AfCitAcode_down	GTTGTCACCGTAGCCGAGC
AfHppDcode2_for	TGCGCAACGGCGACATCAC
AfHppDcode2_rev	TGGCGGGTTCGTTGATGGG
AfHmgAcode_up	ACCTGCTGGAAGGGTGACAC
AfHmgAcode_down	ACCAGACTGGCTTCGACTCC
pAK200rev	TCTTTTCATAATCAAAATCACCTT
Ab01	GGCTTTACCTATAGCCAGCCTATGTGGCG
Ab02	CGCCACATAGGCTGGCTATAGGTAAGCC
sftpD_for	CTGGCGAACCTGGACCAAAG
sftpD_rev	GCACATCTCCTGGGCATCCTC
pAK200for	GCCTACGGCAGCCGCTGG
HppDp-Not1-for	GCGGCCGCTTGTGTTGGTGTGTTTGGATATTGCAG
HppDp-eCFP-rev	CCTCGCCCTTGCTCACCATATTGAAGTCAAGTGAGAAGAGATG
eCFP-Not1-rev	GCGGCCGCTTACTTGTACAGCTCGTCCATGC
HppDp-eCFP-for	CATCTCTTCTCACTTGACTTCAATATGGTGAGCAAGGGCGAGG
arp2_flank_for	ACGTTGGCCGTGCTTATC
arp2_flank_rev	GGAGATGCGGTAGACAAC
arp2_flank_NotI_for	CCGCTCATTGCGCATCTGAAC
arp2_flank_NotI_rev	CCGCTCCGAAGATTGACTAGATAGAG

1.5 Standard media and supplements

For propagation of plasmids, *E. coli* was cultivated in LB-broth (Roth) or 2 × YT-broth (Qbiogene). 2 % (w/v) select agar (Invitrogen) was added for the cultivation on agar plates. Kanamycin (30 µg/ml), tetracyclin (15 µg/ml), ampicillin (100 µg/ml) or chloramphenicol

(30 µg/ml) was added for selection, if required. 2 × YT-broth was applied for phage amplification.

A. fumigatus was cultivated in *Aspergillus* minimal medium (AMM) containing 63 mM NaNO₃, 7 mM KCl, 2.1 mM MgSO₄, 11.2 mM KH₂PO₄, trace elements and 2 % (w/v) agar if required. The filtrated, 1000 × stock solution of trace elements at pH 6.5 included in 100 ml 2.2 g ZnSO₄ × 7H₂O, 1.1 g H₃BO₃, 0.5 g MnCl₂ × 4H₂O, 0.5 g FeSO₄ × 7H₂O, 0.16 g CoCl₂ × 6H₂O, 0.16 g CuSO₄ × 5H₂O, 0.11 g Na₂MoO₄ × 2H₂O, 5 g Na₄EDTA. Unless otherwise noted, 50 mM glucose were used as carbon source and 0.6 M KCl were added to the medium for transformation. Pyrithiamine (Sigma-Aldrich, Germany) in a final concentration of 0.1 µg/ml was applied when selection for pyrithiamine resistance was required. 1 M sorbitol as well as 100 µg /ml Hygromycin B (Roche) were supplemented when *hph* gene was used as selection marker. For inhibition of HppD, sulcotrione (Riedel-de Haën, Germany) was used in a final concentration of 50 µM.

2 Standard molecular biological, microbiological and biochemical methods

2.1 DNA extraction, modification and cloning

Standard techniques for manipulation of DNA were carried out as described (Sambrook & Russel, 2001). Chromosomal DNA of *A. fumigatus* was prepared using the Master pure yeast DNA purification kit (Epicentre Biotechnologies, USA). For isolation of plasmid DNA from bacterial cells, QIAprep® Spin Miniprep Kit (Qiagen, Germany) or FastPlasmid® Mini Kit (Eppendorf, Germany) were applied. DNA was modified by restriction digestion with enzymes purchased from New England Biolabs GmbH, dephosphorylation was achieved with Calf Intestinal Alkaline Phosphatase (JenaBioscience, Germany) and DNA was ligated with Rapid DNA Ligation Kit (Roche, Germany) or T4 DNA Ligase (JenaBioscience, Germany).

Concentration and purity of isolated DNA was determined by absorption measurement at 260 nm and 280 nm with NanoDrop (Thermo Scientific, Germany). Gel electrophoresis was carried out for analysis of ethidium bromide stained DNA fragments with alpha Imager gel documentation system (Alpha Innotech, Canada). For the extraction of DNA fragments from agarose gels, QIAquick® Gel Extraktion Kit (Qiagen, Germany) was applied.

PCR amplification of specific DNA fragments for cloning, analysis or as hybridisation probes was carried out with GoTaq® polymerase (Promega) or with Phusion™ High-Fidelity PCR if proof reading activity was required. Difficult DNA templates were amplified with PCR

Extender System (5Prime, Germany). *In vitro* site-specific mutagenesis was either performed by oligonucleotide-directed mutagenesis in a two step PCR as described (Higuchi *et al.*, 1988) or by performing mutagenesis with QuickChange® II Site-Directed Mutagenesis Kit (Stratagene, Germany).

2.2 Southern blot analysis

For detection of site-specific integration of DNA fragments into chromosomal *A. fumigatus* DNA after transformation, Southern blot hybridisation was carried out. For this purpose, chromosomal DNA of *A. fumigatus* was digested by specific restriction enzymes. DNA fragments were separated by agarose gel electrophoresis and transferred onto Hybond™-N⁺ membranes (GE Healthcare Bio-Sciences, Germany) by capillary blotting. Labeling of the DNA probe, hybridisation and detection of DNA-DNA hybrids were performed using the DIG Labeling System and CDP-Star (Roche Applied Science, Germany).

2.3 Transformation of *A. fumigatus*

Transformation of *A. fumigatus* was carried out using protoplasts as described (Ballance & Turner, 1985). Briefly, *A. fumigatus* was cultured for approximately 16 h in 100 ml AMM at 37 °C. After separation of mycelium from medium by filtration through miracloth and washing (0.6 M KCl, 10 mM Na₂HPO₄, pH 5.8), the incubation with 400 mg Glucanex® (Novozymes, Switzerland) in 20 ml (0.6 M KCl, 10 mM Na₂HPO₄, pH 5.8) for 2-3 h at 30 °C and 60 rpm followed. Protoplasts were separated from non-digested material by filtration through miracloth and pelleted by centrifugation at 4 °C and 1700 *g*. Subsequently, protoplasts were gently resuspended and washed (0.6 M KCl, 0.1 M Tris × HCl, pH 7.0, 4 °C). After a second washing and centrifugation step, protoplasts were resuspended (0.6 M KCl, 50 mM CaCl₂, 10 mM Tris × HCl, pH 7.5) to obtain a concentration of 0.5-2 × 10⁷ protoplasts/ml. 5 to 10 µg DNA in 10 µl were added to 100 µl protoplasts and 25 µl PEG solution (25 % (w/v) PEG 8000, 50 mM CaCl₂, 10 mM Tris × HCl, pH 7.5). After gentle mixing and incubation for 20 min on ice, further 0.5 ml PEG solution was added and the incubation of the mixture for 5 min on ice followed. The mixture was aliquoted after addition of 1 ml solution (0.6 M KCl, 50 mM CaCl₂, 10 mM Tris × HCl, pH 7.5), added to 10 ml AMM liquid transformation agar and plated onto AMM transformation agar plates. Plates were incubated up to 7 days at 37 °C.

2.4 SDS polyacrylamide gel electrophoresis

To analyse protein extracts and purified fractions, proteins were separated by denaturing SDS polyacrylamide gel electrophoresis (SDS-PAGE). When whole extracts were analysed, 50 μ l of pelleted bacterial cultures, which have been adjusted to an $OD_{550nm} = 5$ with 0.9 % (w/v) NaCl, were resuspended in 10–15 μ l a.d.. For the analysis of soluble and insoluble protein fractions, 500 μ l bacteria suspension with an $OD_{550nm} = 10$ were sonicated and centrifuged for 30 min at 4 °C and 16,100 *g*. Soluble proteins were detected in the supernatant and insoluble proteins appeared in the pellet, which was resuspended in 500 μ l 0.9 % (w/v) NaCl. 32.5 μ l of required samples as well as protein samples after FPLC purification steps were mixed with 4 \times NuPAGE[®] LDS Sample Buffer (Invitrogen) and 50 mM DTT. The obtained 50 μ l were subsequently denatured for 10 min at 70 °C. 20 μ l of the sample and 10 μ l of protein standard (SeeBlue[®]Plus2, Invitrogen) were applied onto NuPAGE[®] 4-12 % Bis-Tris precast polyacrylamide gels and electrophoresis was carried out in NuPAGE[®] MES running buffer (both Invitrogen) at 200 V for approximately 35 min. Gels were either stained with Coomassie or analysed by Western blotting.

2.5 Detection of proteins after SDS-PAGE

For Coomassie staining, gels were incubated for 20 min in staining solution (0.2 % (w/v) Coomassie Brilliant Blue R250, 10 % (v/v) acetic acid, 45 % (v/v) methanol) and subsequently decolourised in a mixture of 10 % (v/v) acetic acid and 20 % (v/v) methanol.

For the more sensitive and specific detection of His - tagged proteins, Western blotting was applied. After SDS-PAGE, proteins were electrophoretically transferred via semi-dry blotting to a nitrocellulose membrane using NuPAGE[®] Transfer Buffer (Invitrogen). Subsequently, the membrane was washed twice with TBS (150 mM NaCl, 10 mM Tris \times HCl, pH 7.5) for 10 min, blocked with 3 % (w/v) BSA in TBS for 1 h, washed twice with TBSTT (500 mM NaCl, 20 mM Tris \times HCl, 2 % (v/v) Triton[®]X-100, 0.5 % (v/v) Tween[®]-20, pH 7.5) for 10 min and washed once more with TBS for 10 min before incubation for 1 h with the primary antibody His Tag[®] Monoclonal Antibody (Novagen) in TBS including 3 % (w/v) BSA. Two washing steps with TBSTT and one washing with TBS followed before the incubation with the secondary antibody, the goat Anti-Mouse IgG Alkaline Phosphatase antibody (Sigma Aldrich), for 1 h in TBS including 3 % (w/v) BSA. Afterwards, the membrane was washed five times with TBSTT for 10 min and finally developed with 1-Step NBT/BCIP (Thermo Fisher Scientific).

3 Pigment extraction, synthesis and analysis

3.1 Pigment extraction from *A. fumigatus* cultures

100 ml AMM with 50 mM glucose and 10 mM L-tyrosine were inoculated with 3×10^8 *A. fumigatus* conidia. After cultivation for 53 h at 37 °C and 200 rpm, the supernatant was filtered through Miracloth (Calbiochem, USA). The supernatant was precipitated over night at RT by adjusting to pH 2.0 with 1 M HCl. After centrifugation (16,100 *g* for 20 min), the pellet was resuspended in 2.5 ml water (alkalised with NaOH to pH 12) and dialysed in 3.5 kDa slide-A-Lyzer Dialysis Cassettes (Pierce Biotechnology, USA) against water accompanied by a stepwise reduction of pH from 10 to 7. The lyophilised pigment was then used for Fourier transform infrared (FTIR) analysis.

3.2 Production of synthetic pyomelanin

In vitro synthesised melanin (HGA melanin) was used as a control in FTIR spectroscopy. HGA melanin was produced by auto-oxidation of a 10 mM HGA solution at pH 10 at constant stirring for 3 days (adapted from Ruzafa *et al.*, 1995). Polymerisation was stopped and precipitation started by adjusting the pH to 2 with 6 M HCl. After precipitation over night and centrifugation (16,100 *g*, 20 min), the pellet was resuspended in 2.5 ml alkaline water solution (pH 12) and treated further as described above. The lyophilised sample was applied to FTIR spectroscopy.

3.3 FTIR analysis of natural and synthetic melanin

Synthetic melanin and melanin prepared from *in vitro* cultures were analysed with FTIR spectroscopy. Samples were pressed in KBr disks and spectra were obtained with an FTIR spectrophotometer (FT/IR-4100 Jasco, Easton, USA) equipped with a deuterated L-Alanine Triglycine Sulphate (TGS) detector.

3.4 Preparation of melanin ghosts

Melanin was isolated from conidia according to a method adapted from Youngchim *et al.* (2004). 2×10^9 conidia, grown on AMM agar, were washed three times with PBS. Digestion of cell walls was performed over night with β -glucanases (10 mg/ml Glucanex® (Novozymes, Switzerland) in a solution of pH 5.5 containing 0.1 M sodium citrate and 1 M sorbitol). Particles were washed three times with 2 ml PBS and incubated in the following

step in 2 ml 4 M guanidine thiocyanate solution (Fluka Biochemika, Germany) over night. Again, particles were washed three times and incubated in proteinase K solution (1 mg/ml in 10 mM Tris, 1 mM CaCl₂ and 0.5 % (w/v) SDS (Pharmacia Biotech, Sweden), proteinase K from *Triterachium album* was purchased from Boehringer Mannheim) over night. After three further washing steps, particles were boiled for 1 h in 1 ml 6 M hydrochloric acid. The obtained melanin particles, also referred to as melanin ghosts, were separated from the solution by centrifugation in Filter Units (Ultrafree-MC Centrifugal Filter Units with Microporous Membrane, Ø 0.45 µm, Millipore, Germany), extensively washed with PBS and finally lyophilised by freeze drying with Freeze Dryer ALPHA 2- 4 (CHRIST, Germany).

4 Characterisation of *A. fumigatus* mutant strains *in vitro*

4.1 Determination of colony radial growth

To investigate the growth of the mutant strains the radial extension on solid medium was tested. 2500 conidia in 2.5 µl freshly prepared spore suspension were point inoculated on solid media at 37 °C for up to 96 h. Wild-type, $\Delta arp2$, $pksP$, $\Delta hppD$ and complemented strains were grown on AMM agar plates with 50 mM glucose as carbon source, on AMM without glucose but with 10 mM L-tyrosine and on AMM agar plates supplemented with 50 mM glucose and 10 mM L-tyrosine. Four replicates of every strain were measured in two independent experiments and for each colony, two diameters perpendicular to each other were determined twice a day. At least five time points during the log phase were used to calculate growth rate. The radius of the colonies was plotted against time using leastsquare regression analysis, and the slope of the regression line, which represents the growth rate, was calculated. Each replicate was analysed separately and the mean of the growth rate was calculated.

4.2 Inhibition zone plate assay

The sensitivity of the mutants to H₂O₂ in comparison to the wild type was measured in a plate diffusion assay. The 25 ml top and 25 ml bottom agar consisted of AMM supplemented with 50 mM glucose and 20 mM L-tyrosine. 2.5×10^8 conidia were added to the top agar and poured on top of the bottom agar in a Petri dish. When the susceptibility of fresh conidia was tested, H₂O₂ was added immediately. To test the effect of H₂O₂ on germinating conidia, plates were pre-incubated for 10 h at 37 °C before addition of H₂O₂. For both approaches, 150 µl of 5 % (v/v) H₂O₂ were filled in a hole of 10 mm in diameter and inhibition zones

were measured 22 h after addition of H₂O₂. 8 replicates from 2 independent experiments were used for the calculation of mean and standard deviation.

4.3 XTT-assay for the susceptibility testing to H₂O₂

Additionally, the susceptibility of *A. fumigatus* to H₂O₂ was measured in an XTT assay. Conidia were diluted in AMM or AMM supplemented with 10 mM L-phenylalanine to gain a concentration of 1×10^5 conidia/ml. 150 μ l were applied to a microplate and cultivated for 24 h at 37 °C while mild shaking. Afterwards, 50 μ l of H₂O₂ dilutions in AMM were added and the microplate was further incubated for 3 h at 37 °C. The addition of 50 μ l of freshly prepared Menadione/XTT solution in PBS followed. XTT was applied in a concentration of 200 μ g/ml and menadione at 25 μ M. After 2.5 h of incubation at 37 °C in the dark, colour formation was measured at 450 nm in order to quantify formazan formation. Background OD was obtained by spectroscopic measurements of inocula-free wells processed in the same way as the inoculated wells. Each assay was performed in triplicate and repeated in three independent experiments for each strain. Analysis was carried out with relative ODs, which were calculated (in percent) based on the following equation: $(\text{OD of H}_2\text{O}_2 \text{ containing well} - \text{background OD}) / (\text{OD of corresponding H}_2\text{O}_2 \text{- free well} - \text{background OD}) \times 100 \%$. The absorbance of samples without H₂O₂ provided the 100 % viability values, which were individually calculated for each strain and each repeated experiment. Obtained percentages were finally applied for the non-linear regression analysis by using a three parameter logistic model (sigmoidal curve with standard slope (-1) due to the limited number of data points). The analysis was carried out with GraphPad Prism software. The EC50 concentrations of H₂O₂ and the corresponding 95 % confidence intervals were calculated for comparison of strain susceptibilities (adapted from Meletiadis *et al.*, 2001).

4.4 Homogentisate dioxygenase assay

The homogentisate dioxygenase activity was determined spectrophotometrically by measuring the formation of maleylacetoacetate at 330 nm as previously described (Fernández-Cañón & Peñalva, 1997). In brief, crude extracts were prepared from mycelia grown in liquid media. The mycelia were either frozen in liquid nitrogen and stored or directly lysed by sonification in 50 mM potassium phosphate buffer, pH 7. After 15 min centrifugation at 13,000 *g*, the supernatant was used for enzyme assays, which contained, in a final volume of 1 ml, 50 mM potassium phosphate buffer (pH 7), 2 mM ascorbate, 50 μ M FeSO₄, 200 μ M homogentisate and 50 μ l protein extract at a concentration of 1 mg/ml. The

substrate homogenisate was added just before measurement and after preincubation of the assay mixture for 10 min. The molar extinction coefficient of maleylacetoacetate is $13,500 \text{ M}^{-1}\text{cm}^{-1}$ (Seegmiller *et al.*, 1961). Protein concentrations for calculation of specific activities were determined by using Coomassie Plus protein assay (Pierce Biotechnology, USA).

4.5 Melanin formation and analysis of *A. fumigatus* culture supernatants

200 ml AMM were inoculated with 1×10^7 conidia from wild type, the $\Delta hppD$ and $\Delta hmgA$ mutants, as well as the complemented strains. After 20 h of pre-incubation, L-tyrosine was added to a final concentration of 10 mM. Every 4 hours, 4 ml samples were taken and filtered through Miracloth (Calbiochem, USA). Aliquots were stored at -20°C for further analysis. Pigment production was estimated by direct absorbance measurement at 405 nm of the supernatant of an alkalisied (20 μl 5 M NaOH per ml sample) and centrifuged (16,000 *g* for 2 min) sample. Another aliquot was acidified (20 μl 10 M HCl per ml sample) and glucose concentration was determined (BIOSEN C_line, package GP+, EKF-diagnostic GmbH, Barleben, Germany). Samples for high performance liquid chromatography (HPLC) were additionally filtered through Millex-LCR₁₃ FilterUnits 0.5 (Millipore, Billerica, USA). 20 μl of the sample were injected into a Shimadzu HPLC system fitted with an RP₁₈ column (Eurospher 100C18, 250 mm \times 4.6 mm, 5 μm ; Merck, Darmstadt, Germany). For elution, water with 0.1 % (v/v) TFA was used as buffer A and acetonitrile with 0.1 % (v/v) TFA as buffer B. Peaks were eluted at a flow rate of 1 ml/min applying the following gradient: 8 % B for 12 min, gradient from 8 % B to 95 % B within 3 min, 95 % B for 1 min, gradient from 95 % B to 8 % B within 2 min and finally 5 min at 8 % B for re-calibration. The compounds were detected with a Shimadzu LC-10 AD Diode Array Detector at 280 nm. L-tyrosine and HGA eluted under these conditions at 7.7 and 8.6 min, respectively. The concentrations of L-tyrosine and HGA were determined by calculation of peak areas at 280 nm and comparison with a standard curve for L-tyrosine and HGA. For instrument control, data acquisition and data analysis, the CLASS-VP package (Shimadzu GmbH, Duisburg, Germany) was employed.

4.6 Transcript analysis in liquid cultures

For RNA isolation from *in vitro* grown cultures, *A. fumigatus* was cultivated with and without 10 mM L-tyrosine. 100 mg mycelia were used for RNA extraction employing MasterPure Yeast RNA purification Kit (Epicentre Biotechnologies, USA). After DNase treatment, 10 μg of total RNA were used for first strand cDNA synthesis with SuperScript III

reverse transcriptase and anchored oligo(dT)₂₀ primers (Invitrogen, Germany). Reverse transcription was conducted at 50 °C for 3 hours. RNA was hydrolysed with 15 µl 1 M NaOH for 10 min at 70 °C and subsequently neutralised with 15 µl 1 M HCl. After addition of 6 µl 3 M sodium acetate pH 5.2, 2.5 µl glycogen (5 mg/ml), and 200 µl ice cold ethanol, cDNA was precipitated over night at -20 °C. After centrifugation for 30 min at 4 °C and 16,000 *g*, the pellet was washed with 70 % (v/v) ethanol and resolubilised in 30 µl Tris × HCl buffer (pH 8.0).

cDNA synthesis was used to determine transcription levels of *hmgA* and *hppD* compared with the constitutively formed citrate synthase transcripts (*Afu5g04230*, *citA*) (according to Ibrahim-Granet *et al.*, 2008). For this purpose, oligonucleotides *AfCitAcode_up* and *AfCitAcode_down* were used for the amplification of a 575 bp fragment of *citA* transcripts. Oligonucleotides *AfHppDcode2_for* and *AfHppDcode2_rev* allowed the specific amplification of a 591 bp region of *hppD* transcript. A 563 bp DNA fragment of the coding region of *hmgA* could be detected with oligonucleotides *AfHmgAcode_up* and *AfHmgAcode_down*. Transcript amplification using GoTaq DNA polymerase (Promega, Germany) was carried out in the Veriti Fast Thermal cycler (Applied Biosystems, USA) with 5 ng cDNA as template. As a control, 0.1 ng gDNA were applied under the same conditions.

4.7 Expression analysis of *hppD* via an eGFP-fusion

To study *hppD* gene expression in conidia, germinating conidia and hyphae dependent on L-tyrosine addition and in comparison to *pksP* gene expression, a strain bearing an HppD-eGFP and a PksP-DsRed2 fusion was generated. Wild-type strain served as control. Conidia were inoculated directly from the colonies grown on AMM agar to 150 µl liquid medium on a cover slip. Incubation was carried out in a wet chamber at 37 °C for 8, 16 and 40 h in the dark. The majority of liquid medium was aspirated at the specified time points, and the cover slip was put upside down on a microscope slide, sealed with nail varnish and immediately examined under the microscope without prior fixation.

5 *In vivo* characterisation of *A. fumigatus* strains

5.1 Animal infection model

An optimised low dose mouse infection model of invasive aspergillosis was applied (Kupfahl *et al.*, 2006; Liebmann *et al.*, 2004). Female BALB/c mice (18-20 g, 6-8 weeks old, Charles River, Germany) were housed in groups of five animals in individually vented filter

top cages with food and water *ad libitum*. For immunosuppression, mice were treated with cyclophosphamide and cortisone acetate. Cyclophosphamide was dissolved in PBS (pH 7.4) and administered intraperitoneally at 150 mg/kg starting on day -4 and then reapplied every subsequent third day throughout the experiment. A single dose of cortisone acetate solubilised in PBS was administered subcutaneously at 200 mg/kg on day -1. *A. fumigatus* conidia were grown on malt extract agar (Merck, Germany) for 5 days at RT and freshly harvested using sterile PBS containing 0.1 % (v/v) Tween[®]20. After filtration through a cell strainer (BD Biosciences, Germany) conidia were counted and diluted in PBS to a final concentration of 1.2×10^6 /ml – 1.8×10^6 /ml. Mice were anaesthetised intraperitoneally by a mixture of medetomidin × HCl (Dormitor[®]), midazolam × HCl (Dormicum[®]) and fentanylcitrate (Fentanyl[®]) in PBS to allow the complete intranasal administration of 25 µl of the conidia suspension. To recover from anaesthesia, mice were treated with a mixture of atipamezol × HCl (Antisedan[®]), flumazenil (Anexin[®]) and naloxon × HCl (Naloxon[®]) as antidote. Visual inspections of mice were made twice a day for a period of 14 days post-infection. Animals were euthanised intraperitoneally with ketamine (Ursotamin[®]), when at least two of the predetermined endpoints were reached, e.g., more than 20 % weight-loss in 4 days, moribund state, body surface temperature less than 29 °C, profound dyspnoea, severe lethargy, lateral position. Survival curves were compared using logrank test after Kaplan-Meyer analysis.

5.2 Preparation of stained lung sections

Freshly prepared lungs were immediately fixed in neutral phosphate buffered formaldehyde (Histofix 4 %, Roth, Germany) for 2 to 4 weeks. Subsequently, lungs were washed to remove excess fixative, dehydrated in an ethanol series, embedded in paraffin and cut into 5 µm thin slices. Sections were deparaffinised with xylene and rehydrated. For the observation of tissue conditions, sections were stained with haematoxylin-eosin, and for a better visualisation of fungal mycelium, polysaccharides were stained with periodic acid-Schiff (PAS) stain. In the case of PAS stain, tissues were counter-stained with haematoxylin.

5.3 Transcript analysis in infected lung tissue

Determination of transcript levels of *A. fumigatus* genes in the infected mouse lung was performed according to Ibrahim-Granet *et al.* (2008) with some modifications. Two immunosuppressed female BALB/c mice (Charles River, Germany) were infected intranasally with 25 µl PBS containing 4×10^6 conidia of *A. fumigatus* wild type. As control,

25 µl PBS without conidia were administered to another mouse. 7 days after infection, the mice were sacrificed, and the lungs were directly frozen in liquid nitrogen. The lungs were ground to a fine powder, and 100 mg were used for RNA extraction employing the RiboPure Yeast Kit (Ambion Europe, UK). cDNA synthesis and RT - PCR were performed as described in section 4.6 with slight modifications. As quality control of mouse cDNA, the housekeeping gene *sftpD* encoding surfactant associated protein D (NM 023124), was chosen additionally (Kouadjo *et al.*, 2007). *SftpD* transcripts were amplified with oligonucleotides SftpD_for and SftpD_ leading to a 579 bp DNA fragment. 400 ng cDNA served as a template for transcript amplification.

6 Methods for antibody selection

6.1 General buffers and material for antibody experiments

The antibody pool for the selection was provided by a recombinant antibody library which was developed within the scope of the diploma thesis of Habicht & Siegemund (2002). Annotated sequences of *Camelidae* VHH-domain antibodies served as the basis for this fully synthetic recombinant library. Three CDRs in a conserved framework provide 19 to 29 variable amino acid positions, for 20 different amino acids. Additionally, 9 positions in the framework are variable in two amino acids. Theoretically, the library possesses a variability of 4^{39} amino acid sequences. Practically, the variability is reduced to approximately 10^{11} due to limited transformation efficiencies and the occurrence of frame-shifts and stop codons. Phage display was chosen as a tool for the presentation of peptide sequences encoded in the library.

Panning buffer (PB) at pH 7.4 served as the basis for the working buffers in the panning procedures, in phage and antibody ELISAs as well as in immunofluorescence studies. The standard PB contained 10 mM CaCl_2 , 50 mM Tris and 150 mM NaCl. High salt panning buffer (HS-PB) included 0.5 M NaCl instead of 0.3 M NaCl. The PEG solution for phage precipitation consisted of 17 % (w/v) PEG-6000, 3.3 M NaCl and 1 mM EDTA. The components of PBS solution for phage recovery were 137 mM NaCl, 3 mM KCl, 8 mM Na_2HPO_4 and 1.5 mM KH_2PO_4 at pH 7.4.

A. fumigatus conidia of *pksP* mutant and wild-type strains differ in their surface hydrophobicity which hinders homogeneous binding to various surface - treated ELISA plates. However, quantitative binding studies demand homogeneous binding of the antigen to the bottom of the ELISA plate. Therefore, porous 96 well ELISA plates (Multiscreen-HTS-

BV, Ø 1.2 µm, Millipore, Germany) were used in combination with the Multiscreen® Filtration System (Millipore) to incubate and wash conidia in the panning process and ELISA analysis. This ensured the retention of conidia, whereas washing and binding steps were not hindered.

Absorption measurements of the developed ELISA were carried out with Multiskan Spectrum (ThermoLabsystems) in flat bottom ELISA plates. All steps were carried out at RT but incubations with antibodies were performed on top of a Thermomixer comfort (Eppendorf) at 20 °C.

6.2 Selection of VHH domains against *A. fumigatus* conidia

Binders were selected from non-binders in four competitive panning rounds. Each positive selection (selection against the target, i.e. melanised conidia) was preceded by a negative selection against a negative-antigen (conidia lacking melanin) to avoid the selection of binders against other surface structures than melanin. A brief summary of panning conditions for each round is presented in Table 5.

Table 5. Summary of the conditions in each panning cycle. Presented is the pool of phages which provided the reservoir of binders in the respective selection step, the blocking reagent for conidia, antibody pool as well as for ELISA plate surfaces. The origin of conidia, which served as positive- and negative-antigen, is also depicted.

No.	Pool of binders	Blocking reagent	Negative-antigen	Positive-antigen
1	Library phages	BSA	-	ATCC46645
2	Purified phages from 1 st round	milk powder	<i>pksP</i> mutant	ATCC46645
3	Purified phages from 2 nd round	BSA	<i>pksP</i> mutant	ATCC46645
4	Purified phages from 3 rd round	milk powder	<i>pksP</i> mutant	ATCC46645

500 µl of the antibody pool, with approximately 1×10^{10} – 1×10^{11} purified phages, were introduced in each panning round. At first, phages, the negative-antigen (2×10^8 *pksP* mutant conidia), the positive-antigen (5×10^7 ATCC46645 conidia) and the ELISA plate were incubated with either 2 % (w/v) BSA in PB or 2 % (w/v) milk powder in PB for 1 h at 550 rpm to block unspecific sites. After blocking, the negative-antigen and phages were concertedly incubated for 1 h at 550 rpm and subsequently centrifuged (1 min at 16,000 *g*). Deviant from first and second cycle, negative-antigen and phage pool were mixed and blocked together in the third and fourth selection round. The incubation with the non-melanised conidia allowed the separation of phages binding to other surface structures than

melanin, which appeared in the pellet after centrifugation. The supernatant, which contained phages not binding to the negative-antigen, was added to blocked wild-type conidia. Selection of binders against wild-type conidia occurred for 1 h at 550 rpm. Conidia and bound phages were pelleted at 16,000 *g* for 1 min, and the supernatant, containing unbound phages, was withdrawn. In the next step, the conidia/phage mixture was resuspended in 100 μ l PB and transferred to a blocked ELISA plate. Loosely bound phages were removed in 20 washing steps with PB (containing 0.05 % (v/v) Tween[®]-20). Each washing step included the incubation of conidia/phage mixture in 200 μ l fresh buffer for 2 min at 600 rpm. For elution of bound phages from conidia, conidia were transferred to a blocked tube after resuspension in a total volume of 400 μ l PB including Tween[®]-20. After centrifugation at 16,000 *g*, supernatant was withdrawn and phages were eluted from conidia by incubation for 9 min in 800 μ l glycine \times HCl with a pH of 2.2. Eluted phages were recovered from conidia in the supernatant after centrifugation. For neutralisation, phage solution was transferred into a tube containing 48 μ l 2 M Tris. This phage suspension was used for plate titering and transfection of *E. coli* cells for phage amplification for further selection rounds (B6.3).

6.3 Transfection of *E. coli*, determination of phage concentration, phage amplification and phage recoverage

Eluted phages from the panning cycle were titered in a plate assay to determine chloramphenicol-resistant transducing units, which was essential to estimate panning outcome. XL1-Blue cells were transfected with eluted phages for plate titering and phagemid amplification.

XL1-Blue stocks ($OD_{550nm} = 1$) in 20 % (v/v) glycerol in 2 \times YT were prepared as 10 ml portions and stored at -20 °C for acceleration of the working procedure. A stock was thawed before transfection and cultivated at 37 °C and 200 rpm in 100 ml 2 \times YT supplemented with 15 μ g/ml tetracycline until an $OD_{550nm} \approx 0.5 - 0.7$ was reached.

A dilution series of phages in PB was established until the dilution step 10^{-5} was reached. 10 μ l of diluted phage suspensions were incubated for 30 min at 37 °C with 50 μ l XL1-Blue culture (freshly prepared with an $OD_{550nm} \approx 0.5$) for transfection and afterwards spread onto LB agar plates containing chloramphenicol and incubated over night at 37 °C. The number of bacterial colonies grown corresponded to the number of chloramphenicol-resistant transducing units and thus to the approximate number of phages recovered after the selection cycle.

The other portion of eluted phages was used for transfection of 20 ml XL1-Blue culture for phage amplification. After incubation at 37 °C for 30 min without agitation, centrifugation at RT for 6 min at 3,500 *g* followed. The supernatant was discarded, except for 2 ml, and the pellet was resuspended before spreading onto LB agar plates and incubation at 37 °C for approximately 18 h. Afterwards, the grown colonies were harvested with 5 ml of a mixture of 2 × YT and 25 % (v/v) glycerol. 1 ml was used for phage amplification, and the remaining suspension was frozen at -20 °C for storage.

Harvested transfected XL1-Blue cells were cultivated in 100 ml 2 × YT at 37 °C and 200 rpm at a maximal initial OD_{550nm} ≈ 0.1 until OD_{550nm} ≈ 0.5 - 0.7 was reached. 30 µg/ml chloramphenicol allowed the selected growth of *E. coli* cells which had been transfected with library phages. Subsequently, cells were transfected with VCSM13 helper phages. After incubation of bacteria/phages mixture at 37 °C for 30 min without agitation, the incubation for 30 min at 37 °C with an agitation of 100 rpm followed. 1 mM IPTG was added to induce expression of VHH domains. The amplification of phages occurred at 30 °C and 200 rpm over night.

Candidates for phage ELISA or sequencing analysis were picked from colonies grown in the plate titering experiment. These library clones were cultivated in 15 ml 2 × YT at 37 °C and 200 rpm, containing tetracycline and chloramphenicol, until an OD_{550nm} ≈ 0.5 - 0.7 was reached. Transfection with helper phages was carried out as described above, and protein production was induced by the addition of 1 mM IPTG.

6.4 Purification of phages

VHH-presenting phages had to be purified from *E. coli* cells for a new panning round and for phage ELISA. The overnight culture of transfected *E. coli* after panning was aliquoted in 50 ml falcon tubes and incubated for 30 min on ice. Centrifugation for 20 min with 8,000 *g* at 4 °C followed to separate phages in the supernatant from sedimenting bacteria. After splitting the supernatant into 25 ml portions and the addition of 20 ml PEG solution, the mixtures were incubated for 1 h on ice to precipitate phages and centrifuged for 20 min with 8,000 *g* at 4 °C. The supernatant was removed, and the phage pellet was resuspended in 17 ml PB. Phage precipitation was repeated once more for further purification. The final phage pellet was resuspended in 5 ml panning buffer, aliquoted into 1 ml portions and used directly or frozen at -20 °C.

For amplification of single library clones which have been obtained after panning, 15 ml of bacteria/phage culture were mixed with 10 ml PEG solution, and precipitation was

carried out as described above. For the second purification step, the pellet was resuspended in 1 ml PBS, and phages were precipitated with 700 μ l PEG solution. The final pellet was obtained after centrifugation for 5 min at 16,000 *g*. The purified phage pellet was resuspended in 1 - 1.5 ml PBS for ELISA studies.

7 Methods for antibody production and characterisation

7.1 Phage ELISA

Each well was covered with 5×10^7 conidia, which presented the antigen. The fluid was aspirated and conidia were washed twice with 200 μ l PB. Afterwards, conidia were blocked three times with 300 μ l blocking buffer which consisted of a 1:2 dilution of SuperBlock[®] (PBS) Blocking Puffer (Thermo Fisher Scientific, Germany) and PB supplemented with 0.05 % (v/v) Tween[®]-20. Another washing step followed before addition of 100 μ l phage suspension (from single clone amplification according to B6.3 and B6.4). Conidia were incubated with phage suspension for 1 h under agitation and afterwards washed 6 times with 200 μ l PB. The incubation with HRP/anti-M13 Monoclonal Conjugate (a conjugate of horseradish Peroxidase with mouse anti-M13 monoclonal antibody, GE Healthcare, Germany) in PB followed for 1 h. For this purpose, the HRP conjugate was diluted 1:2500 in PB. After aspiration of the antibody solution, conidia were washed 10 times with PB containing 0.05 % (v/v) Tween[®]-20 and twice with 200 μ l PB without Tween[®]-20. Finally, the ELISA was developed with 150 μ l tetramethylbenzidine substrate (1-Step Turbo TMB-ELISA (Thermo Fischer Scientific, Germany)) for 30 min. Then, the fluid was aspirated into a new 96 well plate, and the reaction was stopped with 100 μ l 1.5 M sulfuric acid solution. The absorption was measured at 450 nm against the blank solution which derived from identical incubations without conidia.

7.2 Antibody ELISA

To characterise the binding of the antibody, a slightly modified phage ELISA was applied. The amount of antigen, hence the conidia concentration, was reduced to 2×10^7 conidia/well. After washing twice with 200 μ l PB, conidia were blocked for 3 h at 300 rpm with PB supplemented with 2 % (w/v) BSA. The incubation with 100 μ l antibody solution (250 μ g/ml in HS-PB supplemented with 1 % (w/v) BSA) for 1 h at 300 rpm followed after two further washing steps with 200 μ l PB. Eight washing steps with an optimised HS-PB (supplemented with 0.05 % (v/v) Tween[®]-20) followed. To eliminate residual Tween[®]-20,

three further washing steps were applied with HS-PB. Developing occurred via PhoA activity determination by incubation with 100 μ l PNPP (*p*-Nitrophenyl Phosphate, Disodium salt, Thermo Fisher Scientific, Germany) as substrate for 22 min. The reaction was stopped by addition of 50 μ l 2 M NaOH. The aspiration of the solution into a new microtiter plate followed, and the absorption was measured at 405 nm.

7.3 Fermentation of the antibody

MelPhoA was produced in RV308 strain carrying plasmid pTetA6H_Mel* via high-cell-density fermentation under non-limited growth conditions (adapted from Horn *et al.*, 1996). Two-step pre-cultures (with chloramphenicol) were grown in shake flasks at 26 °C until $OD_{550nm} \approx 3$ and were used to inoculate 400 ml medium (without chloramphenicol) in the sixfors fermenter (Infors AG, Switzerland) to an initial $OD_{550nm} \approx 0.15$. Induction of protein production was initiated by the addition of 1 mM IPTG when $OD_{550nm} \approx 80$ was reached. Fermentation was continued for 4 h and 20 min to reach $OD_{550} \approx 150$. Finally, cells were pelleted by centrifugation for 20 min at 9,000 *g* and 4 °C before storage at -70 °C.

7.4 Purification of the antibody

A 50 g cell pellet was resuspended in 300 ml high salt buffer (2 M NaCl, 50 mM NaH₂PO₄, 40 mM imidazole, pH 8.0) and homogenised for 20 min at 4 °C (RW 28 basic, KIKA Labortechnik, Germany). Afterwards, cells were lysed with the EmulsiFlex-C50 homogenizer (AVESTIN, Canada), pH was adjusted to 8.0 with 1 M NaOH, and suspension was left for 30 min on ice to precipitate the excess of salts. After centrifugation for 90 min at 25,000 *g* (BECKMAN centrifuge Avanti™ J-20, rotor JA-14), the supernatant was filtered consecutively through 1.2 μ m and 0.44 μ m filtration membranes. Finally, 1 % (v/v) Tween®-20 was added to the buffer, and the volume was adjusted to 500 ml with high salt buffer.

The (His)₆ tag VHH-domain antibody was purified by affinity chromatography on a Fast Protein Liquid Chromatography (FPLC) System (Äkta™ Explorer 900, GE Healthcare) equipped with a column packed with 25 ml of Ni Sepharose 6 Fast Flow (GE Healthcare, Germany). After equilibration of the column with the low salt buffer (0.3 M NaCl, 50 mM NaH₂PO₄, 40 mM imidazole, pH 8.0) supplemented with 1 % (v/v) Tween®-20, the sample was bound to the column at a flow rate of 10 ml/min. The sample was intermediately polished with a stepwise increase (5 CV each) of the imidazole concentration from 40 mM to 80 mM, 100 mM and 115 mM in low salt buffer. Finally, the antibody was eluted with 250 mM imidazole. The detection of alkaline phosphatase activity allowed the identification

of fractions with high concentrations of purified antibody. For this purpose, 100 μ l of each fraction were mixed with 100 μ l PNPP solution (Thermo Fisher Scientific, Germany) in a 96 well plate, and the absorption was measured at 405 nm after developing for 3 min and addition of 50 ml 2 M NaOH.

In a second step, the antibody was further purified, concentrated and desalted via the strong anion exchange matrix Q Sepharose™ Fast Flow (HiTrap™ QFF, 5 ml, GE Healthcare, Germany). Antibody fractions from the first chromatographic step were diluted 10 times with buffer A (20 mM Tris, pH 8.5), and the column was equilibrated with the same buffer. Subsequently, the sample was captured at a flow rate of 5 ml/min, and the antibody was eluted with a gradient over 10 CV from 0 % buffer B to 40 % buffer B (20 mM Tris, 1 M NaCl, pH 8.5). The antibody was aliquoted, mixed with glycerol (1:1) and stored at -20°C for long term storage.

7.5 Biotinylation of the antibody

Before biotinylation, the antibody solution was desalted via gel filtration (PD10 desalting column, GE Healthcare, Germany). Biotinylation of the antibody was performed in PBS (pH 7.9) with EZ-Link® Sulfo-NHS-Biotin Reagent (PIERCE, Germany) for 2 h on ice. The comparison between 5 times, 10 times and 15 times molar excess of biotin to antibody, yielded in best results for the 5 times over-biotinylation. Here, antibody affinity was reduced to a minimal extend, and NeutrAvidin™ HRP conjugate detected the biotinylated antibody well.

7.6 Simultaneous competition antibody ELISA

2×10^7 wild-type conidia were loaded into the porous microplate, washed twice with 200 μ l HS-PB and blocked for 1.5 h with HS-PB supplemented with 2 % (w/v) BSA. Two further washing steps with HS-PB followed before the incubation with 100 μ l antibody mixture for 1 h. Unbound antibodies were discarded in two washing steps with HS-PB supplemented with 0.05 % (v/v) Tween®-20 and two further washing steps with HS-PB. It was proceeded with the addition of NeutrAvidin™ HRP conjugate (diluted 6000-fold in HS-PB, Perbio Science Germany) for 30 min. The unbound conjugate for detection was removed in the following three washing steps with HS-PB containing 0.05 % (v/v) Tween®-20 and 3 further washing steps with HS-PB. The ELISA was developed with 100 μ l HRP substrate (BM Blue POD, soluble; Roche Applied Science, Germany) for 10 min, and the reaction was stopped by addition of 100 μ l of 1 M sulfuric acid. After aspiration of the solution into a fresh

96 well microplate, absorption was measured at 450 nm against 690 nm as the reference wavelength.

7.7 Immunofluorescence studies

Conidia and mycelia of *A. fumigatus*, melanin particles and *Phoma destructiva* samples were prepared before blocking and antibody incubation as follows: For detection of conidia and melanin particles, all incubation and washing steps were carried out in Ultrafree-MC Centrifugal Filter Units with Microporous Membrane (\varnothing 0.45 μ m, Millipore, Germany) and solution volumes of 400 μ l. Approximately 2×10^7 conidia/particle were applied per experiment. To investigate the binding of MelPhoA to mycelia, 3×10^6 conidia of *A. fumigatus* CEA17 Δ akuB^{KU80} strain were cultivated in 1 ml AMM for 48 h. If necessary, 10 mM L-tyrosine was added after the first 10 h of growth. *P. destructiva* was cultivated in 50 ml potato dextrose medium for 45 h. If necessary, 5 μ g/ml cyclosporine A was added after 22 h of cultivation for pigment induction. Cultures of fungi were fixed before treatment with the antibody. For this purpose, mycelia were washed with PBS through miracloth and fixed for 15 min in PBS containing 3 % (v/v) formaldehyde. Fixative was removed by filtration through miracloth and inactivated in 50 mM NH₄Cl solution for 10 min. Further washing steps with PB were carried out in Ultrafree-MC Centrifugal Filter Units. MelPhoA was also applied for detection of *A. fumigatus* in tissue sections of immunosuppressed and infected mouse lungs (mouse infection model is described in B5.1). Lungs were either embedded and frozen in Tissue-tek O.C.T. (Sakura Finetek) before sectioning into 20 μ m slices, or treated as described in B5.2. All washing and incubation steps were carried out on SuperFrost® Plus adhesion slides (Menzel, Germany) with solution volumes of 200 μ l.

Samples containing MelPhoA targets were washed three times with PB (section B6.1) before blocking with 3 % (w/v) BSA in PB for 2 h. Tissue sections were additionally blocked with Avidin D for 15 min and subsequently with Biotin for 15 min (Avidin/Biotin Blocking Kit, Vector Laboratories, USA). The incubation with biotinylated MelPhoA (5 μ g/ml) in PB with 0.5 M NaCl in 1 % (w/v) BSA followed. Before incubation for 1 h at RT with a 500-fold dilution of Streptavidin - Cy3 conjugate (Sigma) in PB for detection, the samples were washed twice with PB supplemented with 0.05 % (v/v) Tween®-20 and 0.5 M NaCl before a further washing step without Tween®-20 followed. Unbound conjugate was removed by five washing steps with PB containing 0.05 % (v/v) Tween®-20 and 0.5 M NaCl and three further washing steps with pure PB. Samples were embedded and conserved in ProLong® Gold Antifade (Invitrogen, Germany).

For the detection of melanin on the surface of mycelia of pyomelanin mutants, a modified method was applied (section C3.5.3.). 5×10^4 or 5×10^5 conidia/ml were inoculated in 100 μ l AMM medium, if necessary supplemented with 10 mM L-tyrosine, on SuperFrost® Plus adhesion slides (Menzel, Germany) for 48 h at 37 °C in a wet chamber. Washing, blocking and incubation steps were carried out with volumes of 400 μ l in the same order and with the same solutions as mentioned above. However, 2 % (w/v) BSA and 2 % (w/v) milk powder in PB were used as blocking solution, and MelPhoA and Streptavidin - Cy3 conjugate were diluted in PB containing 2 % (w/v) BSA and 0.5 M NaCl. A water repellent circle around the sample, created with a PAP Pen, allowed the reduction of solution volumes and avoided the mixing of adjoining samples. During washing steps, the majority of mycelia was discarded, however the residual mycelia adhering to the slide were sufficient for detection.

7.8 2D gel electrophoresis and Western blotting of conidia extracts

Protein extraction, gel electrophoresis and spot identification was essentially carried out (according to Teutschbein *et al.*, 2009). *A. fumigatus* wild-type strain ATCC46645 was grown on YPD agar for 3 days at 37 °C before harvesting of conidia with a solution containing 0.9 % (w/v) NaCl and 0.025 % (v/v) Tween®-80. After washing of conidia twice and resuspension in 0.9 % (w/v) NaCl solution, glass beads were added which facilitated the disruption of conidia with the micro-dismembrator (Sartorius) for 6 min at 2,000 rpm. Glass beads were sedimented by centrifugation for 1 min at 200 rpm, and proteins were precipitated in the obtained supernatant by addition of 13.3 % (v/v) TCA in acetone and 20 mM DTT over night at -20 °C. After washing of the pellet twice in acetone and evaporation of the solvent, extraction of proteins for 15 min at 4 °C under agitation with 500 μ l extraction buffer (50 mM Tris, 5 mM EDTA, 100 mM KCl, 30 % (w/v) saccharose, 200 mM DTT, pH 8.8) and 500 μ l Tris buffered phenol followed. Extraction with 500 μ l extraction buffer was repeated after centrifugation (16,100 *g* at 4 °C for 5 min) with the upper phenolic phase. Phases were separated by centrifugation and precipitation of the proteins in the upper phase started by the addition of 100 mM $\text{NH}_4(\text{CH}_3\text{COO})$ in methanol over night at -20 °C. The pellet obtained after centrifugation (15 min at 16,100 *g*) was washed twice with methanol and once with acetone before evaporation of residual acetone. The subsequent resuspension and extraction in lysis buffer (7 M urea, 2 M thiourea, 2 % (w/v) CHAPS, 30 mM Tris, 1 % (w/v) Zwittergent, 0.8 % (v/v) Pharmalyt 3-10, 20 mM DTT) was supported by ultrasonification for 10 min. Cell debris was precipitated at -70 °C for 1 h, the sample was adjusted to RT and centrifuged (20 min at 16 °C with 16,100 *g*). The supernatant, containing soluble proteins,

was applied to gel electrophoresis. The absolute amount of 100 µg protein was applied via anodic cup loading to rehydrated IPG-strips with a non-linear pH-gradient from 3-11 (GE Healthcare Bio-Sciences, Germany). The second dimension electrophoresis was performed on Criterion 12.5 % Tris-HCl-glycine gels (Biorad). For Western blot analysis, proteins were transferred from unstained gels to PVDF membranes via tank blotting in a solution containing 25 mM Tris, 192 mM glycine, 0.025 % (w/v) SDS and 20 % (v/v) methanol for 2 h at 0.5 A. Then, membranes were blocked for 2 h with TBS-T (10 mM Tris, 150 mM NaCl, 0.1 % (v/v) Tween[®]-20, pH 8.0) containing 5 % (w/v) BSA. The incubation with 4 µg/ml MelPhoA occurred in the same solution at 4 °C over night. Blots were washed three times with TBS-T and finally detected with BCIP/NBT (Millipore). Developing was stopped by washing in water, and blots were conserved after scanning digitally. To facilitate comparison with Coomassie stained gels, wet blots were poststained with colloidal Coomassie Blue R-250 (Neuhoff *et al.*, 1988) and scanned. Preparative gels for mass analysis were stained with colloidal Coomassie Blue R-250. Images were analysed with Delta2D Version 3.6 (DECODON). Protein spots of interest were excised and tryptically digested (Shevchenko *et al.*, 1996). Peptide mass and peptide fragment fingerprint spectra were measured by MALDI-TOF/TOF (Ultraflex 1; Bruker Daltonics, Germany) and subsequently identified by searching the fungi section in the NCBI-database using the MASCOT interface (MASCOT 2.1.03, Matrix Science, UK) with the following parameters: Cys as S-carbamidomethyl-derivative and Met in oxidised form (variable), one missed cleavage site, peptide mass tolerance of 200 ppm. Hits were considered significant according to the MASCOT score (p<0.05).

8 Microscopy

8.1 Electron microscopy

A. fumigatus cultures grown on AMM agar were chosen for raster electron microscopy (REM) to study the surface morphology of conidia and hyphae. For this purpose, 5000 conidia were point inoculated on AMM agar with 20 mM glucose and if necessary with additional 10 mM L-tyrosine. Incubation was carried out in a LAB-TEK[®] 4 well chamber slides (Nalge Nunc International, USA) for two days at 37 °C and for one day at RT. Afterwards, cultures were washed with 250 µl washing buffer (10 mM Tris, 0.1 % (v/v) Tween[®]-20, pH 7.0) and fixation for 2 × 45 min with washing buffer containing 2.5 % (v/v) glutaraldehyde followed. Cultures were washed once more with washing buffer and three

more times with washing buffer without Tween[®]-20. Each washing step was carried out for 3 min with 250 µl buffer while shaking. After dehydration of samples in an ethanol series (30 %, 50 %, 70 %, 80 %, 90 %, 2 × 100 % for 15 min each), probes were gently dried in carbon dioxide in the critical point dryer (Bal-tec CPD 030, BAL-TEC AG, Liechtenstein) to conserve structures. Samples were coated with a gold layer for 90 s at 60 mA (Bal-tec SCD 005) to make their surfaces electrically conductive. Micrographs were taken with a LEO 1450 VP electron microscope (Carl Zeiss, Germany).

8.2 Light and fluorescence microscopy

For light and fluorescence microscopical studies and documentation, a Leica DM4500 B digital fluorescence microscope and a Leica DFC480 digital camera (both Leica Microsystems, Germany) were employed. Table 6 summarises parameters of applied fluorescence proteins and filter cubes. Photographs were processed with FastStone Image Viewer 3.5 software (FastStone Soft).

Table 6. Fluorescence microscopy data. Absorption and emission maxima of fluorescent proteins and the properties of the corresponding applied filter cubes are depicted.

Fluorescent protein	Absorption maximum	Emission maximum	Used filter cube	Excitation filter	Suppression filter	Dichromatic mirror
eGFP	488 nm	509 nm	GFP	470+/-20 nm	525+/-25 nm	500 nm
DsRed2	558 nm	583 nm	RFP	546+/-6 nm	605+/-37.5 nm	560 nm
Cy3	552 nm	565 nm	RFP	546+/-6 nm	605+/-37.5 nm	560 nm

9 Databases and bioinformatics

Gene sequences were obtained from *A. fumigatus* Af293 genome which was sequenced by the Sanger Institute and The Institute for Genomic Research (<http://www.tigr.org/tdb/e2k1/afu1/>). The CBS Prediction Servers (<http://www.cbs.dtu.dk/services/>) and the Central *Aspergillus* Data Repository (<http://www.cadre-genomes.org.uk/>) were used for both conserved domain search and for predictions about protein structures. Clusters in different *Aspergillus* spp. were aligned and compared by the Sybil comparative analysis system (<http://www.tigr.org/tigr-scripts/sybil-asp/sybilHome.pl?db=asp>). Similarity searches were performed using the Basic Local Alignment Search Tool of the National Centre for Biotechnology Information (<http://www.ncbi.nlm.nih.gov/blast/Blast.cgi>).

C RESULTS

1 A camelid antibody domain against fungal melanin

1.1 Selection and synthesis of the antibody

1.1.1 Design of a panning method against conidia

Wild-type conidia of *A. fumigatus* expose DHN-melanin on their surface (Jahn *et al.*, 1997; Langfelder *et al.*, 1998; Tsai *et al.*, 1998) and therefore provide a suitable target for antibody selection against natural melanin. However, conidia are also covered by other cell wall components which essentially demand the exclusion of the selection against these interfering structures. *PksP* mutant conidia of *A. fumigatus* are white coloured and lack the pigment but still possess the other conidial surface components (compare section D1.1). These features make *pksP* mutant conidia to qualified competitors in a selection procedure. A competitive selection includes the withdrawal of binders against structures which should be excluded before the incubation of the remaining binder pool with the actual target. Therefore, *pksP* mutant conidia have to be incubated with the pool of binders before the presentation of the target on the surface of wild-type conidia in order to withdraw binders against other surface structures than melanin. A further prerequisite of a successful selection method is the separation of conidia with bound antibodies from non-binders. The widely applied solid phase separation for proteinaceous targets and cells was not successful for conidia. The attempt to stick conidia to a variety of surfaces resulted in inhomogeneous and loose coating. Moreover, the fixation of conidia on surfaces using the biotin-streptavidin system worked insufficiently (data not shown).

The further attempt to separate phages and conidia in an aqueous solution *via* centrifugation failed since conidia did incompletely sediment after centrifugation leading to an intolerable loss of conidia during washing steps (data not shown). Recently, the BRASIL method was introduced (Giordano *et al.*, 2001) which is based on differential centrifugation. Here, a cell suspension is incubated with phages in an aqueous upper phase and centrifuged through a non-miscible organic lower phase. This method did not allow a sufficient separation of unbound phages from conidia either (data not shown).

Because of the lack of suitable methods, the idea was to use the difference in size of conidia compared to phages as basic principle for a separation method. Conidia display a diameter of approximately 2.5 μm , and filamentous phages are about 6.5 nm in diameter

and 960 nm long. Therefore, a separation by filtration through a porous membrane was tested and finally applied.

In the first selection round, library phages were incubated with BSA as blocking reagent and with melanised conidia. The second selection round was started by the incubation of conidia lacking melanin with library phages obtained in the first round. Then, this was followed by the incubation with melanised conidia. The blocking reagent was changed to skimmed milk to withdraw binders against BSA. The change in blocking reagent and the introduction of the negative-antigen were responsible for the low number of transducing units achieved after the second panning cycle (titers are summarised in Table 5). In the third and the fourth cycle, the incubation of pigmentless conidia to the reduced library pool before the presentation of melanised conidia was continued. The enrichment of binders correlated with the increase of transducing units after the selection process and thus, panning was completed.

Table 7. Titers after panning cycles. For each panning step the reduction of transducing units after panning compared to the units introduced in the panning round before selection are depicted.

Panning cycle	Negative antigen	Titer before selection	Titer after selection
1	none	$1 \times 10^{10} - 1 \times 10^{11}$	$\approx 5 \times 10^3$
2	<i>pksP</i> mutant conidia	$1 \times 10^{10} - 1 \times 10^{11}$	$\approx 3 \times 10^3$
3	<i>pksP</i> mutant conidia	$1 \times 10^{10} - 1 \times 10^{11}$	$\approx 1 \times 10^4$
4	<i>pksP</i> mutant conidia	$1 \times 10^{10} - 1 \times 10^{11}$	$\approx 8 \times 10^5$

1.1.2 Design of phage and antibody ELISA

In the ELISA study a homogeneous presentation of antigens is indispensable due to its character as a quantitative evaluation method. As described in section C1.1.1, conidia did not stick well to commonly applied polystyrene coated surfaces. Therefore, a variety of other surfaces was tested, including poly-L-lysine treated surfaces and Reakti-Bind™ Maleic Anhydride coated ELISA plates (Thermo Fisher Scientific). The attempt to establish a covalent amid link between maleic anhydride and amine groups of proteins and peptides on the surface of conidia failed. Additionally, Reakti Bind™ Streptavidin-coated ELISA plates (Thermo Fisher Scientific) did not efficiently bind the biotinylated conidia. None of these methods allowed a homogeneous coating of surfaces with different types of conidia. Therefore, the same porous microplates as in the panning procedure were used for phage and antibody ELISA.

The amount of conidia used as antigen in the ELISA turned out to be a sensitive parameter. The amount of the conidia had to comply with the following requirements: avoidance of clogging of pores, allowing efficient washing steps and sufficient signal levels. The optimal amount for phage ELISA was determined to be 5×10^7 conidia/well and the amount was reduced to 2×10^7 conidia/well in the antibody ELISA. The reduction was necessary to minimise the signals due to internal alkaline phosphatase activity of conidia.

1.1.3 Sequence analysis of selected VHH domains

Single clones from dilution series after the 4th panning step were amplified and tested in the phage ELISA for their binding properties to wild-type and *pksP* mutant conidia. An example of a phage ELISA is depicted in Fig. 5A. Such clones were selected for sequence analysis which showed a high signal for binding to wild-type conidia but a lower signal after incubation without conidia or with *pksP* mutant conidia, e.g., clone 8, 13 and 15 in Fig. 5A.

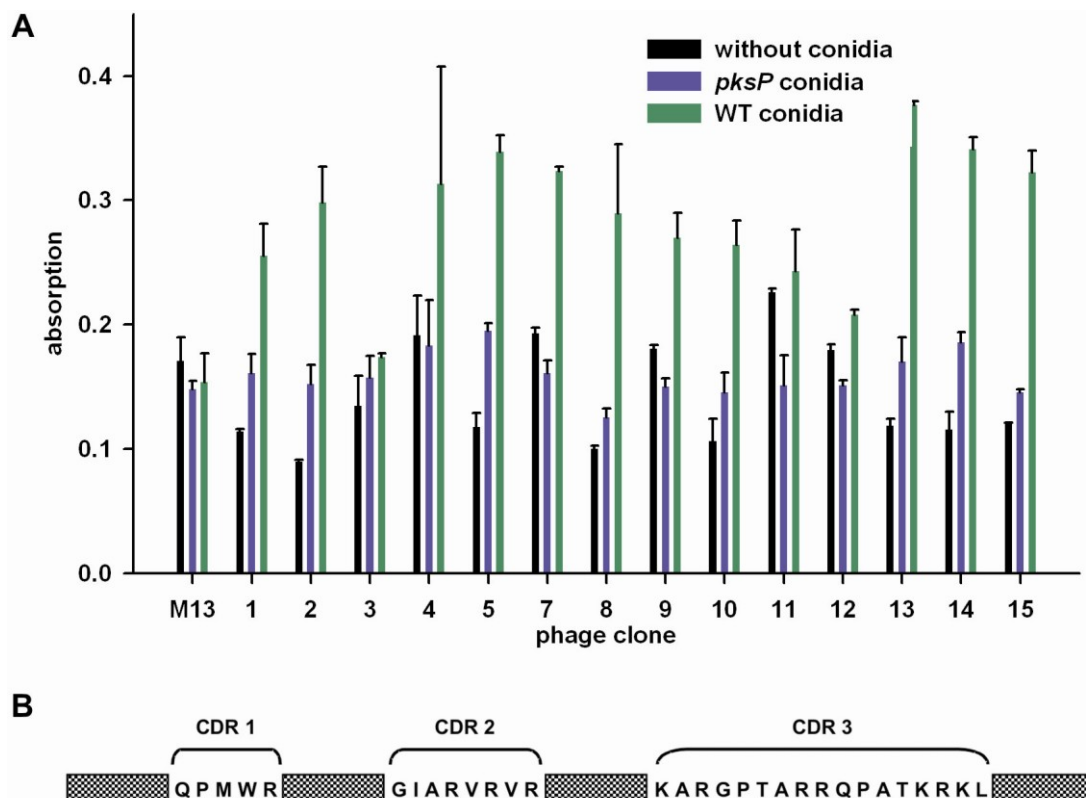


Fig. 5. Phage ELISA and variable domains of the enriched antibody. (A) VHH-presenting phages were tested for their binding to uncovered surfaces, to *pksP* mutant conidia as well as to *A. fumigatus* wild-type (WT) conidia. Binding was compared to the signals of helper phages (M13) which did not expose VHH domains on their surface. **(B)** The amino acid sequence of the variable regions of the selected VHH domain is shown. The constant framework of the VHH domain is shadowed in grey and the variable regions are named CDR 1, CDR 2 and CDR 3.

Twenty phagemid DNAs were chosen for sequence analysis due to their high signal ratio between wild-type conidia and *pksP* mutant conidia as presented antigen in the phage ELISA; 17 clones revealed equal sequences. The remaining sequences did not emerge repeatedly. The enriched VHH-domain sequence (FR1-4 and CDR 1-3) is depicted in Fig. 5B.

1.1.4 Antibody synthesis

Although binding studies can be carried out with phages presenting the antibody domain on their surface, phage handling and antibody modification for specific applications is restricted. Therefore, the heterologous production of the antibody was favoured.

The selected antibody sequence was cloned for the protein synthesis from the phagemid DNA into pTetpA6H via *SfiI* restriction. The obtained plasmid pTetpA6H_Mel provided a tool for the facilitated heterologous production of the antibody in *E. coli* cells. Furthermore, the plasmid improved the antibody for further applications and allowed the essential maturation of disulfide bonds. The modifications included the N-terminal fusion to the *pelB* signal sequence, the addition of a FLAG tag for easy detection in Western blot analysis, the C-terminal fusion of the antibody to alkaline phosphatase (*phoA*) and the attachment of six histidine residues for the facilitated purification via immobilised metal-affinity chromatography (IMAC) (Fig. 6A). The *pelB* signal sequence of the pectate lyase of *Erwinia carotovora* caused the transport of the antibody after cleavage of *pelB* into the periplasm. This led to the formation of native disulfide bonds due to the oxidising conditions in the periplasm and due to periplasmatic proteins. Thus, the antibody was produced in a soluble form. The exclusive synthesis in the cytoplasm would have prevented disulfide bonds because of the reducing condition in this compartment. The C-terminal PhoA fusion allowed its direct detection in ELISA studies and caused the dimerisation of the antibody. Furthermore, a signal enhancement was thereby achieved.

1.1.5 Optimisation of antibody synthesis

The production of the MelPhoA antibody was suboptimal in *E. coli* TG1 strain. The mRNA sequence of the antibody in CDR1 included the *amber* codon UAG. TG1 cells containing the *supE* tRNA allow the translation of that *amber* codon to glutamate and therefore prevent the abortion of peptide synthesis. However, the *amber* codon did not seem to be efficiently translated into glutamate. Protein yields were unsatisfying after high-cell-density fermentation and IMAC purification. Therefore, the mutagenesis of the *amber* codon in CDR1

to CAG, which codes for the amino acid glutamine, was supposed to improve the protein yield.

For the optimisation of the sequence, base T₁₀₈ was exchanged to C₁₀₈ in pAKMel in a two step PCR. Oligonucleotides Ab01 and pAKfor amplified the 5' region of the antibody and Ab02 and pAK rev the 3' region. The oligonucleotides Ab01 and Ab02 brought about the nucleotide exchange. Both fragments served as a template in the second PCR step and the reaction with oligonucleotides pAKfor and pAKrev led to the amplification of the whole mutagenised antibody sequence. The obtained PCR fragment was digested with *Sfi*I and extracted from a gel for its purification. Then, this prepared sequence was ligated into plasmid pTetpA6H after *Sfi*I digestion, dephosphorylation and gel extraction of the plasmid. The plasmid pTetpA6H_Mel* was gained and used for the heterologous production of MelPhoA.

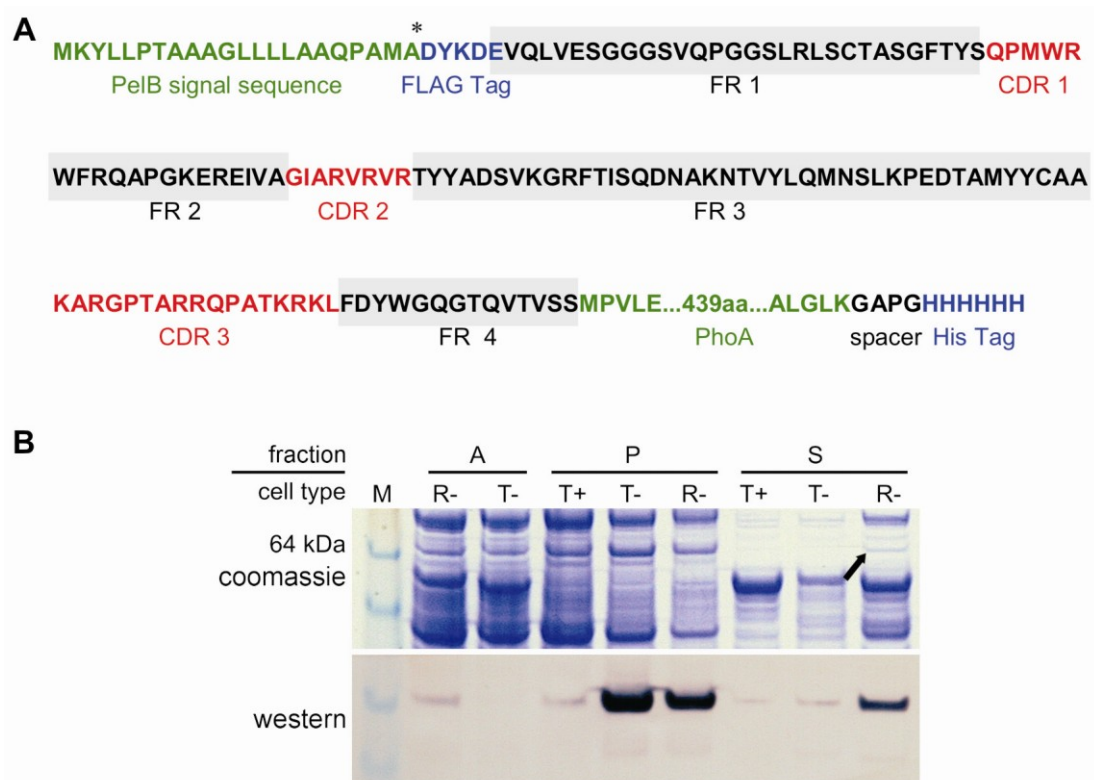


Fig. 6. Sequence of the engineered antibody and optimisation of antibody production. (A) Amino acid sequence of the selected VHH-domain antibody as it is encoded by the expression vector pTetA6H_Mel. Signal sequence of PelB, FLAG- and His Tag and alkaline phosphatase (PhoA) are depicted. The original VHH domain with its framework is shadowed in grey and the variable regions are drawn in red. **(B)** Cell lysate analysis of mutated antibody sequence compared to amber codon containing sequence. Whole cell lysate (A), insoluble fraction (P) and soluble fraction (S) of the antibody with amber codon (+) and without amber codon (-) cultivated in RV308 (R) and TG1 (T) are depicted. Coomassie stain does not clearly prove a higher yield of the mutagenised antibody, but Western blotting with anti-his antibody shows a higher yield in the soluble as well as in the insoluble fraction.

The impact of the mutagenesis on the expression level of the antibody was tested in a small scale fermentation assay. *E. coli* TG1 and RV308 strains were transformed with the plasmid pTetpA6H_Mel* and cultivated. Cells were lysed by ultrasonification 4 h after induction with IPTG. Whole cell lysates, pellet fractions and supernatants obtained after centrifugation were analysed using SDS-PAGE. The pellet fraction contained cell wall components and insoluble proteins, e.g., cell wall associated proteins and inclusion bodies. The supernatants comprised soluble proteins. The upper panel in Fig. 6B presents the Coomassie stained SDS-PAGE which did not clearly reveal the amelioration of the protein yield after mutagenesis. Only Western blot analysis of the same SDS-PAGE with anti-His antibody proved strongly increased yields. The pellet fraction obtained from TG1 transformants showed the highest MelPhoA level. However, pellet fractions contain inclusion bodies and insoluble proteins which would have to be refolded to be functional. Hence, the soluble fraction was most suitable to obtain a functional protein. Highest protein levels in a soluble fraction were obtained with RV308 strain. Consequently, RV308 strain containing the mutagenised plasmid was fermented to obtain elevated antibody yields.

1.1.6 High-cell-density fermentation and purification of the antibody

MelPhoA was produced in *E. coli* RV308 bearing plasmid pTetpA6H_Mel* by high-cell-density fermentation as this plasmid-strain combination yielded in the highest production of soluble protein as observed in C1.1.5. The maximal absorption of approximately 150 at 550 nm was reached during the fermentation process. After harvesting and centrifugation of cells a final biomass of 90 g/400 ml wet weight was obtained.

The C-terminal hexahistidine tag (His tag) allowed the purification of the antibody by IMAC. A high salt buffer containing additionally Tween®20 and a low concentration of imidazole was applied for the loading of the cell lysate onto the column to minimise binding of unspecific proteins to the nickel ions of the column. The elution of the antibody was triggered by an imidazole concentration of 250 mM. The upper panel in Fig. 7A presents Coomassie stained gels obtained after SDS-PAGE of fractions of different purification steps. The size of the protein in the eluted fractions (64 kDa) corresponds to the expected size of a MelPhoA monomer. The lower panel depicts the alkaline phosphatase activity of each fraction. This test allowed the fast identification of the antibody containing fractions, served as in-process control and gave a first hint about the proper folding of the protein. Therefore, MelPhoA was purified and concentrated in its functional conformation by IMAC.

A second chromatographic step was added to further purify and concentrate the antibody as well as for the exchange of the buffer. The isoelectric point of 6.5 and therefore the charge of -2.83 at pH 7 of the antibody permitted the application of anion exchange chromatography. As depicted in Fig. 7B, this method further concentrated and purified the antibody. The appearance of the weak band at approximately 120 kDa corresponds to the dimer of the antibody as expected due to the self association of the alkaline phosphatase domain to dimers.

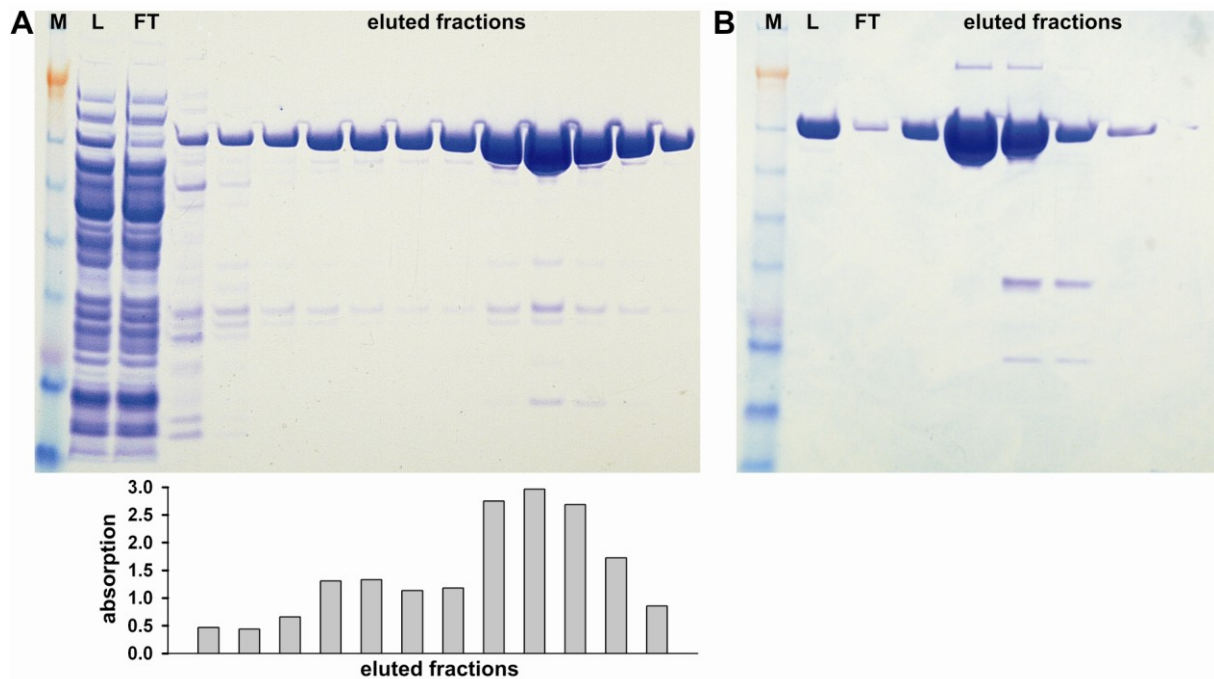


Fig. 7. SDS-PAGE of MelPhoA purification procedure and corresponding alkaline phosphatase activity assay. M denotes Marker (SeeBlue® Plus2 Pre-Stained Standard, Invitrogen), L is the load onto the column and FT stands for flow through during column loading. **(A)** The IMAC purification of the soluble fraction of cell extract and in the lower panel the corresponding activity of alkaline phosphatase of each fraction are depicted. **(B)** The further purification and concentration via ion exchange chromatography is presented.

1.2 Characterisation of the antibody

The phage ELISA already indicated a higher affinity of the selected VHH domain to WT conidia compared to conidia without melanin. In addition, the alkaline phosphatase activity assay showed that the purified VHH-domain fusion to alkaline phosphatase was functional. ELISA studies of the purified MelPhoA were chosen to prove the functionality of its antigen binding domain. The presentation of different targets exposing different types of melanin was essential for obtaining a prediction about the specificity of the antibody. Another prerequisite for the application of the antibody was the analysis of the nature of the

interactions between melanin and the VHH domain which can be carried out by a competitive ELISA.

1.2.1 Displacement of the antibody in the competition ELISA

The interaction between antibody and antigen is characterised by a reversible binding. This interaction can be measured in a competitive ELISA where two protein populations compete for the same target. The excess of one antibody population decreases the signal derived from another antibody type that is applied at constant concentration in a concentration dependent manner. Another antibody against melanin was not available and consequently, a system had to be established which allowed the independent detection of a modified MelPhoA from a second version of MelPhoA. The biotinylation of antibodies allows their detection via streptavidin-conjugates caused by the strong biotin-streptavidin interactions. Applying this approach the biotinylated antibody was separately detectable from non-biotinylated antibodies in an assay containing a mixture of both. In this study, MelPhoA was biotinylated with a 5 fold, 10 fold and 15 fold molar excess of activated biotin derivative. The detection of the biotinylated antibody via alkaline phosphatase revealed that the 5 fold molar excess did not reduce binding of the antibody domain to the target. Higher amounts did slightly reduce the signal probably due to biotinylation of the antigen binding domain or of the catalytic domain of alkaline phosphatase (data not shown). The biotinylated MelPhoA was applied in an ELISA at constant concentration with wild-type conidia as a target. Different concentrations of non-biotinylated antibody were used to displace the former antibody from its target. The biotinylated MelPhoA was detected via a streptavidin-HRP conjugate allowing its independent detection from non-biotinylated MelPhoA by HRP-substrate developing (Fig. 8B). The competition ELISA in Fig. 8A depicts the signal obtained via HRP substrate development and clearly proves the displacement of the biotinylated antibody by increasing concentrations of the competitor MelPhoA.

1.2.2 Binding of the antibody to conidia and melanin particles in the ELISA

The affinity of MelPhoA to conidia of different *A. fumigatus* mutants, other aspergilli and to melanin particles was investigated in a direct ELISA. Here, the antibody was directly used to gain the signal by its internal alkaline phosphatase activity. A secondary antibody was dispensable. The binding of MelPhoA to wild-type conidia was compared to the binding to *pksP* mutant conidia to find the most suitable ELISA conditions. 1 % (w/v) BSA solution was effective for the blocking of conidia. It was not inferior to the blocking with milk powder or

commercially available blocking solutions (SuperBlock Blocking buffer by Thermo Fisher Scientific, data not shown). However, a sufficient number of washing steps was crucial to avoid unspecific signals. High signals in the ELISA with *pksP* mutant conidia resembled insufficient washing or unspecific binding of MelPhoA. Additionally, the increase of the salt concentration to 0.5 M NaCl in the washing buffer reduced the binding of MelPhoA to *pksP* mutant conidia. Higher concentrations up to 1.5 M NaCl did not further improve the specificity. The camelid antibody BMP 2-7 PhoA (gift from P. Hortschansky) was included in the study to exclude that the interaction between MelPhoA and melanin originated from an interaction with the alkaline phosphatase domain of the antibody. BMP 2-7 PhoA was previously selected and is targeted at a Bone Morphogenic Protein. This camelid antibody gave low signals in the ELISA with *A. fumigatus* wild-type conidia (data not shown).

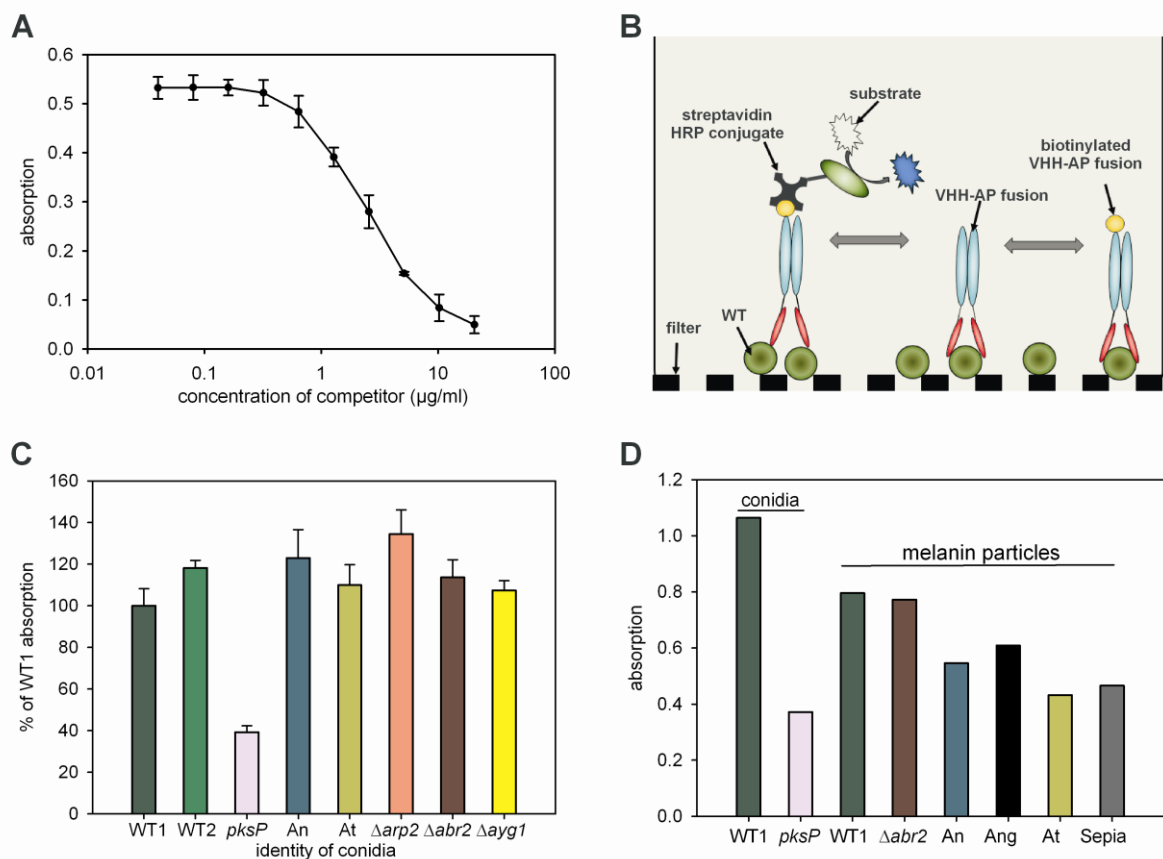


Fig. 8. ELISA studies with MelPhoA. (A) presents a competition ELISA of biotinylated MelPhoA with MelPhoA on wild-type conidia as antigen. In (B) the principle of the competition ELISA is depicted schematically. (C) shows the binding of MelPhoA to different types of conidia. The absorption obtained for the binding to WT1 conidia was defined as 100 %. The absorption obtained for the other antigens was calculated against WT1 absorption. Bars represent means with standard deviations calculated from two independent experiments with 6 replicates each. (D) Absolute absorption values obtained through the binding of MelPhoA to WT1 and *PksP* mutant conidia compared to the binding to melanin particles isolated from different conidia are presented. WT1 is ATCC46645, WT2 stands for CEA17 $\Delta akuBKU80$, An for *A. nidulans* SCF5, At for *A. terreus* i402, Ang for *Aspergillus niger* FSU-871, and Sepia for DOPA- melanin isolated from *Sepia officinales*.

These preliminary experiments resulted in an optimised ELISA procedure for the affinity testing of MelPhoA to conidia and melanin particles as antigen presenting structures. The binding of MelPhoA to different conidia in comparison to the binding to wild-type conidia is summarised in Fig. 8. The affinity of the VHH domain to CEA17 Δ *akuB*^{KU80} and ATCC46645 wild-type conidia was comparable. However, the antibody bound about 2.5 fold stronger to wild-type conidia than to the non-melanised *pksP* mutant conidia.

The affinity of MelPhoA to other DHN-melanin deficient strains was investigated as well. The Δ *arp2* strain exposes a pinkish pigment, the conidia of the Δ *ayg1* mutant strain are yellow and the Δ *abr2* strain produces a brown pigment. Apparently, these modifications did not interfere with the binding of MelphoA. The antibody showed comparable binding to wild-type conidia and to conidia exposing these modified pigments. A high affinity was also observable to the green *A. nidulans* and to the ochre *A. terreus* conidia. Therefore, MelPhoA binds to diversely pigmented conidia of different *A. fumigatus* DHN-melanin mutant strains as well as to the conidia of other aspergilli.

To further exclude that the selected antibody is directed against an antigen exposed on conidial surfaces different from melanin, the affinity to pure melanin particles was tested. For this purpose, melanin particles (often referred to as melanin ghosts (Wang *et al.*, 1996)) were isolated from various conidia. The isolation procedure included the degradation of cell wall glucans, the cell membrane disintegration and the protein denaturation by a chaotropic reagent, the proteolysis and further hydrolysis of other cell components to soluble molecules. This harsh procedure ensured that only DHN- and DOPA-melanins remained insoluble. These melanins are resistant to the whole procedure. Conidia from *A. fumigatus* ATCC46645, Δ *arp2*, Δ *abr2*, Δ *ayg1* and *pksP* mutant strain as well as conidia of *A. terreus*, *A. nidulans* and *A. niger* were subjected to melanin ghost preparation. However, conidia of the mutant strains Δ *arp2*, Δ *ayg1* and *pksP* did not yield insoluble particles. The obtained suspensions of the other strains were lyophilised for a better quantification. However, the electrostatic charging and inhomogeneous resuspension of the melanin particles after lyophilisation interfered with an accurate quantification of MelPhoA binding in the ELISA. Hence, the ELISA evaluation can only give an indication for the affinity of MelPhoA to melanin particles. Though, the 20 μ g of melanin particles applied to each well corresponded approximately to the amount of melanin particles isolated from 2×10^7 conidia, the amount of conidia applied to each well in the conidia ELISA. Fig. 8D depicts the binding of MelPhoA to melanin ghosts and sepia melanin (Sigma Aldrich, Germany) in comparison to the binding to wild-type and *pksP* mutant conidia. The evaluation of the bar chart leads to the conclusion that MelPhoA binds to melanin particles as well as to *Sepia* melanin.

1.2.3 Detection of melanin by MelPhoA applying immunofluorescence

MelPhoA was applied for the detection of conidia, melanin ghosts, mycelia as well as for the detection of *A. fumigatus* hyphae in the tissue of immunosuppressed and infected mouse lungs. In all of the described studies the biotinylated antibody was employed to allow the detection via Streptavidin -Cy3 conjugate as explained in Fig. 9E. This method was based on the avidin-biotin immune detection method and included the blocking of unspecific binding sites, the incubation with the biotinylated antibody, the removal of the unbound antibody and the final microscopical detection of the bound antibody with a Streptavidin-Cy3 conjugate.

The binding of the antibody to melanin ghosts and *A. fumigatus* ATCC46645 wild-type conidia is depicted in Fig. 9A. Melanin ghosts as well as melanised conidia showed a strong Cy3 fluorescence with the described method. In a control experiment, either the Cy3-conjugate or the biotinylated MelPhoA antibody was omitted. Here, only faint background fluorescence was detectable (data not shown). A quantitative comparison of fluorescence signals was not reliable applying this method. The different natures of the targets complicated the application of equal quantities of both targets in the experiment. Still, this study proved the conservation of the target structure of the antibody in melanin ghosts despite of the harsh preparation procedure.

The binding of MelPhoA to hyphae of *A. fumigatus* wild-type strain which were obtained after cultivation with and without 10 mM L-tyrosine was also examined. The mycelia and media did not turn brownish in the culture without L-tyrosine, however a pigment deposition on the surface of hyphae and a pigment release into the medium was visible in cultivations with tyrosine. This visible pigment deposition was confirmed by its recognition by the antibody as shown in Fig. 9B. Although mycelia cultivated without tyrosine were not stained by MelPhoA, mycelia grown with tyrosine were clearly detectable. Furthermore, the affinity of the antibody to hyphae of *Phoma destructiva* was investigated. A transcriptome analysis of this ascomycete fungus revealed that the presence of cyclosporine A induces genes of the DHN-melanin cluster. Additionally, cyclosporine A causes the pigmentation of the fungus which led to the assumption that cyclosporine A induces DHN-melanin production (Friedrich, 2007). As depicted in Fig. 9C, the antibody bound to pigmented mycelia of this fungus. Non-pigmented mycelia only revealed a weak fluorescence with MelPhoA and the Cy3 conjugate. Hence, the pigment produced by *P. destructiva* is a target of MelPhoA, too.

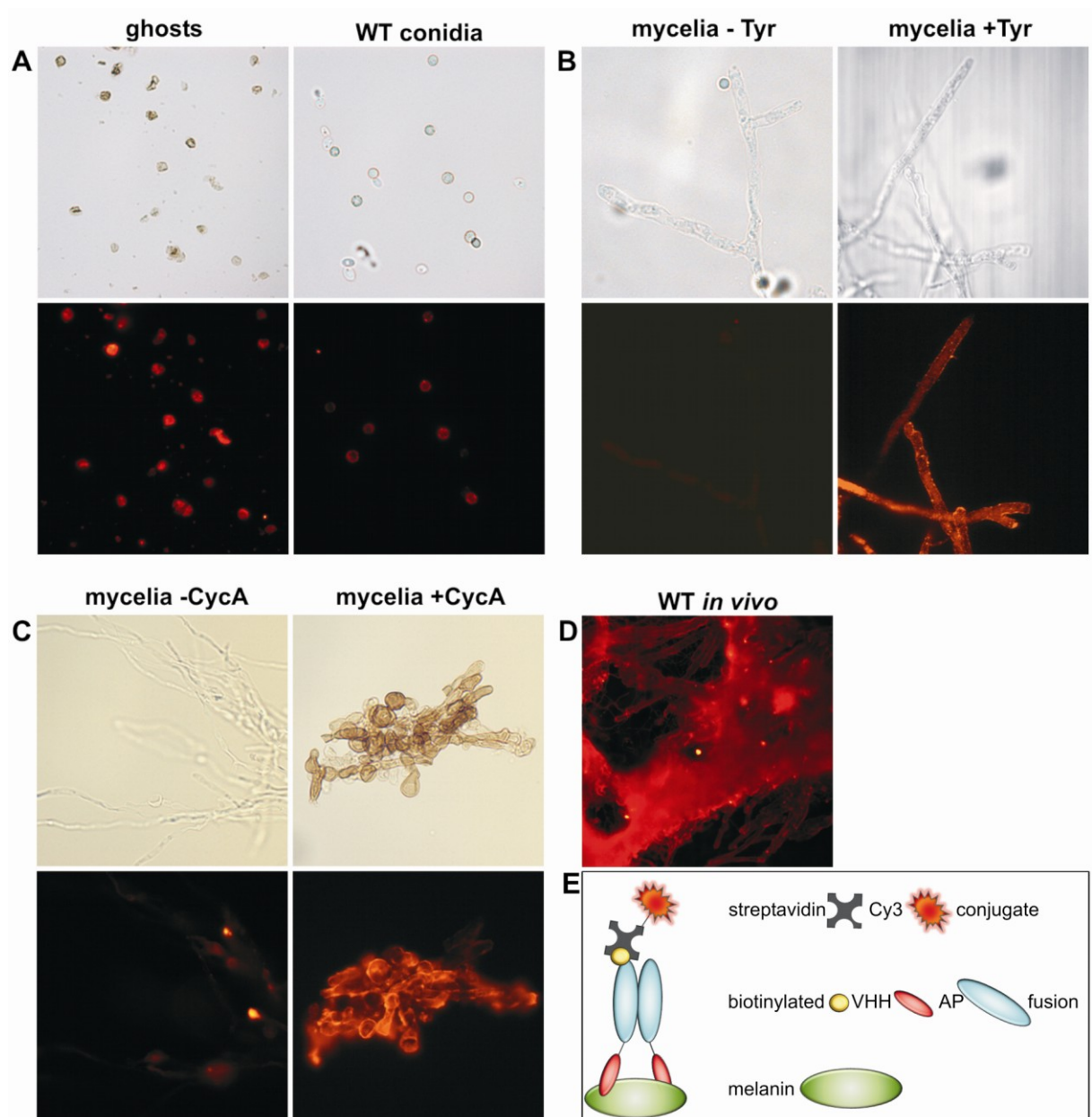


Fig. 9. Immunofluorescence for the detection of melanin with MelPhoA. The biotinylated antibody was detected via a Streptavidin-Cy3 conjugate in all of the experiments presented. Bright-field micrographs are placed above fluorescent micrographs for clarification. **(A)** The left panel depicts binding of MelPhoA to melanin particles isolated from *A. fumigatus* wild-type conidia and the right panel presents its binding to *A. fumigatus* wild-type conidia. **(B)** *A. fumigatus* wild-type mycelia grown in AMM with and without 10 mM L-tyrosine are compared. **(C)** Binding of MelPhoA to mycelia of *P. destructiva*. In the left panel the fungus was cultivated in potato dextrose medium and in the right panel this medium was supplemented with cyclosporine A for pigment induction. **(D)** MelPhoA was used to detect hyphae of *A. fumigatus* wild-type in the lung section of immunosuppressed mice which were infected intranasally with spores of the fungus. **(E)** The principle of detection of bound antibody is explained. The biotinylated VHH domain fused to alkaline phosphatase (AP) binds to the target and is detected microscopically via the fluorescence signal of a Streptavidin-Cy3 conjugate.

A further aim was the application of MelPhoA for the detection of a possible melanisation of hyphae grown in the lung of immunosuppressed. For this purpose, frozen

lung sections of infected tissue, which showed a severe spreading of mycelia, were examined by immunohistochemistry with MelPhoA. Micrograph D in Fig. 9 presents the binding of the biotinylated antibody to hyphae in the lung tissue. However, the tissue was also stained. Several attempts for the reduction of this background fluorescence were carried out. Auto-fluorescence was in frozen sections less prominent compared to sections from paraffin-embedded tissue. To reduce the fluorescence of the tissue due to the binding of MelPhoA several blocking agents were applied, e.g., combined blocking with BSA and milk powder, SuperBlock Blocking Buffer, Blocker™ Casein in PBS (both Pierce, USA) and Avidin/Biotin Blocking. The latter served to mask biotin binding sites probably present in the tissue. Yet, unspecific fluorescence was not excludable by this procedure. Also the inclusion of further washing steps did not provide better results. Hence, the fluorescence of the tissue was not avoidable which impeded the application of MelPhoA in tissue samples. A closer look at the binding of MelPhoA to pyomelanin is presented in section C3.5.3.

1.2.4 MelPhoA in Western blot analysis of conidia extracts

In immunofluorescence and ELISA studies with melanin particles it was shown that MelPhoA binds to melanin (C1.2.2 and C1.2.3). Still, it cannot be excluded that the antibody possesses high association rates to other targets as it also binds to tissue samples and to various conidia that are differently pigmented. Since the selection was carried out on the surface of conidia, the antibody may also be directed against proteins exposed on the conidial surface. Hence, Western blot analysis with proteins extracted from conidia was carried out for clarification. Two-dimensional gel electrophoresis was applied for the separation of proteins. This method allowed a satisfying resolution of the protein extracts and therefore a clear identification of MelPhoA targets. BSA served as blocking agent since it was employed in the selection procedure and found to be suitable in ELISA and immunofluorescence studies. The antibody was applied in concentrations of 1, 2 and 4 µg/ml. All concentrations led to the same results and only required altered incubation times for the developing of the Western blots. The alkaline phosphatase domain of the antibody provided the basis for the direct detection of the blots with a precipitating substrate. Two protein spots were clearly visible in all blots. For the identification of these proteins, the corresponding spots had to be picked from Coomassie blue stained gels. For this purpose, the developed Western blot (Fig. 10, left panel) was additionally stained with Coomassie blue (Fig. 10, middle panel). This post-staining facilitated the correct mapping of the spots identified in the Western blots to the spots in the Coomassie blue stained gels (Fig.

10, right panel). MALDI-TOF/TOF analysis of the protein spots, which have been tryptically digested, gave the same results in all three tested gels which are summarised in Table 8.

Both proteins should be intracellularly located due to their function. In addition, computational analysis with the CBS prediction servers (<http://www.cbs.dtu.dk/services/>) predicted no transmembrane helices and no signal peptides. Therefore, both proteins should not be exposed on the surface during antibody selection.

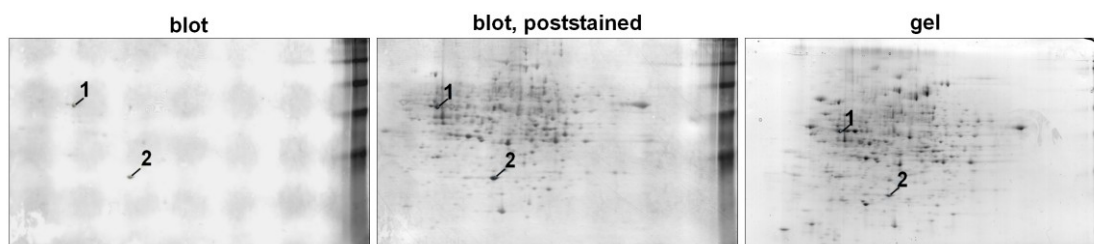


Fig. 10. Target identification of MelPhoA by 2-D gel electrophoresis of conidial protein extracts. The left panel depicts a Western blot of a whole protein extract of *A. fumigatus* ATCC46645 conidia developed with MelPhoA. In the middle panel the Western blot has been additionally stained with Coomassie blue. The Coomassie stained gel provided the material for protein identification and is presented in the right panel.

Table 8. Proteins identified in Western blot analysis with MelPhoA after 2-D gel electrophoresis of conidial extracts.

spot no. ^a	Protein name and locus tag	Sequence coverage (%)	Mascot Score ^b	Protein MW (kDa)	Accession number
1	mitochondrial processing peptidase β subunit; AFUA_1g14200	46.6	139	53.2	gi:70996070
2	sorbitol/xylulose reductase Sou1-like AFUA_2g15430	77.4	155	28.2	gi:71002394

^a spot number according to Fig. 10

^b Mascot score represents the probability that the observed match is a random event. Only protein scores with $p \leq 0.05$ were considered to be significant.

2 The DHN-melanin mutant strain $\Delta arp2$

2.1 Arp2 and DHN-melanin biosynthesis - database search and literature study

The Arp2 enzyme is involved in the pigment biosynthesis based on the polyketide DHN. Its systematic gene identifier (Gene ID) has been assigned to AFUA_2G17560. It is located on chromosome two in the DHN-melanin biosynthesis cluster between the hydrolase *ayg1* and the scytalone dehydratase gene *arp1*. *Arp2* contains no introns and is encoded by 822 nucleotides which are transcribed and translated into a protein of 273 amino acids with a molecular mass of 28.8 kDa. The protein belongs to the short chain dehydrogenase/

reductase family and catalyses the reduction of 1,3,6,8-tetrahydroxynaphthalene to scytalone. Putative homologs in other fungi are summarised in Table 9. Results were obtained after the NCBI Blast search (blastp, Blossum62 matrix) and the search with the help of the Sybil Comparative Database. *A. fumigatus* AFU293 genome, *A. nidulans* FGSC A4 genome, *A. terreus* NIH 2624 strain, *A. clavatus* NRRL 1 genome, *A. oryzae* RIB40 strain, *A. flavus* NRRL 3357 strain and *Neosartorya fischeri* NRRL 181 genome provided the sequences for this analysis. Only the genomes of the fungi *A. clavatus* and *N. fischeri*, which are closely related to *A. fumigatus* and rarely pathogenic, encode an Arp2 enzyme with apparently corresponding activity to the *A. fumigatus* enzyme due to its integration in a DHN-cluster.

Table 9. Putative homologs of *arp2* in fungi closely related to *A. fumigatus*.

Organism	Gene ID	Number of aa ^a	Identity	Gene location ^b	Score ^c
<i>A. nidulans</i>	AN0146.4	265	133/260	encoded next to <i>arp1</i> in an incomplete DHN-cluster	249
<i>A. niger</i>	An07g01830	266	104/262	no DHN-cluster	160
<i>N. fischeri</i>	NFIA_092980	276	254/276	between <i>arp1</i> and <i>ayg1</i> in the DHN-cluster	478
<i>A. clavatus</i>	ACLA_076470	264	218/257	between <i>arp1</i> and <i>ayg1</i> in the DHN-cluster	424
<i>A. terreus</i>	ATEG_06232	284	110/250	no DHN-cluster	180
	ATEG_03632	245	95/250		167
<i>A. oryzae</i>	A0090026000019	500	129/249	no DHN-cluster	242
<i>A. flavus</i>	AAS90030.1	262	129/249	dehydrogenase Ver1 in the aflatoxin biosynthesis cluster	243

^a number of amino acids (aa)

^b the integration into a DHN-cluster was screened with Sybil comparative analysis system

^c the higher the score the better the fit

Neither the gene nor the protein has been characterised experimentally in any of the mentioned fungi. However, *arp2* has been partially examined in *A. fumigatus* (Tsai *et al.*, 1999). The gene was designated as *arp2* for *Aspergillus* reddish-pink because of the reddish-pink coloured conidia of the disruption mutant. The Arp2 protein was identified as hydroxynaphthalene reductase since the disruption mutant accumulated flaviolin and revealed a similar phenotype to the *arp1* disruptant and to cultures treated with the fungicide tricyclazole. This compound inhibits hydroxynaphthalene reductases involved in DHN-melanin biosynthesis in dark fungi specifically (reviewed in Wheeler & Bell, 1988). Furthermore, the *arp1* disruption resulted in the production of reddish-pink conidia as the *arp2* disruption strain. Both transcripts were detected in the conidiation state and the corresponding proteins revealed hydroxynaphthalene reductase activity. The genes were

divergently transcribed and preliminary studies in the murine model of invasive aspergillosis showed a reduced virulence of the *arp1* but not of the *arp2* disruption strain (data were only mentioned in (Tsai *et al.*, 1999). Furthermore, *arp1* disruptants revealed an increased binding of the human complement component C3, an important process for the phagocytosis of inhaled conidia (Tsai *et al.*, 1997). However, local alignment of Arp1 and Arp2 protein sequences does not indicate a high similarity between both (score 46).

2.2 Generation of the *arp2* deletion strain and reintegration of the gene

The first approach to generate an *arp2* deletion mutant was based on the reintegration of the *pyrG* gene, encoding orotidine 5'-monophosphate decarboxylase, into a *pyrG* deficient strain (Weidner *et al.*, 1998). This enzyme catalyses the decarboxylation of orotidine monophosphate to uridine monophosphate and is therefore essential for the growth on substrates lacking uridine or uracil. The exchange of the *arp2* gene by *pyrG* in the *arp2* gene locus by homologous recombination caused a reduced radial colony growth on media without uridine or uracil. The supplementation of these compounds repaired the growth deficiency. Consequently, this deletion strategy was not applicable for the deletion of the *arp2* gene. The phenotype of the mutant did not arise from the *arp2* deletion exclusively; it was also caused by the reduced activity of the 5'-monophosphate decarboxylase. For this reason, the *E. coli* hygromycin B phosphotransferase gene (*hph*) was used as a dominant selection marker in a second approach (Punt & van den Hondel, 1992). Hph protein leads to hygromycin B resistance of the transformed strain.

To construct the *arp2* mutant strain, the entire locus of *arp2* (822 bp) was replaced by a disruption cassette containing the *hph* gene. For the construction of the *arp2* knock-out plasmid, the *arp2* gene, including 1.2 kb upstream and downstream flanking regions, was amplified from wild-type genomic DNA by PCR using oligonucleotides *arp2_flank_for* and *arp2_flank_rev*. The 5' and 3' flanking sequence of *arp2* were included to allow homologous recombination. The 3302-bp PCR product was cloned into plasmid pCR2.1 (Invitrogen, Germany) obtaining pCR2.1*arp2*. After the digestion with *EcoRI*, the 3318-bp product was isolated and ligated into the single *EcoRI* restriction site of plasmid pUC18 (Fermentas, Germany). The resulting plasmid, pUC18*arp2*, was used as the template for an inverse PCR, employing the oligonucleotides *arp2_flank_NotI_rev* and *arp2_flank_NotI_for*, both containing a *NotI* restriction site. Ligation of the PCR fragment which was digested with *NotI* resulted in the generation of plasmid pUC18 Δ *arp2*. The *E. coli hph* gene under the control of the *gpdA* promoter from *A. nidulans* served as dominant selection marker. Therefore, plasmid *coaT_hph_pCR2.1* (gift from C. Fleck) was digested with *NotI* and the *hph* cassette

was ligated into the *NotI* site of pUC18 Δ *arp2* to generate plasmid pUC18 Δ *arp2hph*. For the amplification of the Δ *arp2hph* sequence, oligonucleotides *arp2_flank_for* and *arp2_flank_rev* were applied. The Δ *arp2* strain was gained after transformation of *A. fumigatus* ATCC46645 with the DNA fragment obtained before.

The complementation resulted from the ectopic integration of the *arp2* wild-type gene and the dominant selection marker *ptrA* from *A. oryzae*. *PtrA* activity confers pyrithiamine resistance (Kubodera *et al.*, 2002). For this purpose, plasmid pSK275 (gift from S. Krappmann) was digested with *SpeI* and *HindIII*. The *ptrA* cassette under the control of the native promoter was ligated into plasmid pCR2.1*arp2* after digestion with *SpeI* and *HindIII*. The obtained plasmid, pCR2.1*arp2^c*, was applied for the transformation of the Δ *arp2* strain to gain the complemented strain *arp2^c*.

Transformants with reddish-pink conidia were checked in Southern blot analysis for the correct integration of the DNA fragments after digestion of the genomic DNA with *ApaLI* restriction endonuclease (Fig. 11A). A digoxigenin-labelled probe binding to the upstream region was amplified from plasmid pCR2.1*arp2* with oligonucleotides *arp2_probe_for* and *arp2_probe_rev* for the detection. The Southern blot analysis revealed the correct integration of *hph* in the locus of *arp2* after homologous recombination (Fig. 11A). The wild-type band at 2692 bp was replaced by a hybridisation signal at 3303 bp which was expected for the deletion strain. The complemented strain *arp2^c* showed an additional band which derived from the ectopic integration of the *arp2* wild-type gene as fusion to the dominant selection marker *ptrA*.

2.3 Characterisation of growth and surface of the *arp2* mutant strain

Conidia of the *arp2* deletion strain produced a reddish-pink pigment. The typical grey-green colour of the wild-type strain was lost, regardless of the applied medium. However, the colour of wild-type conidia was regained in the *arp2^c* mutant (Fig. 11B). This is the only but characteristic difference in the colony morphology and growth behaviour of the Δ *arp2* strain compared to wild-type and complemented strain. For example, radial colony growth rates on AMM and malt extract agar were comparable (Table 10). The phenotypic characteristics of *arp2^c* proved that the deletion of *arp2* was a direct effect of the loss of functional Arp2 protein.

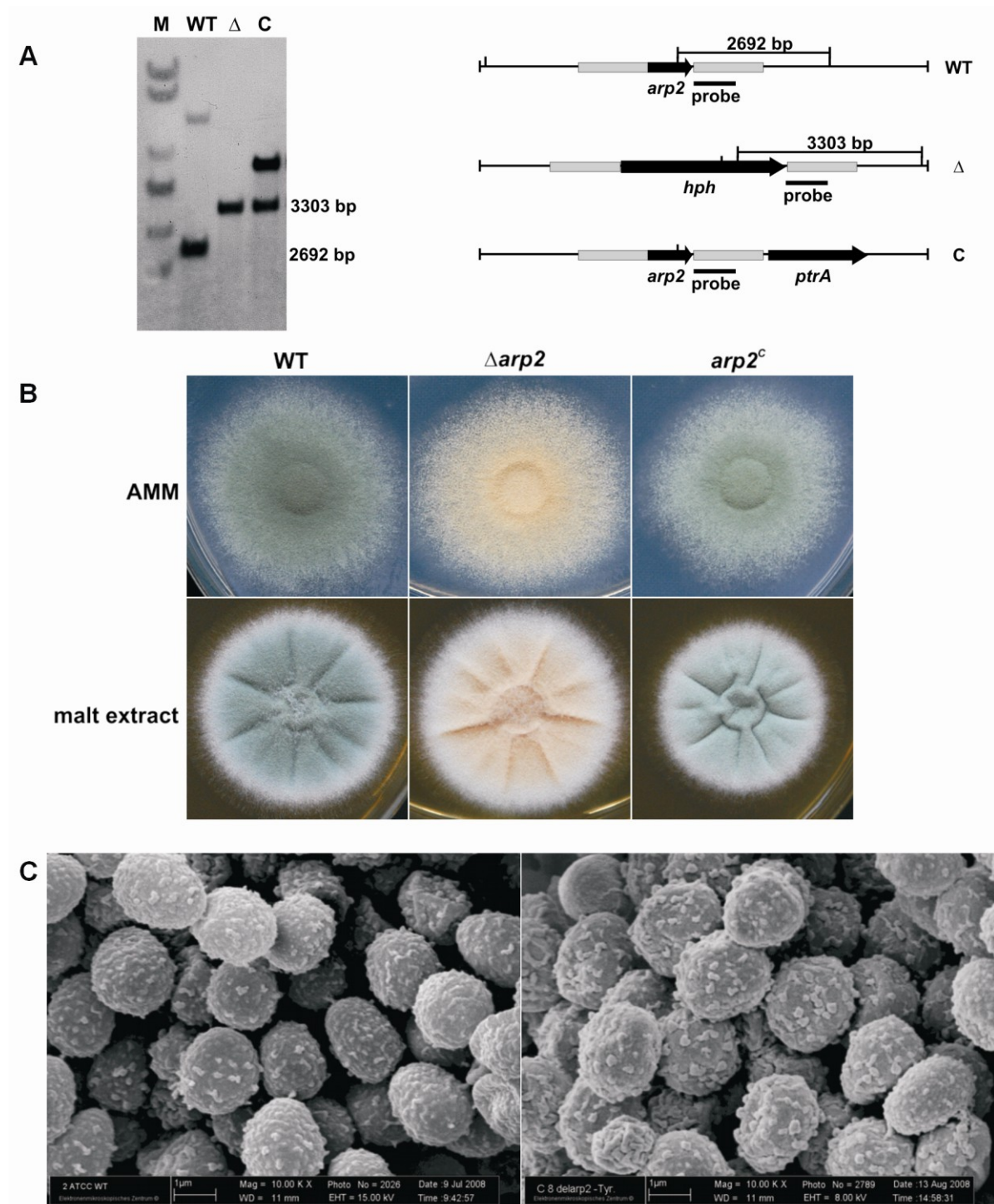


Fig. 11. Characterisation of the *arp2* deletion and the corresponding complemented strain. *arp2* deletion (Δ *arp2*, Δ) and complemented strain (*arp2*^c, C) were compared to ATCC46645 wild type (WT). **(A)** Strategy for the generation of Δ *arp2* and *arp2*^c mutants and corresponding Southern blot analysis. M depicts Hypperladder I in the Southern blot. Grey bars reflect the flanking regions of *arp2* which were used to allow homologous recombination. Vertical bars indicate *Apa*LI restriction sites. The complemented strain contains the deletion locus as well as the complementation fragment explaining the appearance of two bands in the Southern blot. **(B)** Culture morphology after growth on AMM agar and malt extract agar plates. 2.5 μ l of 1×10^6 conidia/ml suspensions of ATCC46645 wild-type strain (WT), Δ *arp2* and *arp2*^c mutant strains were inoculated at 37 °C on AMM containing 50 mM glucose as carbon source for 72 h and on malt extract agar for 48 h. **(C)** Electron scanning micrographs of conidia of ATCC46645 wild-type strain are presented in the left panel and conidia of the Δ *arp2* mutant strain in the right panel.

Although the differences in the conidial colour were obvious, the surface structure was hardly affected by the deletion of the reductase. Scanning electron microscopy revealed a rough surface of conidia of the wild-type as well as of the deletion strain (Fig. 11C). Both exhibited numerous spherical-like depositions above an ornamented surface. However, the ornamentation was slightly smoother in the $\Delta arp2$ strain compared to the wild type. The wild type resembled the results reported before (Jahn *et al.*, 1997; Sugareva *et al.*, 2006).

Table 10. Radial growth rates of the $\Delta arp2$ strain. Growth rates are compared to ATCC46645 wild type and $arp2^c$ strain on AMM and malt extract agar plates.

strain	growth rate on AMM (mm/d)		growth rate on malt extract (mm/d)	
	mean	SD	mean	SD
ATCC46645	16.8	0.5	21.6	0.7
$\Delta arp2$	16.6	0.7	21.8	0.7
$arp2^c$	16.8	0.7	21.8	0.2

2.4 Susceptibility of the $arp2$ mutant strains to ROI

The DHN-melanin free mutant $pksP$ exhibits increased sensitivity to hydrogen peroxide (Langfelder *et al.*, 1998). Although the $\Delta arp2$ mutant conidia are not pigmentless, their pinkish pigment is clearly distinguishable from the grey-green DHN-melanin in wild-type conidia. Hence, the question arose whether this modified pigment scavenges ROI as efficiently as DHN-melanin.

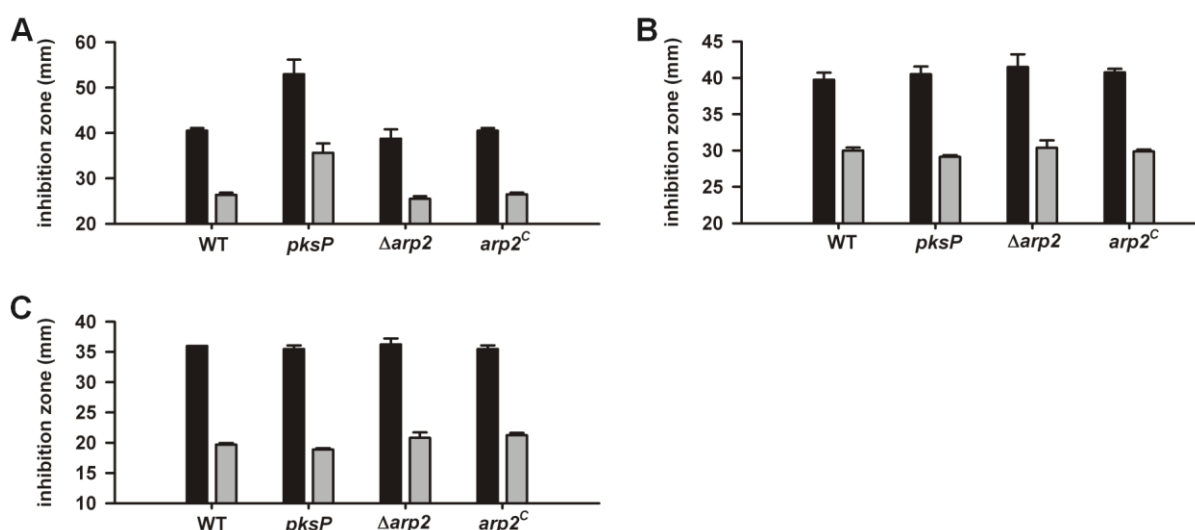


Fig. 12. Susceptibility of $arp2$ mutant strains to H₂O₂, diamide and menadione. AMM with 10 mM L-tyrosine was applied in all experiments to induce pyomelanin formation (see section C3.4) $\Delta arp2$, the corresponding complemented strain $arp2^c$ and wild-type WT (ATCC46645) were compared to the $pksP$ mutant. Each figure depicts means and standard deviations (error bars) of the diameter of the inhibition zones. Black bars represent the result for the direct confrontation assay with conidia and grey bars were obtained with germinated conidia. **(A)** H₂O₂ confrontation assay is shown. In **(B)** diamide is the stress inducing agent and **(C)** shows the impact of menadione on growth.

For this purpose, the $\Delta arp2$ strain was compared to the wild type, its complemented strain and the *pksP* mutant strain in a plate diffusion assay. Conidia as well as germinated conidia were confronted with concentration gradients of H_2O_2 , diamide or menadione as shown in Fig. 12. The reddish-pink pigment exposed by the Arp deficient strain seemed to protect the conidia as efficiently as DHN-melanin.

2.5 Contribution to virulence in a murine model of invasive aspergillosis

To assess a possible role of Arp2 in pathogenesis, the deletion strain and the complemented mutant were tested in the low dose murine model of invasive aspergillosis. Groups of 10 mice, which were immunosuppressed with cyclophosphamide and cortisone acetate, were intranasally infected with wild-type, $\Delta arp2$ or *arp2^c* conidia. A control group of ten further animals remained uninfected to monitor the influence of the immunosuppression on survival. As illustrated in Fig. 13 all strains led to a similar lethality. The statistical evaluation confirmed this conclusion. The Logrank test (Mantel, 1966) after Kaplan-Meier analysis revealed no significant difference (on the significance level 0.05) in survival between wild type and deletant ($p=0.898$) and deletant and complemented strain ($p=0.578$). Thus, Arp2 does not contribute to virulence in the low dose mouse infection model, contrary to the *pksP* mutant strain (Jahn *et al.*, 1997).

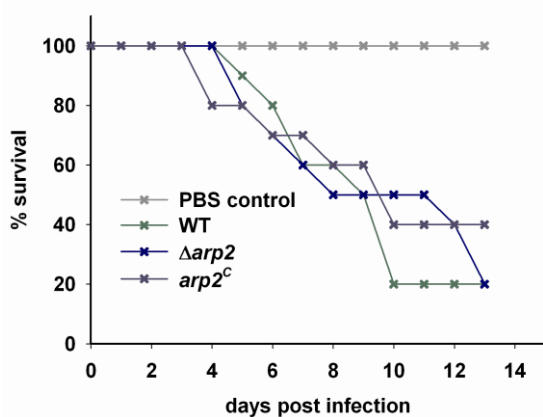


Fig. 13. Virulence of the *arp2* mutant strains in the mouse infection model. The survival after intranasal infection with $\Delta arp2$ conidia compared to the complemented strain, WT (ATCC46645) and to the PBS control in the low dose mouse infection model for IA is depicted.

3 Pyomelanin in *A. fumigatus*

3.1 Organisation of the genes in the L-tyrosine degradation cluster

Pyomelanin is formed as polymerisation product of homogentisic acid, an intermediate of the L-tyrosine degradation pathway (Coon *et al.*, 1994). Genes involved in L-tyrosine degradation via homogentisate are clustered in the *A. fumigatus* genome as depicted in Fig. 14. As the central genes of that pathway, *hmgA*, *fahA* and *maiA*, have already been studied in *A. nidulans* (Fernández-Cañón & Peñalva, 1995a; Fernández-Cañón & Peñalva, 1995b; Fernández-Cañón & Peñalva, 1998), the gene organisation in the *A. fumigatus* genome is shown in comparison to the cluster in *A. nidulans*. In addition to these genes with enzymatic function, further genes might attribute to tyrosine degradation due to their immediate vicinity on the chromosome. A fungal specific Zn(II)2Cys6 transcription factor borders the cluster in both species and thus might be involved in the regulation of homogentisic acid formation and tyrosine degradation. A protein of unknown function and without any predicted domains lies next to *hmgA* and *hppD*. Therefore, the organisation of the genes involved in L-tyrosine degradation resembles each other in both species. The only obvious difference is the existence of an additional protein in the *A. nidulans* cluster which is apparently missing in the *A. fumigatus* genome.

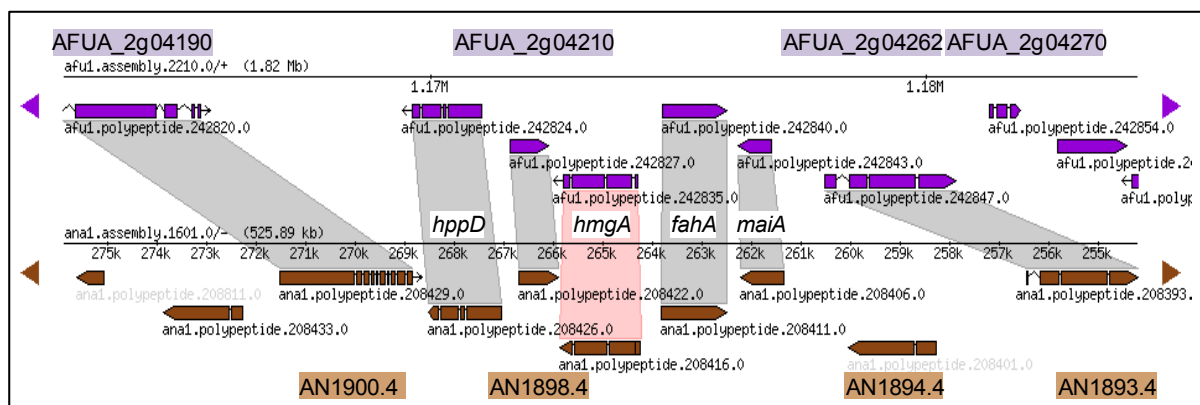


Fig. 14. Organisation of the genes in the tyrosine degradation cluster. *A. fumigatus* genes are drawn in violet and the genes with a brown background depict homologous genes in *A. nidulans*. The function of the genes with white background has already been proven in *A. nidulans*. The grey shadows connect homologous genes. The figure was obtained from <http://www.tigr.org/tigr-scripts/sybil-asp/sybilHome.pl?db=asp> and modified (compare Table 11).

The characteristics of the genes which are probably involved in homogentisic acid synthesis due to their predicted function and their location are summarised in Table 11. The adjacent genes on both sides of the probable cluster are listed as well. It is conceivable that

the phenotypes of deletion mutants in *A. fumigatus* resemble that of the deletion mutants in *A. nidulans* since the identity of the amino acids of the predicted proteins lies between 70 % and 88.7 %. Hence, *hmgA* and *hppD* seem to be suitable targets to study pyomelanin biosynthesis in *A. fumigatus*. Homogentisic acid and consequently pyomelanin should be absent in an *hppD* deletion mutant and accumulate in the *hmgA* deletion strain. This was already concluded in the thesis of V. Sugareva (Sugareva, 2006). However, the strains exhibited severe growth defects probably due to the *pyrG* selection system which impeded a reliable characterisation of the strains.

Table 11. Comparison of the *A. fumigatus* homogentisate cluster with that in the *A. nidulans* genome.

Gene ID	Function	Transcript length (bp)	Number of introns	GC content	Number of aa	Identity
AFUA_2g04190	conserved hypothetical protein	2118	4	50 %	705	39.3 %
AN1900.4		2235	9	50 %	698	
AFUA_2g04200	<i>p</i> -hydroxyphenylpyruvate dioxygenase (HppD)	1212	3	53 %	403	85.6 %
AN1899.4		1322	3	48 %	401	
AFUA_2g04210	conserved hypothetical protein	771	0	56 %	256	60.7 %
AN1898.4		808	0	51 %	252	
AFUA_2g04220	homogentisate 1,2 dioxygenase (HmgA)	1350	3	53 %	449	88.7 %
AN1897.4		1506	3	51 %	448	
AFUA_2g04230	fumarylacetoacetate hydrolase (FahA)	1296	0	56 %	431	86.8 %
AN1896.4		1343	0	53 %	431	
AFUA_2g04240	maleylacetoacetate isomerase (MaiA)	696	0	58 %	231	70 %
AN1895.4		865	0	52 %	230	
AN1894.4	conserved hypothetical protein	1722	1	54 %	503	
AFUA_2g04262	putative Zn(II)2Cys6 transcription factor	2247	3	51 %	748	64.5 %
AN1893.4		2328	3	50 %	775	
AFUA_2g04270	mitochondrial inner membrane translocase subunit (TIM17)	465	2	54 %	154	85.5 %
AN1892.4		1115	3	49 %	153	
AN11319.4	hypothetical protein	159	2	52 %	52	

3.2 Generation of $\Delta hmgA$, $\Delta hppD$ and *pksP* $\Delta hppD$ mutant strains

Genomic DNA from *A. fumigatus* wild type was used as the template for the amplifications of the wild-type genes. DNA fragments were amplified with Phusion™ High-Fidelity DNA Polymerase (Finnzymes, Finland). To construct the *hmgA* knock-out plasmid,

the *hmgA* gene including 1.2 kb upstream and downstream flanking regions was amplified by PCR using oligonucleotides HmgAXbaI_for and HmgAXbaI_rev, introducing *XbaI* restriction sites. The PCR product was cloned into plasmid pCR2.1, yielding plasmid pCR2.1*hmgA*. After digestion with *XbaI*, the 3867-bp product was isolated and ligated into the single *XbaI* restriction site of plasmid pUC18. The resulting plasmid, pUC18*hmgA*, was used as the template for an inverse PCR, employing the primers HmgASfiI_up and HmgASfiI_down, both containing an *SfiI* restriction site. Ligation of the *SfiI*-digested PCR fragment resulted in generation of plasmid pUC Δ *hmgA*. The pyrithiamine resistance gene (*ptrA*) from plasmid pSK275, conferring pyrithiamine resistance, was inserted into the *SfiI* restriction site to yield pUC18 Δ *hmgAptrA*. Finally, the Δ *hmgAptrA* sequence was amplified by PCR using oligonucleotides HmgAXbaI_for and HmgAXbaI_rev. The obtained product was used for transformation of *A. fumigatus*.

For deletion of the *hppD* gene, plasmid pCR2.1 Δ *hppDptrA* was generated. The *hppD* gene, including upstream and downstream flanking regions, was amplified from *A. fumigatus* genomic DNA using the oligonucleotides HppD_for and HppD_rev. The resulting 3660-bp DNA fragment was cloned into plasmid pCR2.1 to obtain pCR2.1*hppD*. This plasmid was used as the template for the amplification with oligonucleotides HppD_Sfi_up and HppD_Sfi_down to modify the ends of the flanking regions with *SfiI* restriction sites and to remove the *hppD* coding sequence. After *SfiI* digestion of the PCR product, the *ptrA* gene was inserted as *SfiI* fragment to give plasmid pCR2.1 Δ *hppDptrA*. Finally, a PCR was performed employing pCR2.1 Δ *hppDptrA* as the template and oligonucleotides HppD_for and HppD_rev. The resulting fragment, containing the *ptrA* gene flanked by *hppD* upstream and downstream regions, was used for transformation of *A. fumigatus* CEA17 Δ *akuB^{KU80}* to gain the Δ *hppD* strain. *A. fumigatus pksP* mutant strain was used in the transformation to generate the *pksP* Δ *hppD* mutant. The deletion strategy and Southern blot analysis of the obtained strains are summarised in Fig. 15.

3.3 Complementation of Δ *hmgA*, Δ *hppD* and *pksP* Δ *hppD* mutant strains

Strains Δ *hmgA*, Δ *hppD* and *pksP* Δ *hppD* were complemented at the original gene locus by the use of modified wild-type genes. A dominant selection marker was not required since the deletion mutants did not sporulate on AMM agar plates when L-tyrosine or phenylalanine was used as the sole carbon source. To distinguish between wild-type and complemented strains by Southern blot analysis, the nucleotide sequences of *hppD* and *hmgA* were slightly modified without affecting the protein sequence.

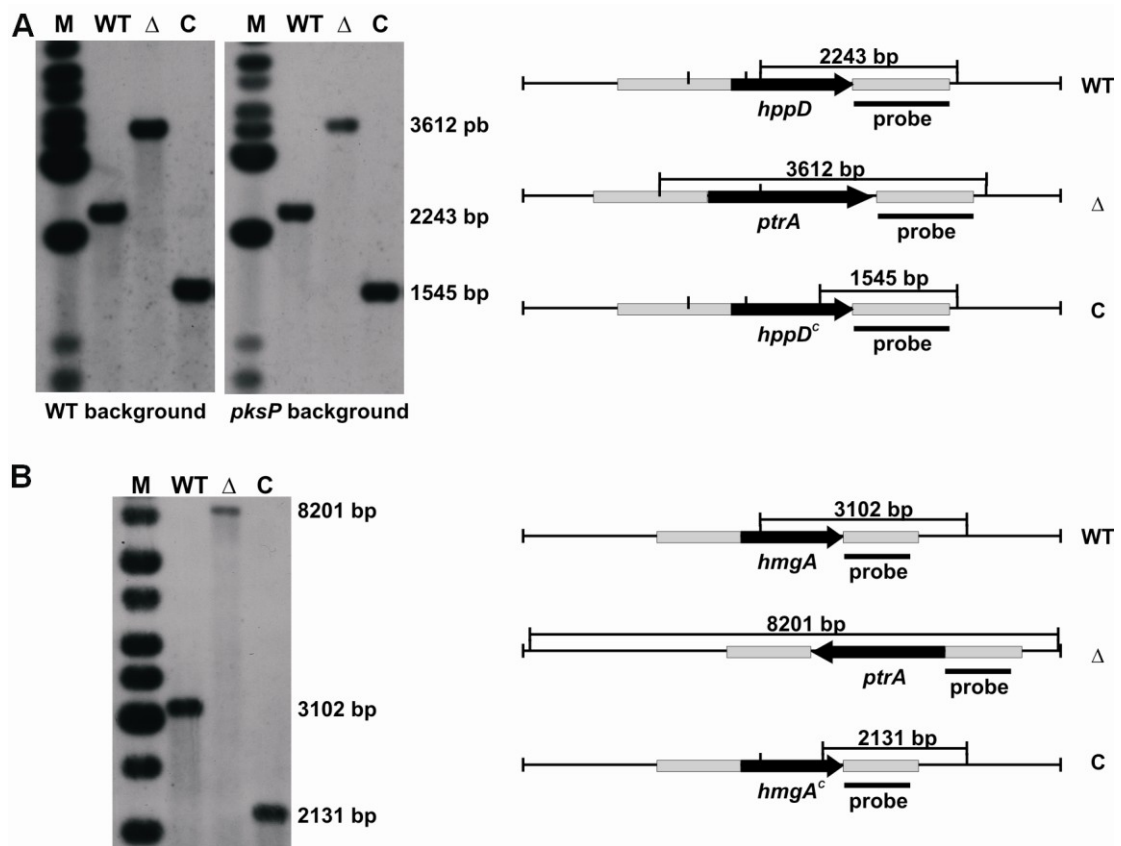


Fig. 15. Deletion and complementation strategy of *hppD* and *hmgA* genes and corresponding Southern blot analysis. (A) The schematic representation of the chromosomal *hppD* locus in the wild type (WT), the *hppD* deletion mutant (Δ) and the complemented (C) strain is illustrated in the right panel. Southern blot analysis proves the deletion of the *hppD* gene in CEA17 Δ *akuB^{KU80}* and *pksP* mutant background. The reintroduction of the point-mutated *hppD* gene containing an additional *XhoI* restriction site is shown in the right lanes. M denotes the lane with the Gene Ruler 1-kb DNA ladder (Fermentas, Germany). (B) The schematic representation of the chromosomal *hmgA* locus in the WT, the *hmgA* deletion mutant (Δ), and the complemented (C) strain is displayed in the right panel. Southern blot analysis verified the deletion of the *hmgA* gene and the reintroduction of the point-mutated *hmgA* gene with an extra *FspI* site. Lane M depicts HyperLadder I (Bioline GmbH, Germany). Restriction endonuclease cleavage sites, the DNA fragments identified by Southern blot analysis and the positions to which the probe hybridises are indicated.

To complement the Δ *hmgA* mutant with the *hmgA* sequence, plasmid pUChmgA^c was generated. In this plasmid, an additional *FspI* restriction site was introduced into the *hmgA* gene by mutagenesis PCR by employing the FlipFlop Site-Directed Mutagenesis Kit (Bioline, Germany) with the help of oligonucleotides hmgA_FspI_for and hmgA_FspI_rev. For transformation of *A. fumigatus* Δ *hmgA* strain, a PCR fragment was generated, using pUChmgA^c as the template and oligonucleotides HmgAXbaI_for and HmgAXbaI_rev. To complement the deletion of the Δ *hppD* and *pksP* Δ *hppD* strains, plasmid pCR2.1*hppD^c* was generated. In this plasmid, an additional *XhoI* restriction site was introduced into the *hppD* sequence by employing the FlipFlop Site-Directed Mutagenesis Kit and oligonucleotides HppD*_C_rev and HppD*_C_for. The *A. fumigatus* Δ *hppD* and *pksP* Δ *hppD* strains were

transformed with a DNA fragment obtained by PCR with pCR2.1*hppD^C* as the template and oligonucleotides HppD_rev and HppD_for. The complemented strains were designated as *hppD^C* and *pksPΔhppD^C*, respectively. The successful reintegration of the modified wild-type genes is depicted in Fig. 15.

3.4 Pigment production and growth of pyomelanin mutant strains

3.4.1 Pigmentation of mycelia, conidia and media

The influence of L-tyrosine addition on colouration of conidia, mycelia and media was investigated for the deletion mutants compared to wild-type and complemented strains (Fig. 16A, B, C). The addition of 10 mM L-tyrosine to AMM liquid cultures stained mycelia of wild-type strains, *ΔhmgA*, *pksP* mutant and the complemented strains *hppD^C*, *hmgA^C* and *pksPhppD^C* brown. The *ΔhmgA* strain was clearly darker pigmented compared to the other strains. On the contrary, the loss of a functional HppD enzyme completely abolished pigment formation in mycelia. This was true for the deletion of *hppD* in *pksP* mutant as well as in the wild-type background, whereas a missing PksP did not influence the degree of pigmentation of the mycelia (Fig. 16B). The pigment release into the medium correlated in all strains with the pigmentation of corresponding mycelia (Fig. 16A). Additionally, phenotypical divergences between deletion and wild-type strains were compensated in the complemented mutants. Monitoring the growth of strains on solid media allowed to report the pigmentation of conidia, the pigment release into the medium and the colouration of mycelia (Fig. 16C). The growth on AMM agar without additional L-tyrosine did hardly lead to phenotypical differences beside the known grey-green pigment loss of conidia of the *pksP* mutant strains. Only mycelia of the *hmgA* deletion mutant showed a slightly darker pigmentation compared to the other strains. Media were not differently stained after 72 h of growth, however prolonged incubations pointed out differences as obtained for the AMM medium with additional L-tyrosine (data not shown). Culturing on AMM agar with 10 mM L-tyrosine led to clearly distinguishable phenotypes already after 72 h of growth. Again, the *ΔhmgA* strain showed a brown colouration of mycelia as well as the release of a brown pigment into the medium. The pigmentation of the wild type and the complemented strains as well as of the *pksP* mutant strain was not as evident as in liquid cultures, but mycelia of the *hppD* deletion in the *CEA17ΔakuB^{KU80}* background as well as in the *pksP* mutant background did not reveal a brown colouration at all. The addition of tyrosine did not influence the colour of the conidia compared to the growth on media without external tyrosine.

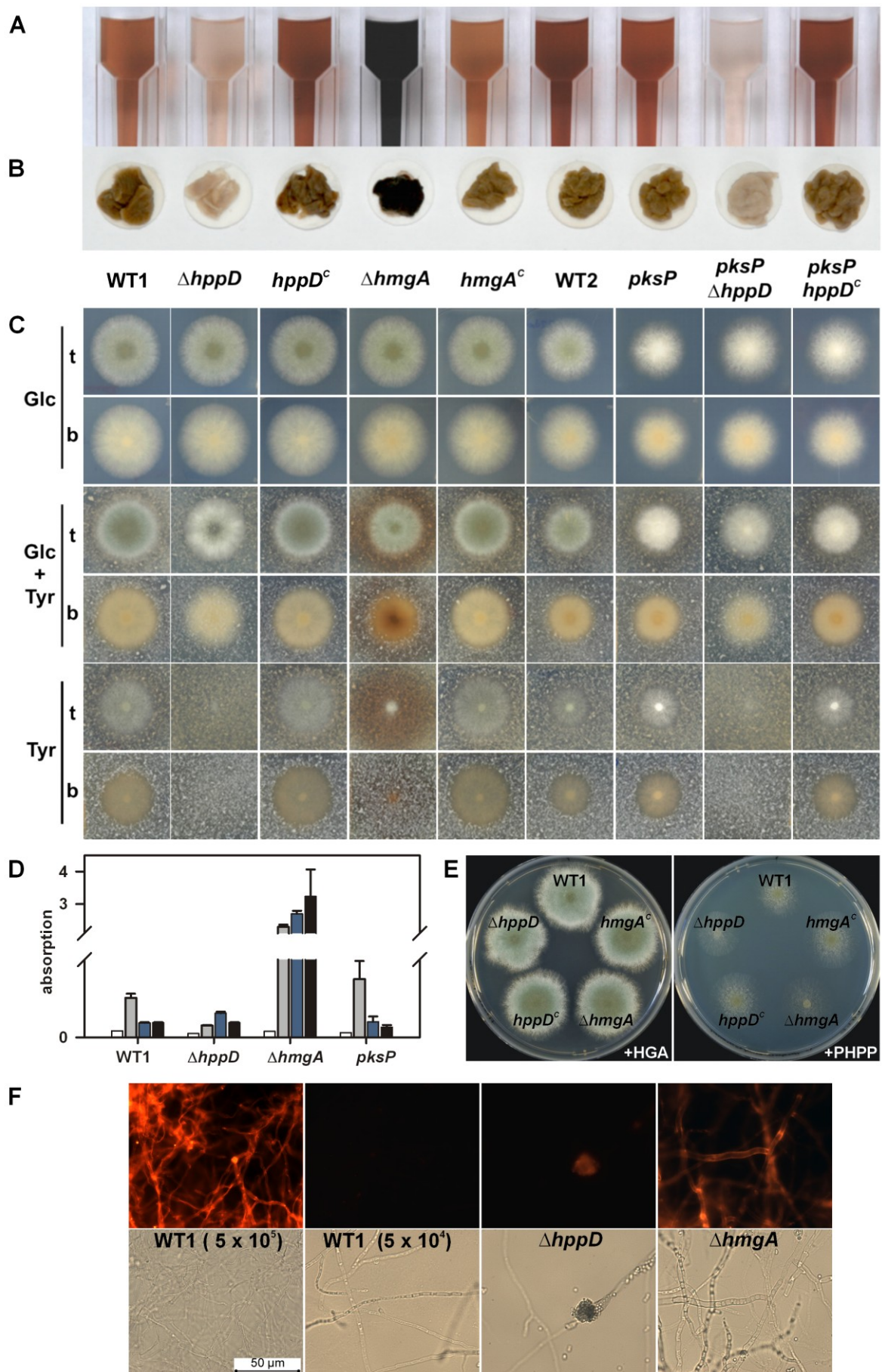


Fig. 16. Characterisation of growth and pigmentation of pyomelanin mutant strains.

Fig.16 (continued) (A) and (B) Pigment production of different wild-type strains and pyomelanin mutant strains grown in AMM with 10 mM L-tyrosine. The strains were inoculated with 5×10^7 conidia and cultivated in 50 ml AMM for 64 h. **(A)** The culture permeates are displayed. **(B)** The mycelia which were separated from media by filtration through miracloth are shown. **(C)** Growth phenotypes of the same strains on agar plates are displayed. Top (t) and bottom (b) view from colonies grown on AMM agar plates with 50 mM glucose (Glc), on AMM agar plates with 50 mM glucose and 10 mM L-tyrosine (Glc+Tyr) as well as on AMM agar plates without glucose but with 10 mM L-tyrosine as sole carbon source (Tyr) are presented. In each case, 2.5 μ l of a conidia suspension containing 1×10^6 conidia/ml were point-inoculated for 72 h at 37 °C. **(D)** Quantification of pigment production by measuring absorption at 405 nm. Wild-type, $\Delta hppD$, $\Delta hmgA$ strains as well as *pksP* mutant strain were inoculated with 1×10^5 conidia/ml for 68 h in AMM (white bar), AMM with 10 mM L-tyrosine (grey bar), AMM with 10 mM L-phenylalanine (blue bar) and AMM with 10 mM phenylacetate (black bar). Media containing the inducer but no conidia were subtracted as blank. The experiment was repeated three times in duplicate. Standard deviations were calculated from two independent experiments. **(E)** The growth on AMM agar plates supplemented with 10 mM HGA (left panel) and alternatively supplemented with 10 mM PHPP (right panel) of wild type, *hppD* and *hmgA* deletion and complemented mutants is depicted. Strains were cultivated for 68 h at 37 °C. **(F)** Wild-type strain, *hppD* and *hmgA* deletion strains were cultivated with tyrosine supplementation and the binding of biotinylated MelPhoA was microscopically detected with a Streptavidin-Cy3 conjugate. 5×10^5 or 5×10^4 conidia/ml of wild-type and 5×10^4 conidia/ml of *hppD* and *hmgA* deletion strains were inoculated in 100 μ l AMM containing 10 mM L-tyrosine for 48 h at 37 °C before the detection with MelPhoA and a Streptavidin-Cy3 conjugate according to B7.7.

Furthermore, L-tyrosine was applied as sole carbon source in AMM agar plates without glucose. Growth of both $\Delta hppD$ and $\Delta hmgA$ mutants was severely impaired. Mycelia were less dense, conidiation was strongly reduced and white, long shaped tyrosine crystals were not consumed in contrast to the observations for wild-type and complemented strains. Still, the pigment release was clearly visible in the $\Delta hmgA$ strains probably due to residual mycelial growth based on carbon sources present in the agar. The same was true for the growth on L-phenylalanine as sole carbon source (data not shown). The poor growth on L-tyrosine as sole carbon source confirms the essential role of HppD and HmgA in the recycling of that amino acid.

3.4.2 Pigmentation dependent on the nature of the inducer molecule

To analyse whether the accumulation of HGA or PHPP affects colony growth, HGA and PHPP were artificially added to the medium. As shown in Fig. 16E, the addition of HGA did not impair growth. The addition of PHPP, the accumulation product of the $\Delta hppD$ mutant, led to reduced growth and sporulation of the wild-type strain, even more so with the deletion strains. Therefore, PHPP apparently needs to be degraded for detoxification. Integration of a functional gene cured the defects of the deletion strains on all applied media, again demonstrating that the phenotypes are a direct result of the loss of HmgA and HppD activity.

A further examination of pigment release in liquid cultures (see Fig. 16D) indicated that beside tyrosine, phenylalanine and phenylacetate also triggered pigment formation. However, the presence of tyrosine resulted in the highest pigment formation in wild-type cultures which is the reason why tyrosine was used in most experiments as inducer molecule. Furthermore, when tyrosine was added to *pksP* mutant cultures the induction of pigmentation was even stronger, probably due to the ATCC background of the *pksP* mutant strain (compare Fig. 16A, B).

3.4.3 The influence of pyomelanin on the surface structure of conidia and hyphae

Cultures of the wild type and pyomelanin mutant strains depicted differently coloured mycelia, especially after addition of L-tyrosine to the media. This observation led to the question whether the pigment does deposit on the surface and whether a deposition of pyomelanin alters the structure of the surface. Scanning electron microscopy was chosen to answer this question as this method possesses potential in studying the surface morphology of conidia as shown before (Jahn *et al.*, 1997).

For the preparation of samples, colonies were grown on solid agar plates to provide conidia and hyphae simultaneously. The addition of tyrosine to cultures resulted in irregularly shaped precipitates on the surface of conidia and hyphae (Fig. 17). These depositions were present in the *hpdD* as well as in the *hmgA* deletion strain and in the wild type. Due to the absence of pyomelanin production in the pigmentless hyphae of $\Delta hpdD$ strain these depositions did not reflect the pyomelanin accumulation. It is rather conceivable, that tyrosine crystals stuck to the surface. Furthermore, $\Delta hmgA$ cultures revealed a slightly smoother surface, probably because of the consumption of tyrosine. The surface of the *pksP* mutant conidia was less ornamented than wild-type conidia as reported before (Langfelder *et al.*, 1998). However, $\Delta hpdD$ conidia also depict a rather smooth surface. This characteristic possibly depends on the ripening of the DHN-melanin pigment. $\Delta hpdD$ colonies turned later grey-green than wild-type conidia, their sporulation was slightly retarded. However, observed colonies were grown for the same period of time and thus the pigments might not have been in equal stages at the time-point of the preparation of the samples.

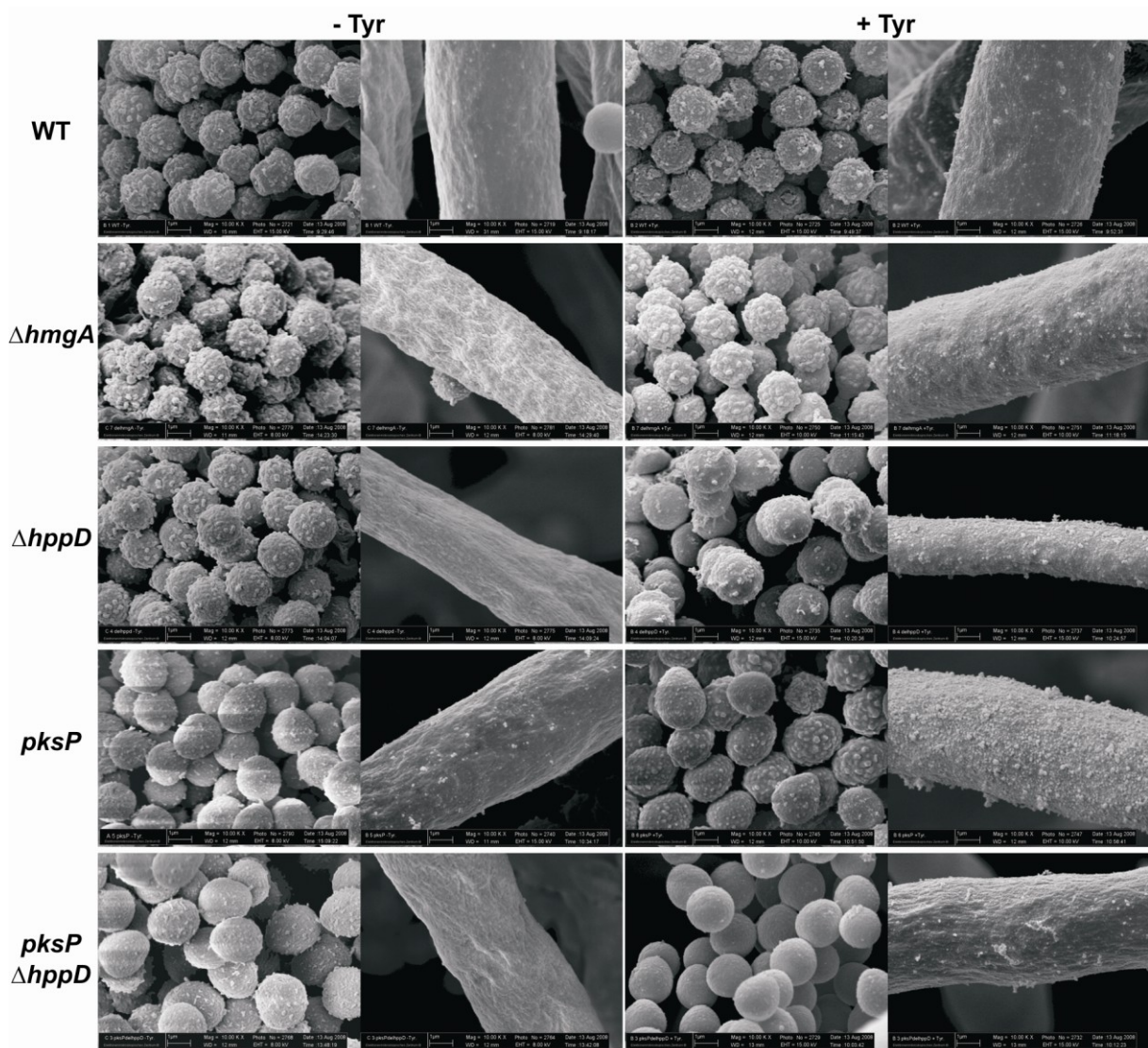


Fig. 17. Scanning electron microscopy of pyomelanin mutant strains. Wild type, $\Delta hmgA$, $\Delta hppD$, $pksP$ mutant as well as $pksP\Delta hppD$ mutant strain were grown on AMM agar plates with 20 mM glucose and with or without 10 mM L-tyrosine. Pictures were taken with a magnification of 10,000. 1st and 3rd column depict the surface of conidia and the 2nd and 4th column show the corresponding micrographs of the hyphae.

3.4.4 Radial growth of pyomelanin mutant strains

Radial diameters of colonies grown on AMM agar plates with and without tyrosine were measured to substantiate the growth phenotypes seen in Fig. 16. Furthermore, the knowledge about radial growth is a prerequisite for susceptibility studies. As summarised in Table 12, mycelia of all strains grew similarly fast on AMM agar with and without tyrosine when glucose was available. However, L-tyrosine as sole carbon source strongly impaired growth of the $hppD$ deletion mutant. Mycelia of the $hmgA$ deletion strain were only slightly reduced in their growth rate. Its hyphae, however, were clearly thinner and less dense

compared to those of the wild-type and the complemented strain. The phenotypes of the complemented strains resembled the growth of the wild type.

Table 12. Radial growth rates of pyomelanin mutant strains. *HppD* and *hmgA* deletion strains were grown in comparison to the corresponding complemented strain and to wild type. AMM agar plates with and without supplementation of 10 mM L-tyrosine as well as AMM with 10 mM L-tyrosine as sole carbon source were applied.

strain	growth rate (mm/d) on					
	glucose		glucose +tyrosine		tyrosine	
	mean ^a	SD ^b	mean	SD	mean	SD
CEA17	18.1	0.2	17.3	0.2	18.5	0.3
<i>ΔhppD</i>	17.9	0.2	16.6	0.2	10.5	0.1
<i>hppD</i>^c	17.9	0.2	16.9	0.1	17.9	0.2
<i>ΔhmgA</i>	18.0	0.1	16.4	0.2	16.6	0.1
<i>hmgA</i>^c	18.3	0.2	17.0	0.1	18.2	0.2

^a means are growth rates calculated from 8 colonies at 5 time points

^b corresponding standard deviations

3.5 Characterisation of the pigment triggered by tyrosine addition

3.5.1 FTIR analysis of natural and synthetic melanin

FTIR spectroscopy is regarded as the most informative method for structural analysis of melanins (Bilinska, 1996). Therefore, this method was applied to analyse the pigment which accumulated in cultures of *ΔhmgA* strain in AMM supplemented with L-tyrosine. This purified and lyophilised pigment was compared with the *in vitro* synthesised pigment which was obtained by alkaline polymerisation of HGA. Both pigments were investigated spectroscopically as potassium bromide disks. The overlay of the FTIR spectra of synthetic pyomelanin and pigment extracted from fungal cultures showed a high degree of similarity (Fig. 18). Both spectra depict a broad absorption at 3,420 cm⁻¹, which is due to associated or polymeric OH groups. Pyomelanin as well as residual water can cause this broad absorption at around 3,400 cm⁻¹. The stretching vibrations for aliphatic CH bonding appear at 2,952 cm⁻¹ and 2,925 cm⁻¹ for natural and synthetic melanin, respectively. At 1,586 cm⁻¹, the symmetric carboxylate stretching vibrations (COO⁻) are detectable according to the basic isolation procedure. However, residual water can cause this absorption as well. The fingerprint regions between 1,450 cm⁻¹ and 650 cm⁻¹ resemble each other closely. The high level of identity between the synthetic pyomelanin and the pigment extracted from fungal cultures indicates that the *ΔhmgA* mutant produces pyomelanin when cultivated with L-tyrosine.

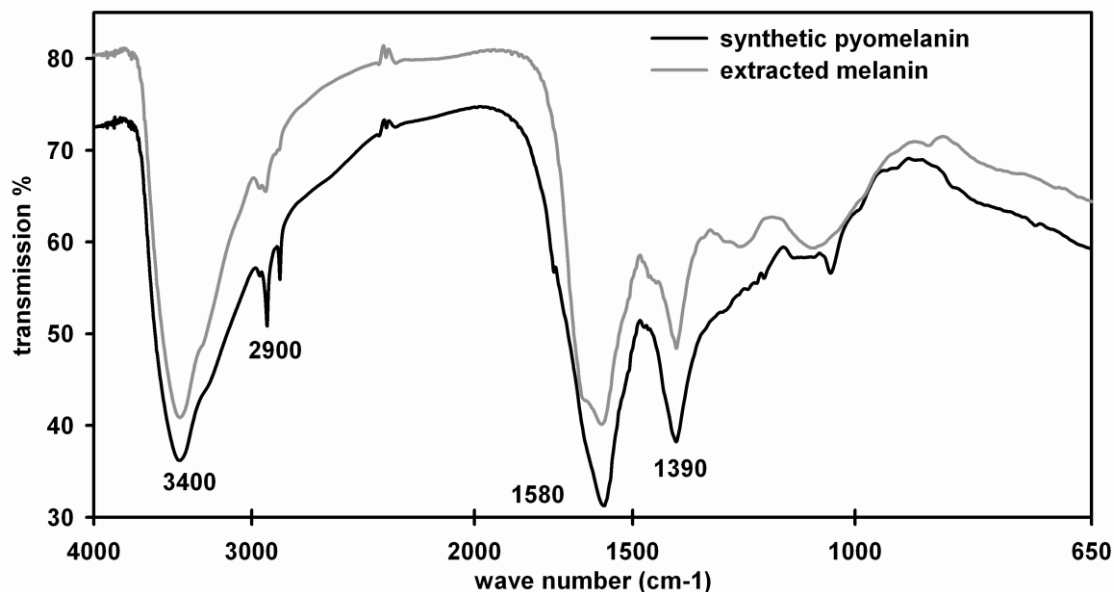


Fig. 18. FTIR analysis of pyomelanins. The overlay of FTIR spectra from melanin synthesised by alkaline polymerisation from HGA (black line) and from melanin isolated from cultures of *A. fumigatus* $\Delta hmgA$ mutant strain (grey line) is shown.

3.5.2 Pigment accumulation, tyrosine consumption and HGA synthesis

To provide evidence for pigment formation from L-tyrosine via the accumulation of HGA, tyrosine catabolism in *A. fumigatus* liquid cultures was analysed. Melanin accumulation was observed by measuring absorption at 405 nm. L-tyrosine and HGA concentrations were determined by HPLC analysis. In wild-type cultures grown without L-tyrosine, pigment accumulation and HGA formation were lacking (Fig. 19A). For wild-type and $\Delta hmgA$ AMM tyrosine cultures, the consumption of L-tyrosine and the formation of HGA were clearly visible (Fig. 19B and F). In the $\Delta hmgA$ strain, HGA concentration as well as absorption values were even higher than those of the wild type. In this mutant, HGA accumulated because of the deficiency of the strain to cleave HGA to maleylacetoacetate (Fig. 3). $\Delta hmgA$ cultures showed a decelerated decrease in L-tyrosine concentration, probably due to a feed-back inhibition via the accumulation of HGA. The analysis of wild-type cultures grown with the HppD inhibitor sulcotrione (Ellis *et al.*, 1995) led to results very similar to those for the $\Delta hppD$ mutant, i.e., HGA formation was not detected and absorption was hardly increased (Fig. 19C and D). The appropriate sulcotrione concentration was identified in a preliminary study. 50 μ M sulcotrione did not inhibit growth of the wild-type strain but prevented formation of the pigment when cultivated with 10 mM L-tyrosine (data not shown).

Additionally, glucose consumption and changes of pH values were followed. Glucose was completely exhausted after 40 to 50 h of cultivation. An increase in pH was detectable at the

same time (Fig. 19F). Therefore, the strains showed similar growth rates in liquid cultures. This was an important prerequisite since tyrosine consumption correlates with growth. Furthermore, high pH values accelerate the process of pigment formation and glucose can apparently repress tyrosine catabolism in *Yarrowia lipolytica* (Carreira *et al.*, 2001).

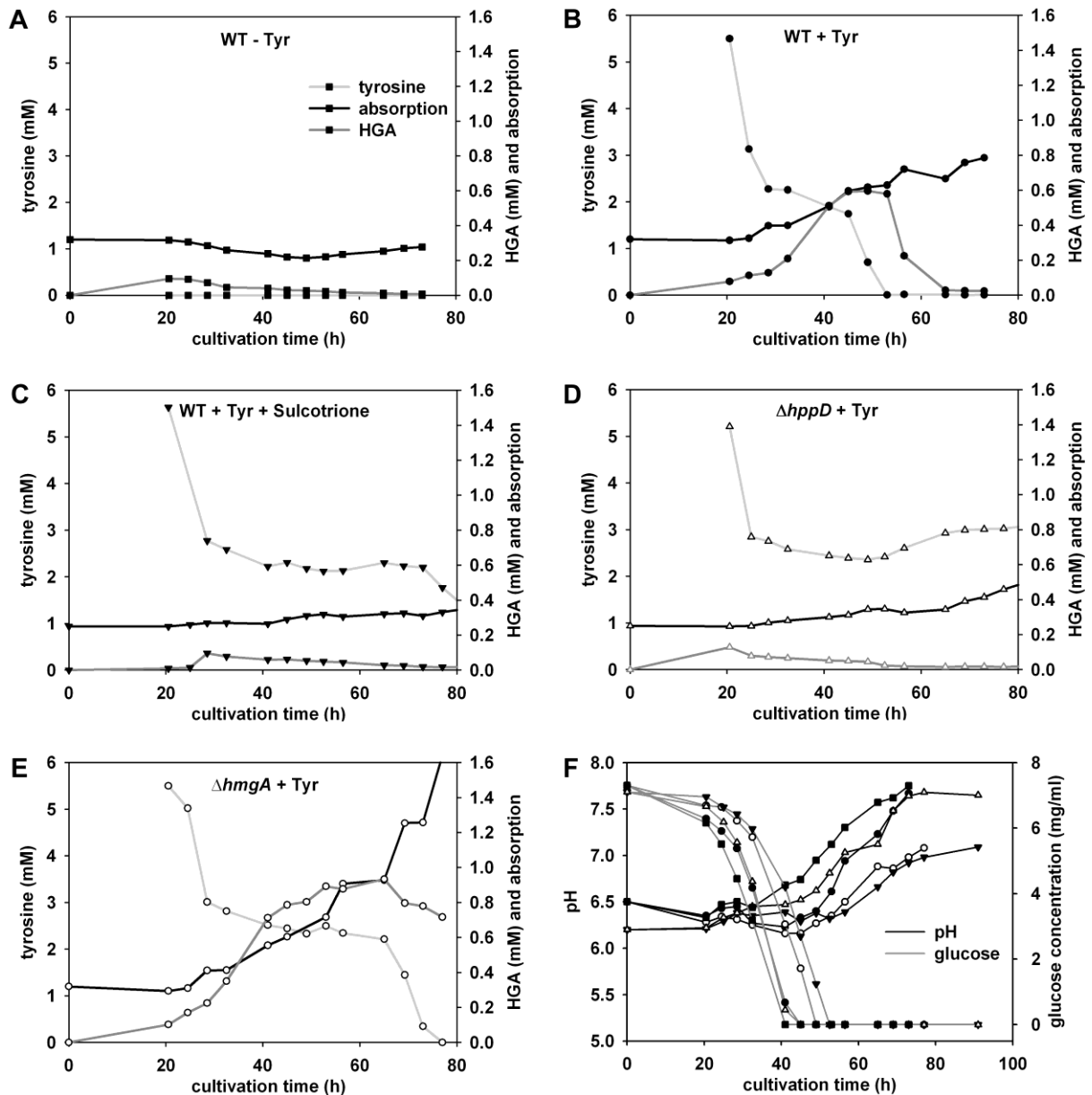


Fig. 19. Pigment formation, HGA synthesis and L-tyrosine consumption in pyomelanin mutant strains. Wild type with (C) and without (B) the HppD inhibitor sulcotrione, $\Delta hppD$ (D) and $\Delta hmgA$ (E) strains were pre-cultivated with 1×10^7 conidia in 200 ml AMM for 20 h prior the addition of L-tyrosine. Additionally, the wild type was cultivated without tyrosine for comparison (A). Pigment formation is reflected by an increase in absorbance at 405 nm (black line). HGA (dark grey line) and L-tyrosine concentrations (light grey line) were measured by HPLC. (F) Glucose consumption and pH change of the cultures mentioned above were monitored. Cultures are depicted as follows: wild type without tyrosine (black square), wild type with tyrosine (black dot), wild type with tyrosine and sulcotrione (black triangle), $\Delta hppD$ with tyrosine (white triangle) and $\Delta hmgA$ with tyrosine (white dot).

The complemented strains *hmgA^C* and *hppD^C* gave the same data as the wild-type strain (data not shown). Taken together, these experiments proved the inability of the $\Delta hmgA$ strain to degrade HGA, observable by the accumulation of HGA and by the formation of high quantities of the brown pigment. Beyond, the missing HGA detection and pigment synthesis proved the deficiency of $\Delta hppD$ strain to form HGA. Thus, it was verified that *hppd* and *hmgA* code for 4-hydroxyphenylpyruvate dioxygenase and homogentisate dioxygenase, respectively. Moreover, the data show a positive correlation between HGA accumulation and melanin formation.

3.5.3 Binding of the anti-melanin antibody to mycelia

MelPhoA, the camelid antibody generated against the conidial pigment of *A. fumigatus* (see section C1), was tested for its binding capacity to melanised and non-melanised mycelia. Melanisation was triggered by the addition of 10 mM L-tyrosine to AMM cultures. The hypermelanised $\Delta hmgA$ strain was cultivated beside wild-type and $\Delta hppD$ strain. The biotinylated MelPhoA was applied to allow the detection of melanin with a Streptavidin-Cy3 conjugate (Fig. 16F). The binding of MelPhoA to mycelia was clearly detectable in wild-type and $\Delta hmgA$ cultures. However, wild-type cultures demanded a denser inoculation compared to $\Delta hmgA$ cultures. Glucose was used up at an earlier time-point in denser inoculated cultures which resulted in a faster degradation of L-tyrosine. The antibody was not directed against mycelia of the $\Delta hppD$ strain, still a Cy3-signal appeared due to the affinity of MelPhoA to melanised conidia. Freshly formed conidiophores gave the Cy3-signal as well (compare the bright-field micrographs in the lower panel of Fig. 16F).

3.6 Regulation of the cluster

3.6.1 Transcription of *hppD* and *hmgA* dependent on the addition of tyrosine

A semiquantitative transcript analysis by reverse transcription-PCR served for the comparison of *hppD* und *hmgA* mRNA steady-state levels of mycelia grown with and without tyrosine. Similar sizes of the DNA fragments allowed the comparison of the amounts of PCR products and therefore of expression levels. Transcripts of *citA* (citrate synthase) showed constant steady-state level under the applied growth conditions and served as reference level. Furthermore, the oligonucleotides for transcript amplification were chosen in the way to be able to distinguish between cDNA amplification and amplification products deriving

from genomic templates (compare Fig. 20B). The comparison with DNA fragments obtained from genomic DNA served as quality control and additionally ensured a DNA free RNA preparation. The left panel in Fig. 20A clearly depicts the resulting different sizes of amplification products on genomic DNA compared to cDNA.

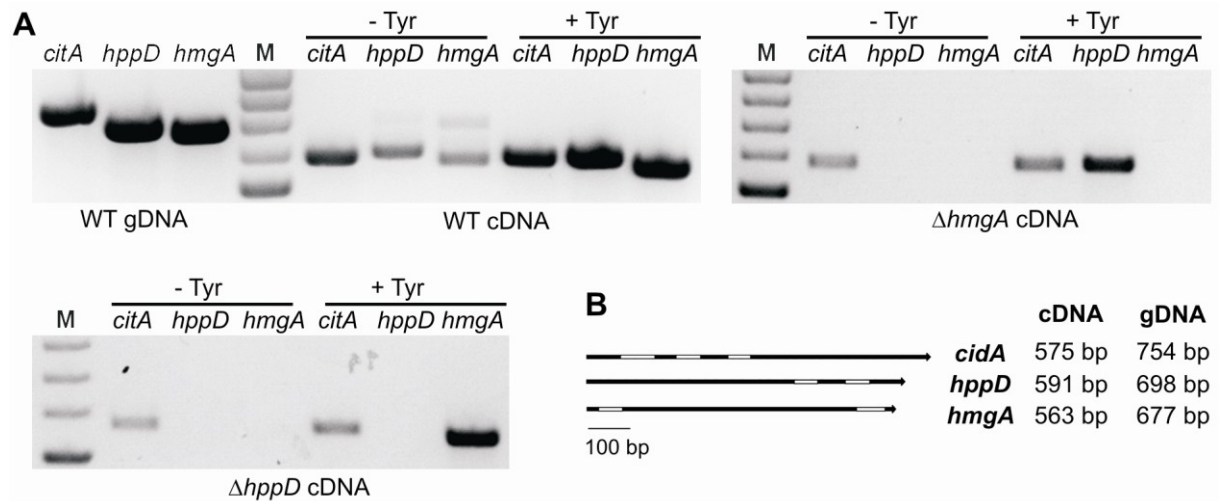


Fig. 20. Semiquantitative transcript analysis of *hmgA* and *hppD* in *A. fumigatus* liquid cultures. (A) Analysis of wild-type (WT), $\Delta hmgA$ and $\Delta hppD$ strain grown in AMM with (+Tyr) and without (-Tyr) the addition of 10 mM L-tyrosine. (M) denotes 100 bp DNA ladder, gDNA is genomic DNA, cDNA marks first strand synthesised complementary DNA. *citA*, transcript of citrate synthase used as a control; *hppD*, transcript of *p*-hydroxyphenylpyruvate dioxygenase; *hmgA*, transcript of homogentisic acid dioxygenase. *CitA* showed a constant mRNA steady-state level and served as reference for expression levels. **(B)** Scheme of the expected fragment sizes for *citA*, *hppD* and *hmgA*. White bars indicate introns. Since the amplified regions from gDNA include introns, the PCR products obtained from cDNA were smaller.

In cultures grown in AMM without L-tyrosine, mRNA steady-state levels of the genes *hppD* and *hmgA* were low in comparison to those of the *citA* reference gene (Fig. 20A). In contrast, the steady-state mRNA level of *hmgA* and *hppD* was strongly increased by the addition of L-tyrosine. This finding correlated well with the increase of the HmgA activity upon the addition of L-tyrosine to the medium (C3.6.2) and shows that the genes are induced by tyrosine at the transcriptional level.

$\Delta hmgA$ and $\Delta hppD$ cultures served as additional quality controls. *HmgA* amplification in the $\Delta hmgA$ strain revealed no product. The amplification of *hppD* transcripts in $\Delta hppD$ cultures was also negative. Consequently, these genes were correctly deleted in the corresponding deletion mutants and gene specific primers were selected for the amplification of *hppD* and *hmgA* transcripts.

3.6.2 HmgA activity dependent on the addition of tyrosine

The activity of HmgA enzyme was observed in the soluble fraction of whole cell lysates to support the results obtained in the study about the transcriptional activation of the cluster. The impact of tyrosine addition to cultures of the deletion strains was compared to wild type and complemented mutants, as illustrated in Fig. 21. Firstly, the absence of tyrosine was associated with the absence of HmgA activity. Secondly, the presence of tyrosine correlated with HmgA activity in the wild type, in the complemented strains and in the *hppD* deletion mutant. The *hppD* deletion strain even showed an increased HmgA activity. Thirdly, the activity of HmgA was totally abolished in the $\Delta hmgA$ strain. This implies that HmgA has no homolog in the *A. fumigatus* genome which is also activated by tyrosine. Furthermore, the lacking activity of HmgA confirms the correct deletion of *hmgA*.

Thus, the transcriptional activation of *hmgA* gene directly correlates with the presence of functional HmgA protein. It is likely, that HmgA activity is directly controlled by gene activation rather than by post-translational modification.

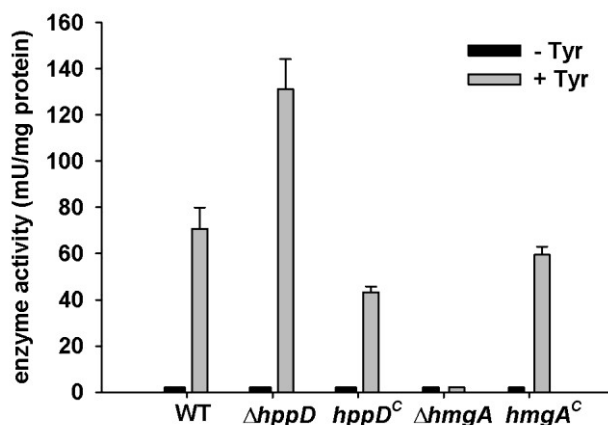


Fig. 21. HmgA activity assay dependent on the addition of L-tyrosine. The soluble fraction of whole cell lysates obtained from cultures of wild type, *hppD* and *hmgA* deletion strains and the corresponding complemented strains were subjected to a spectroscopic HmgA activity assay.

3.6.3 Transcript analysis in the infected mouse lung

To study a potential role of the tyrosine degradation cluster in the pathogenicity of *A. fumigatus*, the transcription of *hppD* and *hmgA* gene was observed in the infected mouse tissue. For this purpose, immunocompromised mice were intranasally infected with *A. fumigatus* wild-type conidia. The mice were sacrificed seven days post infection and the cDNA was synthesised from isolated lung tissue. By reverse transcription-PCR analysis, fungal mRNA steady-state levels of *hmgA* and *hppD* were compared to *citA* transcripts (Fig. 22). Analysis of *citA* mRNA levels did not only serve for the quantitative comparison as explained in section C3.6.1 but also as evidence for the successful isolation of *A. fumigatus*

RNA. As the majority of RNA derived from mouse tissue, *citA* detection was highly dependent on the degree of infection of the lung. Additionally, cDNA synthesised from non-infected mice lungs was tested with the same oligonucleotides to ensure that the amplification products of *hppD* and *hmgA* did not derive from murine cDNA. As a quality control for the murine cDNA, the constitutively transcribed gene *sftpD*, encoding murine surfactant protein D, was used (Kouadjo *et al.*, 2007).

In the uninfected control lung, transcripts of *sftpD* were detected, whereas no amplification of the *A. fumigatus* specific genes *citA*, *hppD* and *hmgA* occurred. Similar mRNA steady-state levels for *hmgA*, *hppD* and *citA* were found in cDNA samples obtained from infected lungs. The ratios of *hmgA* and *hppD* compared to *citA* indicated the induction of the L-tyrosine degradation cluster *in vivo* (compare section C3.5.3). Therefore, L-tyrosine seems to be available in the lung. Moreover, L-tyrosine is metabolised to HGA by *A. fumigatus* during invasive growth.

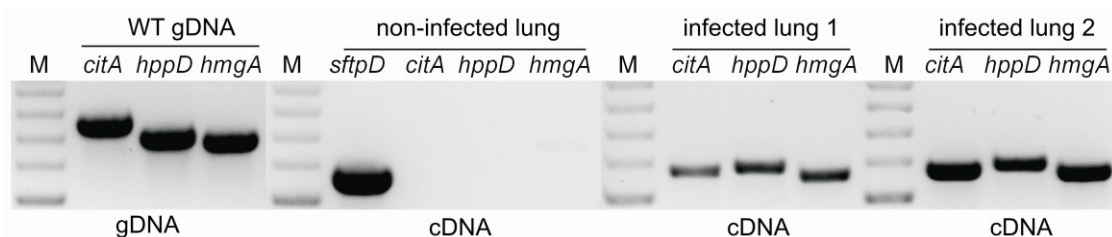


Fig. 22. Semiquantitative transcript analysis of *hmgA* and *hppD* in the infected mouse lung. Genomic DNA (gDNA) from *A. fumigatus* wild-type strain was applied for a control reaction. Two lungs isolated from immunosuppressed mice, which were intranasally infected with *A. fumigatus* conidia, provided material for cDNA synthesis as well as one non-infected lung. The transcripts of the following fungal genes were investigated by reverse transcription-PCR: *citA*, transcript of citrate synthase; *hppD*, transcript of *p*-hydroxyphenylpyruvate dioxygenase; *hmgA*, transcript of homogentisic acid dioxygenase. Transcripts of murine surfactant protein D (*sftpD*) ensured the quality of mouse cDNA. (M) denotes 100 bp DNA ladder.

3.6.4 Activation of *hppD* in different developmental stages

The fusion of the nucleotide sequence of a fluorescence protein to a promoter is a suitable system to study gene activation. In particular, the fusion of the *hppD* promoter to the coding sequence of the green fluorescence protein (eGFP) permits the study of the activation of the tyrosine degradation cluster dependent on the developmental stage. Pyomelanin formation in conidia, germinating conidia, hyphae and conidiophores can be followed. The integration of this fusion into the *pksPp-red* mutant (Behnsen, 2005) permits studying *pksP* gene expression and *hppD* gene expression simultaneously. The *pksPp-red* strain contains a fusion of the *pksP* promoter and parts of the *pksP* gene with the red fluorescence protein, dsRed. Therefore, the resulting double mutant strain allows the observation of DHN-melanin synthesis in direct comparison with pyomelanin formation.

To generate the *hppDp-eGFP* mutant strain, which translates *egfp* under the control of the *hppD* promoter, 598 bp of the 5' upstream region of *hppD* were fused to the coding sequence of eGFP. This sequence was combined with the *ptrA* gene on a plasmid for ectopic integration. The oligonucleotides *hppDp-Not1-for* and *hppDp-eCFP-rev* were applied for the amplification of the 5' upstream region of *hppD* (-598 to -1), using gDNA from *A. fumigatus* wild type. *Egfp* was amplified from plasmid pEGFP with oligonucleotides *eCFP-Not1-rev* and *HppDp-eCFP-for*. *NotI* restriction sites were introduced in both fragments. The amplification products were fused in a PCR with oligonucleotides *hppDp-Not1-for* and *egfp-Not1-rev*. The PCR product was cloned into plasmid pCR2.1, yielding plasmid pCR2.1*hppDp-egfp*. To clone the *ptrA* gene in 3' position of the *egfp* gene, plasmid pCR2.1*hppDp-egfp* was digested with *NotI* and the *hppdp-egfp* cassette was ligated into the *NotI* restriction site of plasmid pSK275. The ligation product pSK-*hppDp-egfp* was used for transformation of the *pksPp-red* strain. The combination with the *ptrA* gene allowed the selection on pyrithiamine containing media. Positive transformants were identified by observing the fluorescence during growth on media supplemented with L-tyrosine.

The expression of *hppD* and *pksP* gene was investigated in mutants grown in AMM with and without 10 mM L-tyrosine. Wild-type strain, which was cultivated in AMM with tyrosine, served as control to exclude that the observed fluorescence derived from background fluorescence. Samples were microscopically analysed for green and red fluorescence and compared to the bright-field micrographs. Freshly harvested conidia were observed as well as germlings obtained after 8 h of cultivation. The expression of *hppD* and *pksP* gene in hyphae was analysed after 16 h of cultivation. Freshly produced conidia in conidiophores were examined 40 h after inoculation. Fig. 23 presents the bright-field and the corresponding red and green fluorescent micrographs. Neither red, nor green fluorescence was detectable in wild-type strain (Fig. 23C). Thus, the fluorescence signals in the *hppDp-egfp* strain originated from *pksP* and *hppD* expression. Green fluorescent protein was visible in conidia, germlings, hyphae and conidiophores when tyrosine was available (Fig. 23A). However, red signals were only obtained in conidia and conidiophores. Red signals were independent from the availability of tyrosine, whereas green fluorescence was hardly detectable when tyrosine was absent. Consequently, *hppD* transcription is strongly induced in the presence of tyrosine which is in agreement with the results obtained in section C3.6.1. Additionally, these results confirm the expression of *hppD* in different developmental stages of the fungus. However, *pksP* gene expression is independent from tyrosine availability and only present in conidia and phialides as shown before (Langfelder *et al.*, 2001).

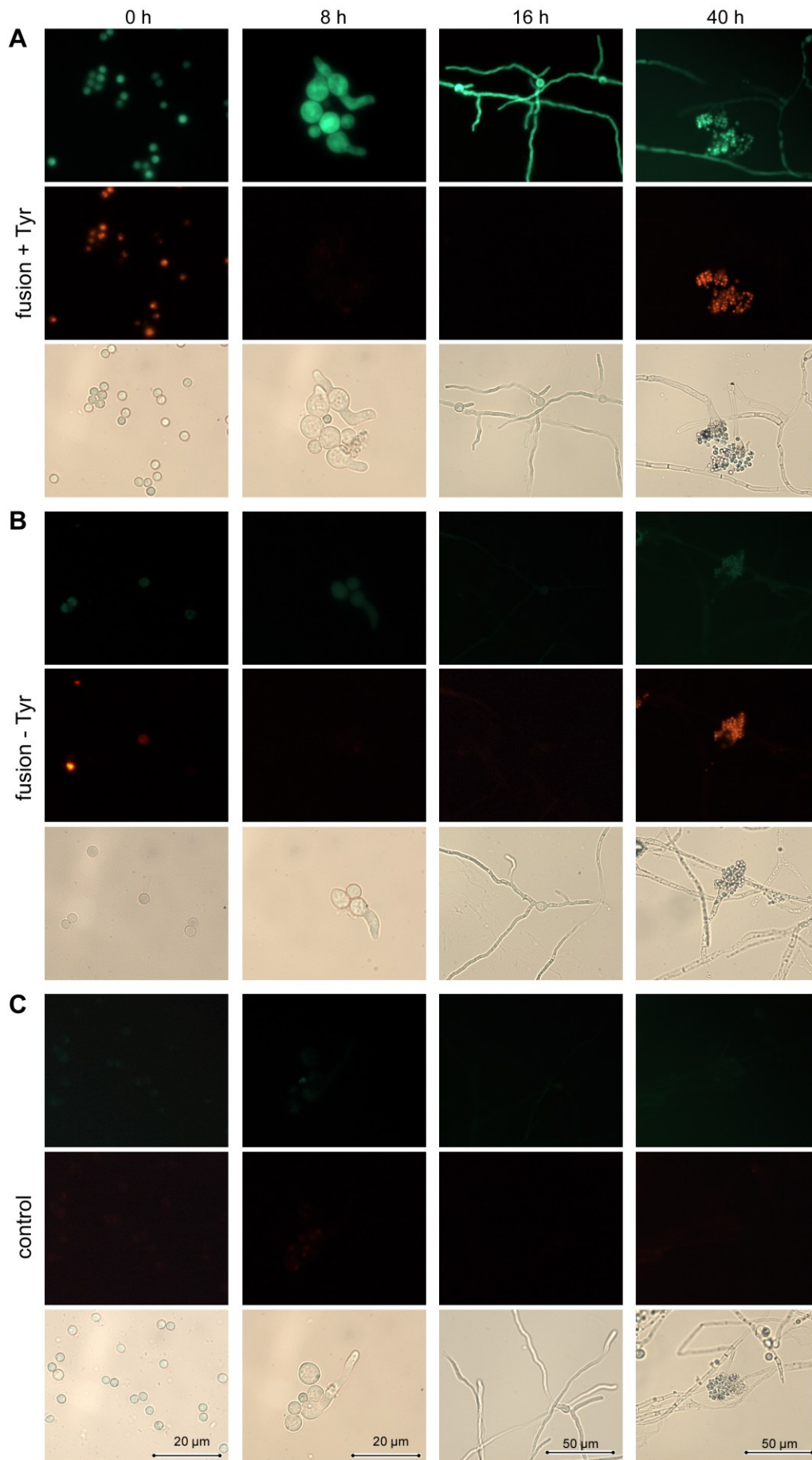


Fig. 23. Simultaneous analysis of *hppD* and *pksP* gene expression by fluorescence microscopy.

Fig. 23 (continued). *HppDp-egfp* strain, containing an *hppD*-promoter fusion to *egfp* and a *pksP*-promoter fusion to *rfp*, was cultivated in AMM with **(A)** and without **(B)** 10 mM L-tyrosine. **(C)** shows the cultivation of wild-type strain with tyrosine. Freshly harvested conidia, germlings (8 h), vegetative growing hyphae (16 h) and conidiophores (40 h) were microscopically examined. The upper panel of each picture presents the detection of green fluorescent protein, the middle panel depicts the red fluorescence and the lower panel shows the corresponding bright-field micrographs.

3.7 Susceptibility of pyomelanin mutant strains to ROI

The possible role of pyomelanin in the protection of *A. fumigatus* pyomelanin mutants against ROI was studied with agar plates containing a concentration gradient of H₂O₂, diamide or menadione. The $\Delta hmgA$ mutant displayed the hypermelanised strain and the $\Delta hppD$ mutant was the pyomelanin-free representative. The *pksP* $\Delta hppD$ strain provided a tool to answer the question whether DHN-melanin and pyomelanin are able to complement each other. AMM supplemented with 10 mM L-tyrosine was used as growth medium. The stress-inducing agents applied differ in their mode of action. Diamide causes an imbalance in the glutathion redox cycle by the fast oxidation of glutathione. As a result, proteins containing thiols are increasingly oxidised to form disulfides (Kosower *et al.*, 1972). Menadione also affects the reduced glutathione pool, but it mainly interferes by elevating superoxide and peroxide radical levels (Sakagami *et al.*, 2000; Thor *et al.*, 1982). Hydrogen peroxide is a frequently used ROI inducing agent which leads to the generation of hydroxyl radicals under iron catalysis by the Haber-Weiss reaction (Haber & Weiss, 1934; Kehrer, 2000). Lipid peroxidation, modifications of amino acids, carbohydrates and nucleotides result from hydroxyl radical generation.

The direct confrontation of freshly harvested conidia with H₂O₂ revealed no differences between wild-type and pyomelanin mutant strains except for strains with *pksP* mutant background (Fig. 24A). Here, conidia are not protected by DHN-melanin which increases sensitivity to hydrogen peroxide and sodium hypochlorite (Jahn *et al.*, 1997). To test the sensitivity of germinating conidia, conidia were preincubated for 10 h in AMM before the addition of H₂O₂. In this experimental approach, the $\Delta hppD$ strain showed a significant ($p < 0.05$) increase in ROI sensitivity compared to the other strains with wild-type background. *PksP* mutants strains were not further impaired in their growth when *hppD* was additionally deleted. All three tested *pksP* mutant strains revealed comparable inhibition zones. The pigmentation of hyphae and media was only absent in the $\Delta hppD$ strain as shown in the lower panel of Fig. 24A. This finding implies that the loss of the formation of homogentisic acid and consequently the loss of pyomelanin synthesis increases the sensitivity to ROI.

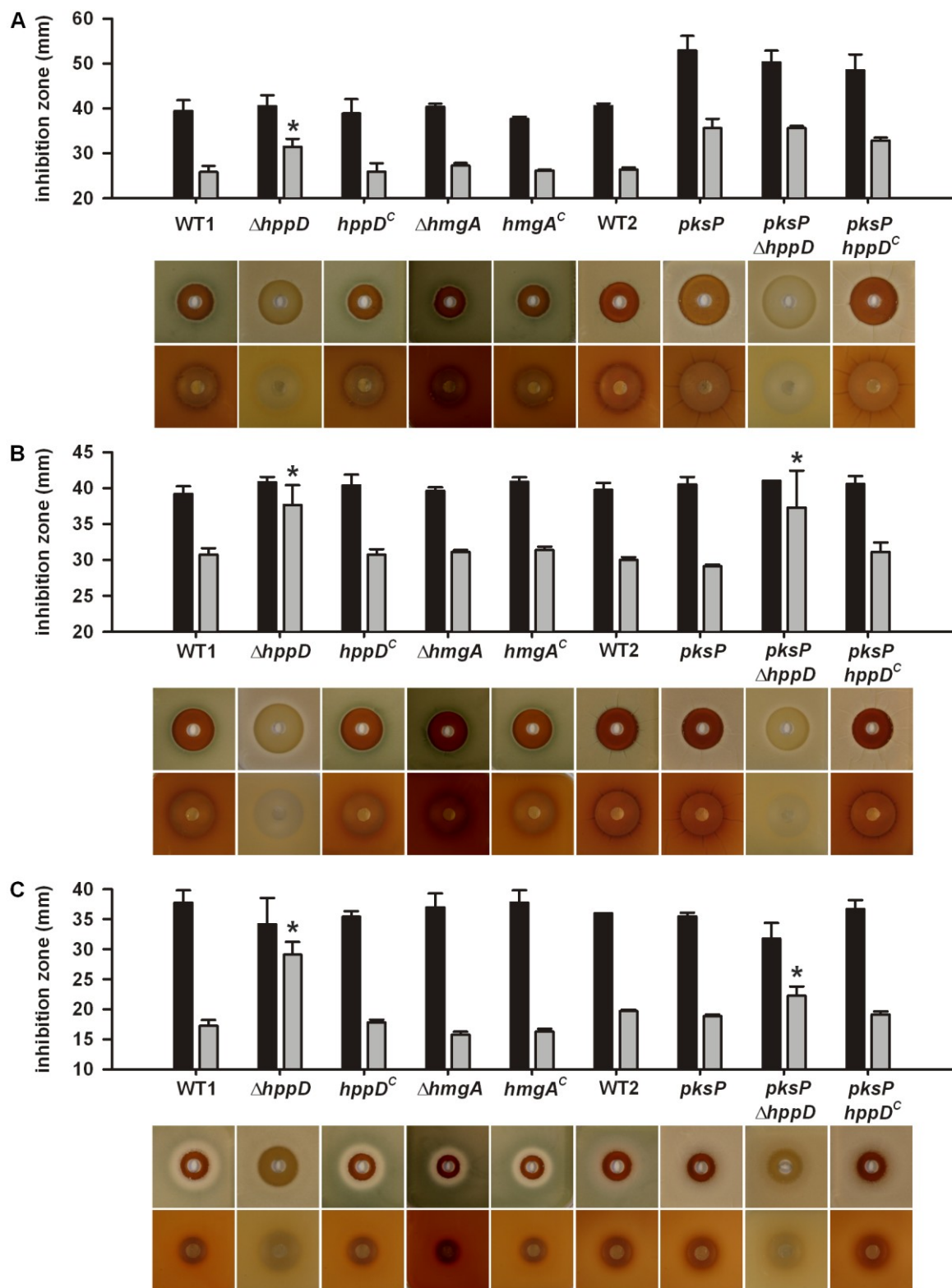


Fig. 24. Susceptibility of pyomelanin mutant strains to H₂O₂, diamide and menadione. Strains were grown on AMM with 10 mM L-tyrosine to trigger pigmentation. Different pyomelanin mutants were investigated: $\Delta hppD$, $\Delta hmgA$, $hppD^C$, $hmgA^C$ and the corresponding wild type WT1 (CEA17 Δ akuB^{KU80}) are depicted as well as the $hppD$ deletion in the $pksP$ mutant ($pksP\Delta hppD$), the $pksP\Delta hppD^C$ and the corresponding wild-type strains ($pksP$ mutant and WT2 for ATCC46645). The means and standard deviations of the diameter of the inhibition zones are shown in the upper panels. Black bars represent the direct confrontation assay with conidia and grey bars were obtained with germinated conidia. In the lower panels the corresponding pictures of the assays are displayed to follow pigmentation. The top views are presented in the upper lines and the lower lines show bottom views of the assays. In **(A)** the H₂O₂ confrontation assay, in **(B)** the diamide assay and in **(C)** the impact of menadione on growth is shown.

The confrontation with diamide and menadione revealed different results (Fig. 24B and C). In the confrontation assay with freshly harvested conidia, the *pksP* mutant strains were not more susceptible than those with wild-type background. Germlings of *hpdD* deletion strains, however, showed significantly increased inhibition zones in both *CEA17ΔakuB^{KU80}* and *pksP* mutant background.

The pigment particularly accumulated at the border of the inhibition zone in all cases except for the *hpdD* deletion strains, most evidently in the *ΔhmgA* strain assay, and independent from the stress inducing agent. However, this accumulation was less evident in the menadione diffusion assay. Despite the strong pigmentation of the *ΔhmgA* mutant strain, the inhibition of growth was comparable to that of the wild-type strain. The increase of the pigment deposition due to the accumulation of HGA in the *ΔhmgA* strain did not further increase the resistance to ROI. To confirm that the effects mentioned above derived from the deletion of the *hmgA* and *hpdD* gene, the complemented mutant strains were also studied. All three complemented strains revealed inhibition zones similar to those of the wild-type strains. These results suggest that the accumulation of homogentisic acid and its conversion to pyomelanin protects the fungus against ROI.

To confirm the results obtained with the plate diffusion assay, a spectroscopic assay based on the reduction of the tetrazolium salt XTT was established. XTT can be reduced to a coloured formazan derivative by receiving electrons from the hydrogen transport system or from artificial electron transporters. Since XTT readily penetrates into intact cells and into subcellular membranes, the degree of its reduction correlates with mitochondrial respiration and is therefore a suitable indicator for cell metabolism and viability. Menadione is the primarily applied electron-coupling reagent to facilitate formazan formation. Established protocols for the performance of the assay for antifungal susceptibility testing exist (Meletiadiis *et al.*, 2001). The protocol was adapted for the sensitivity testing of *A. fumigatus* mutants to H₂O₂ within the scope of this work.

The incubation of *A. fumigatus* cultures with different concentrations of H₂O₂ inhibited the growth of the fungus to a certain degree. This reduced growth correlated with a decreased mitochondrial respiration and resulted in a decrease of the formazan formation. Preliminary experiments revealed that the application of 1 mM, 2 mM, 4 mM and 8 mM H₂O₂ was suitable in this approach. The measured absorptions served for the calculation of the half maximal effective concentration (EC₅₀) of H₂O₂. This concentration reflects the 50 % inhibition of growth. The calculated 95 % confidence intervals of the EC₅₀ values are summarised in Table 13. The results obtained in the plate diffusion assay were confirmed

with the XTT assay. Though here, the susceptibility of mycelia was investigated as H₂O₂ was added to the cultures 24 h after inoculation. The pigmentless $\Delta hppD$ mutant showed again an increased susceptibility to H₂O₂. The $\Delta hmgA$ mutant was not more resistant compared to the wild type, as observed in the plate diffusion assay. Interestingly, the addition of L-tyrosine to the medium did not increase the resistance of the strains.

Table 13. Inhibition of growth by H₂O₂ in the XTT assay. 95 % confidence intervals of the concentration of H₂O₂ which caused a 50 % growth inhibition of *A. fumigatus* cultures in AMM with (+Tyr) and without (-Tyr) 10 mM L-tyrosine.

strain	EC50 (mM); -Tyr	EC50 (mM); + Tyr
WT	2.1-2.6	2.1-2.7
$\Delta hppD$	1.4-1.6	0.9-1.0
$\Delta hmgA$	1.8-2.3	1.9-2.2

3.8 Pyomelanin mutant strains in the murine model of invasive aspergillosis

Transcript analysis revealed the activation of the tyrosine degradation cluster during invasive growth of *A. fumigatus* in the immunosuppressed mouse lung. To assess a possible role of the cluster in pathogenesis, the pyomelanin mutant strains were tested in the murine model of invasive aspergillosis. Groups of 10 mice, which were immunosuppressed with cyclophosphamide and cortisone acetate, were intranasally infected with wild-type, $\Delta hppD$, $\Delta hmgA$, $hppD^C$ or $hmgA^C$ conidia. A control group of further ten animals remained uninfected to monitor the influence of the immunosuppression on survival. All strains caused a similar lethality as illustrated in Fig. 25.

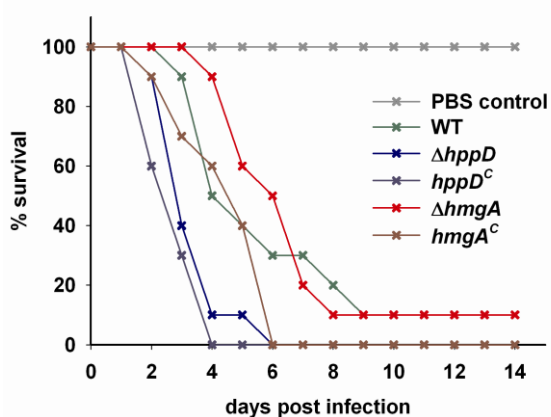


Table 14. Differences in lethality of the strains

strain	CEA17 WT	$hppD^C$	$hmgA^C$
$\Delta hppD$	0.012	0.243	
$\Delta hmgA$	0.684		0.0232

Fig. 25. Virulence of pyomelanin mutant strains in the mouse infection model. The comparison of the survival of mice in the low dose mouse infection model after intranasal infection with $\Delta hppD$, $\Delta hmgA$, WT (CEA17 \DeltaakuBpyrG^+) and the complemented strains $hppD^C$ and $hmgA^C$ is depicted. PBS controls (non-infected immunosuppressed mice) excluded the decrease of mice due to other factors.

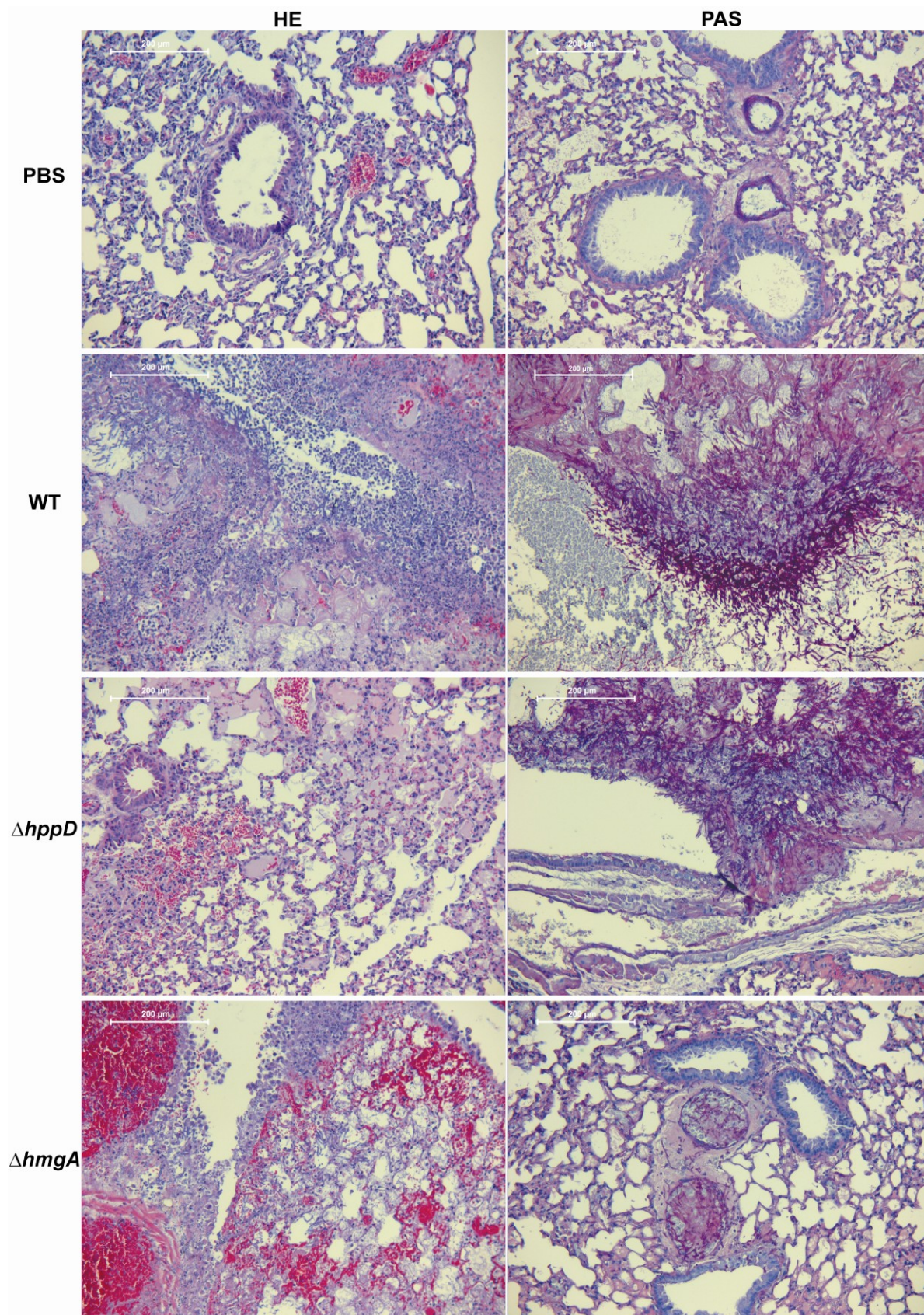


Fig. 26. Histopathology of infected and non-infected mouse lungs. HE (haematoxylin-eosin) stained sections are depicted in the left columns and in the right columns PAS (periodic acid-Schiff) stained sections are shown. Preparations of non-infected but immunosuppressed mice (PBS) and of mice which have been intranasally infected with conidia of the wild-type (WT), the *hppD* deletion ($\Delta hppD$) and the *hmgA* deletion strain ($\Delta hmgA$) are presented. Pictures were taken with a 10-fold magnification.

The application of $\Delta hppD$, $hppD^C$ or $hmgA^C$ conidia caused 100 % mortality after 6 days. Mice infected with wild-type conidia and with the $hmgA$ deletion strain showed a slightly less steep decline in the survival curve with one surviving mouse in each group during the period of observation. Still, the statistical evaluation with logrank test (Mantel, 1966) after Kaplan-Meier analysis revealed no significant difference (on the significance level 0.05) in survival between wild type, deleted and complemented strains. It was assumed that both wild type and complemented strain had to be significantly different from the deleted strain to reject null hypothesis (Table 14). Thus, the tyrosine degradation cluster does not contribute to the virulence of *A. fumigatus* in the low dose mouse infection model applied despite its induction during invasive growth.

Lungs of sacrificed mice were visually inspected for signs of an invasive *Aspergillus* infection. The majority of the infected lungs showed a typical liver colouration due to a hyperaemia. Additionally, these lungs did not collapse, another sign for vigorous growth of mycelia in the lung tissue. Furthermore, lungs slides were analysed histopathologically. Infected tissue sections were observed after paraffin preparation with haematoxylin-eosin stain for a better visualisation of the conditions in the tissue. Periodic acid-Schiff staining was applied to stain polysaccharides and highlight fungal mycelia. Tissue preparations of non-infected but immunosuppressed lungs and sections of lungs infected with wild-type, $\Delta hmgA$ or $\Delta hppD$ conidia are presented in Fig. 26. Lungs infected with wild-type conidia show vigorous growth of mycelia accompanied by large areas of necrosis, cell nuclei fragmentation and oedema of the alveolar. Furthermore, hyperaemia and angioinvasion is clearly visible, a sign for the spreading of the fungal infection. The appearance of fibrin fibers indicates the global inflammation. Lungs infected with $\Delta hmgA$ or $\Delta hppD$ conidia resembled very much the lungs infected with wild type, though the signs of infection are sometimes less prominent. Noticeable is the prevailing focalised growth without spreading in the $\Delta hmgA$ tissue slides and the pronounced hyperaemia.

Taken together, all lungs possess clear indications for an invasive *Aspergillus* infection and no clear difference in the fungal burden between the different strains applied is detectable. These results further confirm that pyomelanin formation is not essential for the virulence of *A. fumigatus* in the low dose mouse infection model.

D DISCUSSION

The opportunistic human pathogen *A. fumigatus* is a major cause of death in immunosuppressed patients. The increasing susceptible population due to advances in transplantation medicine, imprecise and late diagnostics and the emerging resistance of the fungus against established medical treatments contribute to its prominence in the intensive care. A variety of virulence factors has been attributed to its pathogenicity. However, its outstanding role compared to other aspergilli is still not fully understood. Although not unique, DHN-melanin biosynthesis is a distinctive feature for *A. fumigatus* and contributes to its pathogenicity (Jahn *et al.*, 1997; Tsai *et al.*, 1998). Hence, further knowledge about the nature, biosynthesis and properties of pigments in this fungus might provide the basis for advanced methods in the treatment of aspergillosis. Furthermore, the reduction of mortality rates among transplant patients due to *A. fumigatus* infections demands improved diagnostic tools (Brakhage, 2005; Latgé, 1999). DHN-melanin provides a possible target for the earlier and more differentiated diagnosis. Therefore, this work aimed to obtain novel insights into these aspects of pigmentation in *A. fumigatus*.

1 A camelid domain antibody directed against fungal melanin

VHH domains are the terminal variable domain of heavy-chain antibodies present in the *Camelidae*. Their specificity is encoded within a single polypeptide chain. The light chain is missing (Muyldermans *et al.*, 1994). These features enable the fast selection via phage display and the large-scale production of selected VHH domains in *E. coli* cells. Furthermore, these antibodies are amenable to genetic manipulation for their facilitated functional analysis (Holliger & Hudson, 2005). A camelid VHH-domain antibody was selected from a fully synthetic recombinant antibody library within the scope of this work.

1.1 The challenging generation of an anti-melanin antibody

The absence of a published, specific anti-melanin antibody is an indication for the challenge to generate such an antibody. The uncertainty about structural modifications of synthetic melanins and melanin ghosts compared to the naturally exposed melanin hinders the selection of antibodies against pure melanin. The isolation of melanin ghosts from conidia requires harsh conditions (compare section B3.4). Though, in a study melanin particles were used for the immunisation of mice to generate monoclonal antibodies in

hybridomas (Youngchim *et al.*, 2004). Consistently, the obtained antibodies did not discriminate between DHN-melanin and DOPA-melanin. In addition, an appropriate negative-control, e.g. *pksP* mutant conidia, was missing and the antibodies have not been employed in tissue sections. Further monoclonal antibodies against melanin of *Cryptococcus neoformans* were generated in the same way (Rosas *et al.*, 2000). Data about the specificity of these antibodies have not been provided either.

An approach involving the precursor of DHN-melanin was also not drawn into consideration. Although the generation of antibodies against 1,8-DHN appears to be practicable, there is a risk of losing the presented epitope in the natural polymer. Similar concerns affect the *in vitro* synthesis of DHN-melanin. It is doubtful that *in vitro* synthesised DHN-melanin reveals the same conformation as natural DHN-melanin since its synthesis involves an oxidative polymerisation (Tsai *et al.*, 1999). Furthermore, the precursor 1,8-DHN is commercially not available requiring its complex synthesis.

Pure melanin would be an essential prerequisite for the generation of antibodies with the help of the hybridoma technique. This method is based on the fusion of spleen cells of immunised mice to myeloma cells for the generation of monoclonal antibodies (Goding, 1980; Köhler & Milstein, 1975). The lack of a competitive selection makes this method inefficient for the selection against an antigen exposed on a surface among other antigenic structures. Applying this method, antibodies reacting with a variety of surface-exposed molecules would be produced and a large number of hybridomas would have to be screened for the production of the appropriate antibody. Although the “surface-epitope masking” method, that mimics a competitive selection, has already been developed in 1994, the complexity of the procedure impedes its prevalent application (Shen *et al.*, 1994). The outcome of a panning procedure against conidia and hyphae without the involvement of a competitor was shown by Lionakis *et al.* (2005). The authors confronted a peptide-based phage library with wild-type conidia and hyphae and applied the BRASIL approach for the panning procedure (Giordano *et al.*, 2001). The missing competitive selection led to the identification of a variety of binders. Only proteinaceous targets were predictable in this study on the basis of blast searches in protein databases. Consequently, this approach would feature two main drawbacks for the target melanin: (i) the simultaneous selection of antibodies against a variety of surface antigens and (ii) the challenging identification of the binders against non-proteinaceous targets, such as melanin.

Hence, phage display and a competitive selection procedure against conidia were combined for the generation of anti-melanin antibodies in this work. A competitive system for the selection against DHN-melanin was available. The DHN-melanin-free conidia of the

pksP mutant strain allowed the minimisation of unwanted cross-reactivity of antibodies selected against DHN-melanin which is exposed on the surface of *A. fumigatus* wild-type conidia. The preincubations with *pksP* mutant conidia reduced the antibody pool by binders against other conidial surface structures than DHN-melanin. Beside the unavailability of an appropriate, purified antigen, the problem of the complete separation of unbound phages from phages bound to the conidia of the competitor had to be solved. The adsorption of conidia to the bottom of ELISA plates was not possible, most likely due to their large diameter and differing surface hydrophobicities of wild-type and *pksP* mutant conidia. The adaptation of the BRASIL method (Giordano *et al.*, 2001), which implies the separation of phages from conidia by a centrifugation through an organic layer, failed for the competitive approach, too. Thus, the idea to exploit the different size of phages and conidia was realised. This is the first description of the use of a filtration method for the generation of antibodies.

Applying this method, one VHH-presenting phage population was clearly enriched after three selection rounds which ranged over six days. Therefore, this method permitted a fast selection demanding *in vitro* experiments only; another benefit compared to the time-consuming animal depended antibody production methods.

1.2 An elegant antibody engineering

The selected antibody, designated MelPhoA, was successfully produced and purified in high amounts after the adjustment of its coding sequence. The selected sequence was encoded by a phagemid DNA. Since phagemids feature modifiability and handling analogous to plasmids, the transfer of the VHH-domain sequence into a plasmid was easy to perform, and it allowed the recombinant production of the antibody in *E. coli* cells. This host-vector system permitted a straightforward method for the genetic manipulation of the VHH-domain sequence. Within this work, the antibody was modified by the fusion to the alkaline phosphatase at the C-terminus. Due to the independent association of alkaline phosphatase molecules to dimers, the fusion of the VHH domain to alkaline phosphatase triggered the dimerisation of the camelid antibody fragments (Wels *et al.*, 1992). The benefit of the obtained bivalency was an increased binding affinity compared to monovalent constructs (Martin *et al.*, 2006). Additionally, the structure of dimers of VHH domains resembles more the natural HCAbs than monomers. Besides, alkaline phosphatase provided a convenient tag allowing direct enzymatic detection of the VHH-domain fusions without the need for secondary reagents. In crude protein extracts, the alkaline phosphatase activity assay gave a hint about the functional expression and purification of the antibody. Thus, the detection of

high alkaline phosphatase activity in the soluble cell fraction allowed a fast and simple prediction about the proper folding of the antibody.

The functional production of antibody fragments containing disulfide bonds in *E. coli* requires the transportation of the cytosolically expressed antibody into the periplasm for maturation or a refolding from inclusion bodies (Skerra, 1993). Here, the secretion into the periplasm was chosen since this is generally the faster method. The latter has not to be adapted for every specific molecule, whereas the effort for refolding from inclusion bodies is protein specific and not predictable (Cabrita & Bottomley, 2004). A variety of leader peptides using the post-translational Sec translocation pathway or the co-translational single recognition particle (SRP) pathway have been proven to be suitable for the passage of heterologous proteins through the cytoplasmic membrane (Thie *et al.*, 2008). Though, leader sequences are not in every case exchangeable as shown for the translocation of the thioredoxin (Schierle *et al.*, 2003). The targeting to the Sec pathway resulted in an inefficient translocation due to a rapid folding of the protein. However, the *Erwinia carotovora* pectate lyase B leader peptide (*pelB*) has already been successfully applied for the recombinant synthesis of functional camelid domains in *E. coli* (Habicht *et al.*, 2007). Thus, this Sec dependent leader peptide was also used for the transport into the periplasm in this work. By this, a large fraction of the anti-melanin antibody was functionally expressed although an insoluble fraction of the antibody appeared as well. These antibody aggregates were discarded as the establishment of suitable refolding procedures requires time-consuming efforts in the majority of cases (Cabrita & Bottomley, 2004). Due to the production of the antibody by high cell density fermentation, the obtained amounts of soluble and functional antibody were sufficient for the aims of this work.

Disadvantageous in the production of the antibody was the appearance of triplet codons inappropriate for the protein synthesis in *E. coli*. Although an optimised strain was applied, which contained *supE* tRNA, protein yields were low. It has been shown that the amber codon is not properly translated to glutamate even in cells with amber suppressor *supE* activity because of an inefficient read-through (Miller & Albertini, 1983). Therefore, a successful antibody production required the inconvenient modification of the nucleotide sequence into well translated codons. The basis of this drawback is found in the construction procedure of the applied VHH-domain library. A library synthesis by codon-corrected trinucleotide randomisation rather than oligonucleotide randomisation could circumvent low protein yields due to an inefficient read-through (Krumpe *et al.*, 2007). Furthermore, the library synthesis with codon-corrected trinucleotides could provide a significant enhancement of the functional diversity of the library (Rodi *et al.*, 2002). Thus,

this method would allow the avoidance of stop codons and would favour the integration of more uniform amino acid sequences.

A pure antibody was required for the characterisation and application of the VHH domain. The expression plasmid provided the fusion of a hexahistidine tag at the C-terminus of the antibody fragment which facilitated the purification by IMAC. Pure and concentrated antibody solutions were obtained after a terminal anion exchange chromatographic step. To sum up, the applied recombinant production procedure of the VHH domain in *E. coli* cells provided high amounts of the pure and engineered antibody in a fast and convenient way.

1.3 Uncovering targets of the selected camelid domain

The interaction between MelPhoA and the target was reversible which is characteristically for antigen-antibody interactions (Tijssen, 1985b). These interactions are based on Van der Waals forces, hydrogen bonds, ionic and hydrophobic interactions. Therefore, an antibody can be displaced from its epitope by another protein in a competitive ELISA (Tijssen, 1985a). MelPhoA dissociated from its target by the addition of a modified antibody and thus the establishment of covalent bonds was excluded.

Recombinant VHH libraries can provide binders of high affinity and high specificity. The VHH library applied comprises such an antibody pool as shown by Habicht *et al.* (2007). There, a VHH domain was selected that distinguishes A β amyloid fibrils from disaggregated A β peptides as well as from specific A β oligomers. The antibody selected in this study binds to different types of melanin. MelPhoA revealed comparable binding in the ELISA to ATCC46645 and CEA17 Δ *akuB*^{KU80} wild-type conidia of *A. fumigatus*, to *A. nidulans* and to *A. terreus* conidia. Both *A. fumigatus* strains synthesise DHN-melanin (Langfelder *et al.*, 1998; Tsai *et al.*, 1998). Presumably, conidia of *A. nidulans* do not expose DHN-melanin on their surface since the application of the fungicide tricyclazole does not result in a colour change of the conidia (personal communication, A. Brakhage). Tricyclazole inhibits tetrahydroxynaphthalene reductases and therefore interferes with the DHN-melanin synthesis which is visible in a colour change of the pigment (Wheeler & Bell, 1988). Furthermore, *A. nidulans* and *A. terreus* genomes revealed no complete DHN-melanin synthesis cluster after alignment with the *A. fumigatus* DHN-melanin cluster. Hence, the identity of the pigment produced by both strains remains ambiguous although it had been proposed that *A. nidulans* possesses the capacity to produce homogentisate, the precursor of pyomelanin (Fernández-Cañón & Peñalva, 1995b). The binding capacity of MelPhoA to the *A. fumigatus* DHN-melanin mutant strains, Δ *arp2*, Δ *abr2* and Δ *ayg1*, was also comparable to

the wild-type strains. Supposedly, these strains expose a DHN-melanin like pigment which is the result of the polymerisation of precursors of 1,8 DHN ((Sugareva *et al.*, 2006; Tsai *et al.*, 1999), also compare section C2). The low affinity of MelPhoA to pigmentless *pksP* mutant conidia provided evidence that the signals did not derive from other conidial surface structures. Moreover, the affinity to melanin ghosts and pure DOPA melanin supported the statement mentioned before. Furthermore, the antibody did only detect hyphae of *A. fumigatus* when pyomelanin synthesis was triggered by the addition of tyrosine (compare section C3.5.3). Immunofluorescence studies indicated that MelPhoA does not exclusively recognise pigments deriving from aspergilli. MelPhoA was also directed against pigmented mycelia of the ascomycete fungus *Phoma destructiva* and obviated to bind to non-pigmented mycelia. Although the nature of the melanin pigment produced by *P. destructiva* has not been identified, this fungus provided an elegant control as its melanisation is inducible by cyclosporine A (Friedrich, 2007).

The application of MelPhoA for the detection of melanisation of *A. fumigatus* in infected tissue samples was less successful. A Streptavidin-Cy3 conjugate was used for the detection of the biotinylated MelPhoA. This approach minimised necessary washing and incubation steps which was advantageous for the preservation of the target structure. Presumably, high background fluorescence caused the failure of this two-step approach. A reason for a high background fluorescence may be the binding of a Streptavidin-Cy3 conjugate to endogenous biotins because biotin is widely dispersed in mammalian tissues (Bussolati *et al.*, 1997). However, endogenous biotin was blocked before the incubation with the antibody and thus, this assumption is questionable. The direct detection of the antibody by its alkaline phosphatase domain was not under consideration since one-step approaches with a directly labelled antibody usually lack sufficient sensitivity for the detection of most antigens (Ramos-Vara, 2005). Furthermore, this method requires the inactivation of endogenous alkaline phosphatase activity of tissue and mycelia which might damage the epitope. Alternatively, biotinylated antibodies are detectable by a Streptavidin-HRP conjugate. However, this method was not applied as endogenous peroxidase activity needs to be inactivated by hydrogen peroxide, especially in tissues with abundant haemorrhages (Straus, 1979). Haemorrhages were prevalent in some tissue sections of this study. In addition, hydrogen peroxide bleaches melanin (Korytowski & Sarna, 1990) and thus, it is conceivable that the target structure may be destroyed by the treatment with this oxidising agent. Another drawback of the peroxidase method is the colour of the most commonly applied stain diaminobenzidine for the detection of peroxidase activity. This chromogene

gives a brown colour which interferes with the presence of melanins in tissues (Ramos-Vara, 2005).

In general, the establishment of an immunohistochemical approach for the detection of antigens requires expert knowledge and the optimisation of a variety of factors. For example, the preservation of the antigenic structure or a proper antigen retrieval, the application of a suitable fixation procedure, the avoidance of background fluorescence due to unspecific antibody interactions or due to interactions of the reagents with the tissue, efficient blocking steps and the right concentrations of all reagents are essential for the success of an immunohistochemical detection method (Ramos-Vara, 2005). Thus, the applied histochemical procedure might have been inappropriate for the study of the desired antigen-antibody system. Still, it is not excludable that MelPhoA is directed against an epitope also present in tissue sections. In this case, a modified panning procedure might avoid such an affinity. Besides *pksP* mutant conidia, homogenised lung tissue could be used as a competitor. Binders against *pksP* conidia as well as against tissue structures would be withdrawn. However, the feasibility of this approach is questionable; it requires the reestablishment of the method due to a different handling of homogenised tissue samples.

To sum up, MelPhoA can discriminate between melanised and non-melanised conidia and hyphae but does not provide the specificity to discriminate between DHN-melanin, DOPA-melanin, pyomelanin and DHN-melanin derivatives.

1.4 Elucidating the specificity of the VHH-domain antibody

A. fumigatus conidia expose DHN-melanin in its natural conformation (Langfelder *et al.*, 1998; Tsai *et al.*, 1998) and therefore provided the antigenic structure for the selection of the desired antibody. The absence of DHN-melanin in humans as well as its restricted presence in the fungal kingdom qualified the polymer as a suitable target for diagnostics. Because of the application of DHN-melanin exposing conidia as antibody target, the presentation of other conidial surface structures was not excludable. For example, polysaccharides like branched β 1,3, 1,6-glucans, chitin, galactomannan and β 1,3, 1,4-glucan account for more than 90 % of the cell wall components (Latgé, 2007). The outermost cell-wall layer of conidia is additionally covered by rodlets which are composed of moderately hydrophobic proteins, also called hydrophobins (Paris *et al.*, 2003). Finally, cell wall associated proteins and GPI anchored proteins are exposed as well (Asif *et al.*, 2006). Despite of the competitive approach with the melanin-free *pksP* mutant conidia, it is conceivable that the selected antibody also identifies one of the structures mentioned before. Presumably, wild-type and *pksP* mutant conidia do not exclusively differ in the

presence of DHN-melanin due to the impact of melanin on the overall composition of conidial surfaces. For example, resting *pksP* mutant conidia reveal higher amounts of accessible β 1,3 glucan than wild-type conidia (Luther *et al.*, 2007). Thus, the hydrophobicity of the cell surface and the composition of non-covalently bound proteins might be changed. The loss of the ornamentation of *pksP* mutant conidia compared to wild-type conidia is a further indication for a loss of hydrophobic proteins. Rodletless mutants have also lost their ornamentation and reveal a rather amorphous surface (Paris *et al.*, 2003). Therefore, the panning procedure applied is not comparable to standard methods which exclude the selection against undesired targets. Such methods involve the panning against a purified antigen or a competitor that “truly” resembles the antigen presenting structure minus the antigen.

To disprove the recognition of other surface structures by MelPhoA, the VHH domain was confronted with purified melanin particles and DOPA-melanin isolated from *Sepia officinales* as discussed before. Besides, an attempt for the identification of the target by a proteomic approach was carried out. To exclude a proteinaceous target of MelPhoA, the VHH domain was applied in Western blot analysis of conidia extracts after separation by 2-D gel electrophoresis. Indeed, MelPhoA detected two proteins, the mitochondrial processing peptidase β subunit and the sorbitol/xylulose reductase. Presumably, both proteins are intracellularly located due to their function, the lack of signal peptides and the missing transmembrane domains. These proteins were also identified in conidial extracts by 2-D gel electrophoresis with a non-linear pH gradient from 3-11 in the study of Teutschbein *et al.*, (2009). There, the same method for the extraction of proteins was applied. Proteins of whole conidia extracts were analysed. Although the appearance of intracellular proteins on cell surfaces has been described (Wartenberg, 2008), it is doubtful that the mentioned peptidase and the reductase are exposed on the conidial surface. These proteins were not detectable when conidial surface proteins were selectively analysed (Asif *et al.*, 2006). Additionally, the mitochondrial processing peptidase is equally expressed in *pksP* mutant and wild-type conidia as shown by Wolke (2007). These data suggest that the identified proteins are not present on the conidial surface and thus, did not interfere in the selection procedure of MelPhoA. Their recognition of MelPhoA appeared rather incidental but still supports a limited specificity of the antibody.

One reason for a restricted specificity might be a limitation of the library. A disadvantage of fully recombinant libraries is the lack of somatic hypermutations. The later occur during *in vivo* maturation of the immunoglobulin repertoire to achieve a functional diversification (Weigert *et al.*, 1970). Recently, methods have been developed to mimic the hypermutation

in *in vitro* selection methods. Ribosome display, for example, allows the directed evolution of binding proteins through the insertion of random mutations by error-prone polymerases (Hanes *et al.*, 2000). Furthermore, the library diversity is not limited by cellular transformation efficiency applying ribosome display or mRNA display (Amstutz *et al.*, 2001).

Probably, changes in the panning procedure itself might improve the specificity of a selected binder. An increased salt concentration during the selection process might potentiate the selection pressure and result in improved binders. However, a considerable enhancement of the specificity is unlikely since the buffer used for the generation of MelPhoA already contained a high salt concentration. Whereas, it is very likely that the conidial pigment displays an unfavourable target due to its peculiar structural features. The biosynthesis of melanins includes a final oxidative polymerisation. However, intermediates of the pathways own a limited stability and are susceptible to auto-oxidation (Riley, 1997). These characteristics cause the inhomogeneous structure of the polymers. Therefore, the overall structure of none of the polymers has been fully elucidated, yet it is conceivable that all melanins contain similar features. Presumably, hydroxylated aromatics might occur abundantly because DHN-, DOPA- and pyomelanin pigments have aromatic precursors in common (see section A2).

To sum up, a promising competitive selection methodology against conidial melanin has been developed. Additionally, ELISAs with antigen presenting conidia have been designed. These methods circumvented the difficulties in the handling of melanin due to its unique physical and chemical properties. The unsatisfying specificity of the selected antibody is rather attributable to the presented target itself. The inhomogeneous structure of melanin and similarities in the structure of different types of melanin are most probably accountable for the cross-reactivity of the selected antibody domain.

2 DHN-melanin and pyomelanin in *A. fumigatus*

2.1 Pink versus grey-green – does the colour make the difference?

The DHN-melanin pathway is involved in the virulence of *A. fumigatus* as it had been demonstrated for the white conidia of the *pksP* deletion strain (Langfelder *et al.*, 1998; Tsai *et al.*, 1998). In contrast to the influence of the loss of PksP activity, neither a missing laccase Abr2 nor the loss of the hydrolase Ayg1, both involved in DHN biosynthesis, result in an increased sensitivity to ROI or a reduced virulence in the mouse model of invasive

aspergillosis (Sugareva, 2006; Sugareva *et al.*, 2006). Thus, the question remains to be answered whether the pigment itself, an intermediate or a shunt-product of the pathway contribute to the virulence of *A. fumigatus*. The study of the Arp2 reductase, which is also part of the DHN biosynthesis cluster, aimed to elucidate this issue.

A database search discovered homologs of Arp2 in other closely related species. However, the enzyme was in most cases not integrated in a complete DHN-melanin biosynthesis cluster. Only the rarely pathogenic fungi *Aspergillus clavatus* and *Neosartorya fischeri* revealed complete DHN-clusters after analysis of their genomic sequences (Fedorova *et al.*, 2008).

The deletion of the Arp2 reductase encoding gene resulted in reddish-pink conidia as observed for the disruption mutant by (Tsai *et al.*, 1999). Hence, this mutant still produces a pigment which, however, differs from the grey-green wild-type melanin. The complete absence of a pigment would have led to the appearance of white conidia as it is the case for the *pksP* deletion strain. The deficiency in the reductase combined with the reddish-pink colour is a hint that, beside 1,8-dihydroxynaphthalene, other intermediates of the DHN-pathway can be polymerised to melanin. The high degree of conjugation of carbonyl-bonds and unsaturated carbon bonds in the polymer brings about a wide spectral absorbance of melanins (Riley, 1997). Therefore, structural differences in the monomers can explain an absorbance shift causing different colouration of wild-type and $\Delta arp2$ conidia. This assumption is supported by the fact that other DHN-melanin pathway mutants also produce distinctly coloured conidia (Tsai *et al.*, 1999).

Further divergent characteristics compared to the wild-type strain were not detected. The colony morphology as well as the radial growth rate of the mutant resembled the wild-type phenotype. In addition, the modified pinkish pigment did not alter the surface structure as described for the *pksP* mutant conidia (Langfelder *et al.*, 1998). The surface of wild-type conidia is characterised by a strong ornamentation which derives from the presence of hydrophobic proteins, e.g., hydrophobins. This protein layer seems to protect the conidia from environmental stress and alveolar macrophages (Paris *et al.*, 2003). In contrast, *pksP* mutant conidia reveal a smooth surface which implies that the loss of DHN-melanin coincides with the loss of surface proteins (Langfelder *et al.*, 1998). Thus, the observation of the rough and ornamented surface of the Arp2 deficient conidia leads to the conclusion that the pinkish pigment does allow the attachment of surface proteins as the wild-type melanin. The sensitivity to diamide, menadione and H_2O_2 was also comparable to that of the wild type. Consequently, the polymerisation products of precursors of 1,8-DHN seem to scavenge ROI as sufficiently as 1,8-DHN-melanin.

The virulence of the *arp2* deletion mutant also resembled to that of the wild-type strain in the murine model of invasive aspergillosis. The efficient scavenging of ROI of the Δ *arp2* strain in combination with its virulence can neither withdraw nor confirm the essential role of DHN-melanin or modified DHN-melanins in the pathogenicity of *A. fumigatus*. Arp2 does obviously not produce wild-type DHN-melanin, but it is conceivable that the modified DHN-melanin is similarly effective in the protection of the fungus. However, the importance of the ROI scavenging activity for virulence is still a matter of debate. By means of the pigmentless *wA* deficient mutant of *A. nidulans* it was shown that the pigment protected conidia from artificial oxidative damage, human polymorphonuclear leukocytes and monocytes (Jahn *et al.*, 2000). Though, the pigment does not play a role in the virulence due to the apathogenicity of *A. nidulans*. These data are not completely transferable to *A. fumigatus*, however, as *A. nidulans* produces apparently a different type of melanin than DHN-melanin. Still, it is likely that other properties of the pigment play an essential role in the virulence of *A. fumigatus*. Since an elevated C3 deposition has been described for conidia of the Δ *arp1* disruption strain deficient in scytalone dehydrogenase and for the conidia of the *pksP* mutant (Tsai *et al.*, 1998; Tsai *et al.*, 1997), a deeper look at the complement deposition might be helpful to elucidate this problem. In the *arp1* disruption mutant an elevated C3 deposition is in accordance with its attenuated virulence which has been noted but not verified by Tsai *et al.* (1999). It is conceivable that melanin and derivatives of DHN-melanin reduce the recognition and the defense of the immune system due to a hindrance of C3 deposition. In addition to this hypothesis, these pigments may serve as a shield in general. Other antigenic structures might not be accessible for their recognition by the immune system.

Alternatively, Jahn *et al.* suggested the synthesis of a shunt product of the DHN-melanin pathway which might be indicative for pathogenicity (Jahn *et al.*, 2000). Indeed, fungal polyketides comprise diverse secondary metabolites with various biological activities (Schümann & Hertweck, 2006). Well known examples for bioactive polyketides are lovastatin and griseofulvin produced by *A. terreus* and *Penicillium griseofulvum*, respectively. For the identification of a potential shunt polyketide of the DHN-biosynthesis pathway, targeted gene inactivation might be a suitable method (Bok *et al.*, 2006). HPLC analysis with cell extracts of a DHN-melanin mutant strain compared to those of the wild-type can be carried out to find additional peaks in chromatograms deriving from the accumulation of shunt products in the mutant strain. This approach has been followed with the *arp2* mutant strain. However, no obvious additional peaks appeared in the chromatograms of the deletion strain (data not shown). For a more successful approach, the optimal extraction

method has to be identified and other deletion strains have to be analysed. The *ayg1* deletion mutant might be a promising candidate since this strain is equally virulent as the wild type (Sugareva, 2006) and in addition, this heptaketide-shortening enzyme is involved in DHN-melanin synthesis just after the polyketide synthase. Consequently, considering the presence of an unidentified ketide it should most likely accumulate in the *ayg1* mutant strain.

To summarise, the grey-green pigment is certainly not decisive for the virulence of *A. fumigatus*. Conidia with pinkish, yellowish or brownish pigments are similarly effective protected as the wild-type conidia. Therefore, it remains to be elucidated whether DHN-melanin or modifications of the pigments are essential for virulence or whether a shunt product makes *A. fumigatus* such an aggressive pathogen.

2.2 Pyomelanin – a novel melanin produced by *A. fumigatus*

Beside DHN-melanin, *A. fumigatus* is able to produce another type of melanin. The presence of a second melanin was assumed since *pksP* mutant cultures turned brown after addition of L-tyrosine although this mutant is deficient in DHN-melanin biosynthesis. A proteomic approach revealed the tyrosine dependent upregulation of proteins of the tyrosine degradation pathway (Sugareva, 2006). This pathway is associated with inherited diseases in humans, such as alcaptonuria and tyrosinaemia. Due to the relevance for humans, the molecular basis of this pathway has been intensively studied in the model organism *A. nidulans*. The transfer of the results to humans showed that alcaptonuria is associated with enzymatic defects in the catabolism of phenylalanine and tyrosine (Fernández-Cañón & Peñalva, 1998; Peñalva, 2001).

The alignment of the chromosomal region encoding for central enzymes of the pathway in *A. nidulans* with the *A. fumigatus* DNA sequence revealed a high similarity between both species. Corresponding proteins show identities between 60 and 89 %. The genes succeed in the same order on the chromosome. The only obvious difference is the additional AN1894.4 gene in the *A. nidulans* genome. It remains to be answered whether the corresponding gene product has an impact on the regulation of the cluster and on the apathogenicity of *A. nidulans*. The genes *hppD*, AFUA_2g04210, *hmgA*, *fahA*, *maiA* and AFUA_2g04262 have been assigned to the cluster because of their predicted function and their chromosomal location.

Clustering of genes, encoding proteins involved in the same catabolic pathway, is not uncommon for filamentous fungi. Enzymatic and regulatory genes for well-studied catabolic pathways, such as quinate, ethanol, proline and nitrate utilization, were found to be

clustered in various filamentous fungi (reviewed in Keller & Hohn, 1997). Furthermore, fungal genes involved in secondary metabolism biosynthesis are clustered, e.g., the genes involved in DHN-melanin biosynthesis form a cluster and are additionally associated with the virulence of the fungus (Brakhage *et al.*, 2008). The organisation of the tyrosine degradation genes in a cluster suggests that these genes are regulated in a common manner which is characteristic for gene clusters (Yu & Keller, 2005). This is supported by the finding that both genes studied here in more detail, *hmgA* and *hppD*, were shown to be induced at the transcriptional level by L-tyrosine. It is unclear, yet how this tyrosine regulation is mediated. Very recently, the global transcription factor Ace2 was found to suppress an orange-brownish pigment release into the medium (Ejzykowicz *et al.*, 2009). It is likely that the released pigment is pyomelanin. Possible other regulatory genes, AFUA_2G04210 and AFUA_2G04262, are part of the cluster. It has been shown previously that bacterial homogentisate clusters possess at least one regulatory protein. For example, in *Pseudomonas putida*, the *hmgR* regulatory gene located upstream of *hmgA*, *fahA* and *maiA* codes for an IclR-type regulator which acts as a repressor of an aromatic catabolic pathway. It controls the inducible expression of the genes in the homogentisate cluster. HGA is the inducer molecule (Arias-Barrau *et al.*, 2004). Additionally, in the pyomelanin producer *Streptomyces coelicolor* it has been shown that *hppD* transcription is controlled by a complex regulatory system involving repressor and activator regulatory genes (Yang *et al.*, 2007). However, homologs of these bacterial genes are not present in the *A. fumigatus* cluster and analogies in the regulation remain to be elucidated. Particularly, the comparison of the regulation of the tyrosine degradation pathway between *A. nidulans* and *A. fumigatus* will be interesting in order to find out whether a major principle in the difference of the virulence of both strains is based on pyomelanin production.

Several indications exist for an evolutionary origin of the cluster or of parts of the cluster in bacteria. GC contents of the genes are unusually high compared to the average GC content of *A. fumigatus* A1163, a derivative of CEA17, with 49.4 % (Nierman *et al.*, 2005). Especially the genes *maiA* and *fahA* reveal striking GC contents with 58 % and 56 %, respectively. The average GC content of the *A. nidulans* genome of 50 % (Galagan *et al.*, 2005) is also less compared to the genes of the tyrosine degradation cluster although here, the differences are not as obvious as in *A. fumigatus*. In contrast, *S. coelicolor*, representative of the group of soil-dwelling filamentous bacteria, is characterised by a GC content as high as 72.1 % (Bentley *et al.*, 2002). Beside GC contents, the frequent occurrence of streptomycetes and aspergilli in the same natural habitat and the widely present pyomelanin formation in

bacteria compared to the rare description of this pigment in fungi support the assumption of a horizontal gene transfer.

Pyomelanin results of the polymerisation of HGA which derives from L-tyrosine via a tyrosine degradation pathway (Coon *et al.*, 1994). Thus, mutant strains which accumulate or lack HGA can give evidence of the nature of the pigment. The characteristics of $\Delta hmgA$ and $\Delta hppD$ provide several arguments for the presence of the tyrosine degradation pathway and its connection to pyomelanin formation in *A. fumigatus*. The converse phenotype of the *hppD* mutant compared to a *pksP* mutant, deficient in the polyketide synthase essential for DHN-melanin formation, is one example. The *pksP* mutant strain produced white conidia and released a brown pigment when cultivated with L-tyrosine. Thus, the brown pigment is different from DHN-melanin. Although the conidia of the $\Delta hppD$ strain exposed a grey-green pigment, melanin accumulation and HGA detection were not observable in cultures supplemented with L-tyrosine. The inability to produce HGA totally abolished the brown pigment formation. Moreover, the addition of the HppD inhibitor sulcotrione resulted in the same phenotype, further confirming that the tyrosine degradation pathway is responsible for the observed pigment formation.

An *A. nidulans* $\Delta hmgA$ mutant (Fernández-Cañón & Peñalva, 1995a) bears some analogy to the results obtained in *A. fumigatus*. In this study, the focus was on the degradation of tyrosine since it is a closer precursor of HGA than phenylalanine. In addition, tyrosine induced a stronger pigmentation in the *A. fumigatus* wild-type strain than phenylalanine. As shown for *A. nidulans*, *A. fumigatus* also contains one single functional gene coding for homogentisate dioxygenase. The deletion of *hmgA* entirely abolished HmgA activity. The same is true for *p*-hydroxyphenylpyruvate dioxygenase. The deletion of *hppD* prevented the formation of homogentisic acid as well as the pigment synthesis in submerged cultures. Therefore, predicted homologs of these enzymes (AFUA_4G10620 and AFUA_6G10810) do not possess activity under the tested conditions. The pigmentation is induced by tyrosine, phenylalanine and phenylacetic acid which also well agrees with the observations in *A. nidulans* (Fernández-Cañón & Peñalva, 1995b). Additionally, the accumulation of the pigment was strongly triggered by a non-functional HmgA enzyme. The accumulated pigment was clearly identified as polymerisation product of HGA. FTIR spectroscopy resulted in similar spectra as obtained for a synthetic pyomelanin and for pyomelanins produced in *Shewanella algae* (Turick *et al.*, 2002) and *Alcaligenes eutrophus* (David *et al.*, 1996).

The functional tyrosine degradation pathway was dispensable during growth on minimal agar plates with glucose as carbon source but essential for the growth on agar plates containing L-tyrosine as sole carbon source. Furthermore, the visible production of pyomelanin required L-tyrosine or L-phenylalanine in the medium. This makes pyomelanin a typical secondary metabolite. DHN-melanin is a secondary metabolite which has been associated with the virulence of *A. fumigatus*. Hence, the question arises whether pyomelanin is a further natural product involved in the pathogenicity of the fungus.

2.3 Pyomelanin – a novel virulence determinant of *A. fumigatus*?

DHN-melanin and DOPA melanin contribute to the virulence of several fungi (reviewed in Langfelder *et al.*, 2003; Nosanchuk & Casadevall, 2003). However, literature dealing with pyomelanin and virulence is scarce. Only recently, hyperpigmentation based on pyomelanin has been suggested to be involved in an increased adaptation to chronicity of some clinical *Pseudomonas aeruginosa* isolates (Rodríguez-Rojas *et al.*, 2009).

A prerequisite for a role of the tyrosine degradation pathway in the infection process is the availability of tyrosine in the lung tissue since the activation of the pathway is linked to this amino acid. It seems likely that L-tyrosine is present in the lung of immunosuppressed patients, allowing *A. fumigatus* to produce pyomelanin. Consistently, *A. fumigatus* secretes a variety of proteases that are secreted during colonisation of the lung tissue (Monod *et al.*, 2002). It was proposed that protein degradation of the lung tissue is essential for host invasion (Kogan *et al.*, 2004). In fact, this was proven by the finding that mutants in the methylcitrate synthase of *A. fumigatus* exhibited a strongly attenuated virulence due to the accumulation of toxic propionyl-CoA which derives from the degradation of isoleucine, valine or methionine (Ibrahim-Granet *et al.*, 2008). Thus, amino acids are available and serve as nutrient source during invasive growth. This argument is also supported by the presence of L-tyrosine in sera at a concentration between 21 and 107 μM (Gressner, 2007) to serve as precursor for a variety of biocompounds, e.g., catecholamines, thyroid hormones and dihydroxyphenylalanine-melanin. Furthermore, it can be synthesised from L-phenylalanine by the phenylalanine hydroxylase. Transcript analysis of *hppD* and *hmgA* revealed their activation in the infected mouse lung, a further indication for the presence of tyrosine and its metabolisation during infection.

A current model concerning pathogenicity of *A. fumigatus* suggests that conidia are protected against ROI to a certain extent by the DHN-melanin pigment and that its biosynthesis genes are also involved in the production of an immunosuppressive compound

(Brakhage, 2005). When conidia germinate and hyphae grow out, e.g., from macrophages, it is likely that the formation of pyomelanin further protects the germlings and outgrowing hyphae against ROI, e.g., produced by neutrophils.

Consistently, the $\Delta hppD$ strain displayed a higher susceptibility to ROI when the mutant strain was compared to the wild type during growth on agar plates supplemented with L-tyrosine. The entirely abolished pyomelanin formation in this strain increased the susceptibility of germlings to hydrogen peroxide, diamide and menadione. However, hyperpigmentation in the $\Delta hmgA$ mutant did not further increase the resistance to ROI. The basal level of pigmentation of the wild-type strain was apparently sufficient for the protection. Similar findings were previously reported for *Burkholderia cenopacia*. Pyomelanin was shown to protect the bacterium from *in vitro* and *in vivo* sources of oxidative stress (Keith *et al.*, 2007). However, the role of ROI in the killing of *A. fumigatus* has been recently challenged since the deletion mutant of the main regulator for the ROI response of *A. fumigatus*, AfYap1, did not influence the killing of *A. fumigatus* by immune effector cells (Lessing *et al.*, 2007). Additionally to the protective role, another effect of pyomelanin biosynthesis may be hypothesised. In humans, reactive intermediates of the pathway or the deposition of the pigment itself correlate with severe arthritis in alcaptonuria patients with ochronosis (concentrated pigment depositions). The exact mechanism of the joint inflammation and degeneration remains to be elucidated, yet (La Du, 2002). Still, it is likely that the intermediates released by the fungus contribute to the pathogenicity of *A. fumigatus*. Intermediates of the pathway can readily function as electron donors leading to the formation of toxic semiquinoid and quinoid derivatives. Additionally, the electrons produce the highly reactive HO· radical via the Fenton reaction and thereby evoke cytotoxicity (Hegedus, 2000). As a consequence, the host's immune response may be weakened

Despite the increased susceptibility of the pyomelanin-free strain to ROI and the toxicity of intermediates of the pathway, neither the *hppD* deletion strain nor the *hmgA* mutant revealed an attenuated or increased virulence in the mouse infection model. However, very recently the suitability of the applied mouse infection model has been questioned for the virulence study of secondary metabolites (Kwon-Chung & Sugui, 2009). The applied immunosuppressive regime appeared to be the key factor for discrepancies in the impact of gliotoxin on survival of mice, for instance. The neutropenic model, which implies the immunosuppression with corticosteroids in combination with cyclophosphamide, showed gliotoxin to be not essential for virulence (Kupfahl *et al.*, 2006). By contrast, the sole application of cortisonacetate revealed a role of gliotoxin in the pathogenicity of

A. fumigatus. It was concluded that the neutropenic mouse model is inadequate to reveal the pathobiological importance of fungal secondary metabolites (Kwon-Chung & Sugui, 2009). However, the *pksP* mutant is reduced in its virulence in the neutropenic mouse model. Thus, this model can still provide indications for the virulence of some secondary metabolites (personal communication, Thorsten Heinekamp).

The greater wax moth *Galleria mellonella* is a further not suitable model for the testing of the impact of mutations in pigment biosynthesis though it is used for other fungal pathogens. Various DHN-melanin mutants were hypervirulent compared to the wild type in this infection model (Jackson *et al.*, 2009). Thus, the influence of pyomelanin remains to be reinvestigated in the corticosteroid model.

An attenuation of the pyomelanin deficient strain in this mouse infection model would reveal interesting aspects. Tyrosinaemia type I is successfully treated with the potent HppD inhibitor Nitisinone (Orfadin[®]) which interrupts the pathway after *p*-hydroxyphenylpyruvate formation and prevents the accumulation of hepatotoxic intermediates. This drug might also be suitable for the inhibition of *A. fumigatus* HppD. A successful application of that inhibitor might therefore influence the pathogenic potential of *A. fumigatus* in the case of the involvement of pyomelanin in virulence. Recently, Nitisinone has been suggested for the treatment of paracoccidioidomycosis, a disease caused by the thermodimorphic fungus *Paracoccidioides brasiliensis* (Nunes *et al.*, 2005). This drug inhibits the differentiation of the fungus into the pathogenic yeast phase. These observations and the approved application of Nitisinone in humans propose its possible applicability for the treatment of severe fungal infections as new anti-infective drug.

Summing up, despite a variety of indication for a possible involvement of pyomelanin formation in the virulence of *A. fumigatus*, the neutropenic mouse model did not reveal a positive correlation between the pathogenicity and pyomelanin. However, the behaviour of mutants of the pathway needs to be additionally studied in the non-neutropenic mouse model to confirm the unimportance of pyomelanin in the virulence of *A. fumigatus*.

2.4 Two types of melanin in *A. fumigatus*– a benefit for the fungus?

Based on the results of this work, *A. fumigatus* has the capability to produce two different types of melanin, i.e., DHN-melanin pigment via the polyketide biosynthesis pathway (Langfelder *et al.*, 1998; Tsai *et al.*, 1998) and pyomelanin via L-tyrosine degradation. DHN-melanin is present in many different fungi both pathogens and non-pathogens (reviewed in Langfelder *et al.*, 2003; Wheeler & Bell, 1988). Until now,

pyomelanin was rarely detected in filamentous fungi. The presence of DHN-melanin in the fungus raises the question about the reason for the synthesis of a second type of melanin. Tyrosine degradation is an essential pathway for the recycling of that amino acid and for its utilisation as carbon and energy source. This supports the statement that pyomelanin is only a side product of that pathway in the presence of an excess supply of tyrosine or phenylalanine. The comparison of the synthesis of melanins subject to the developmental stage, however, provides insights into a possible complementary role of DHN- and pyomelanin.

DHN-melanin is the pigment characteristic for the conidia. Hyphae grown in *in vitro* cultures are apparently DHN-melanin free. Transcripts of the DHN-melanin gene cluster were only detectable in the conidiation state and not in the mycelia as shown by Northern blot analysis of *A. fumigatus* grown in AMM (Tsai *et al.*, 1999). Furthermore, 2D-gel electrophoresis revealed the presence of proteins of this pathway in conidia but not in extracts of mycelia (Wolke, 2007; Olaf Knemeyer, personal communication). Although the *pksP* gene was found to be expressed in the lungs of infected mice, the presence of DHN-melanin under these conditions is still a matter of debate (Langfelder *et al.*, 2001). In contrast, pyomelanin synthesis is not restricted to conidia; it is additionally strongly produced in germlings and hyphae as shown by the *hppD* promoter eGFP fusion. The detection of HGA in culture supernatants led to the conclusion that the pigment deposits after its extracellular synthesis on surfaces. Pigmentation was clearly visible on the surface of mycelia grown in submerged cultures and on solid media, whereas *pksP* mutant conidia remained white. In fact, in none of the examined strains a visible colour change of the conidia occurred due to tyrosine consumption. Hence, a deposition of pyomelanin on the surface of conidia is doubtful despite the activation of the genes involved in tyrosine degradation in conidia. It is conceivable that differences in the hydrophobicity of the conidial and hyphal surface provoke this observation. The rodlet surface of conidia is uniformly hydrophobic, whereas the subjacent cell wall, which appears during swelling, germination and on the surface of hyphae, is hydrophilic (Dague *et al.*, 2008). Additionally, pyomelanin shows under the applied neutral to slightly acidic culture conditions a rather hydrophilic character visible by its solubility in the medium. Thus, opposing surface properties may explain the primarily deposition of pyomelanin on germlings and hyphae.

Consistently, germlings of the pyomelanin deficient $\Delta hppD$ strain were clearly more susceptible to H₂O₂, diamide and menadione, in contrast to conidia which revealed wild-type sensitivity. Furthermore, the susceptibility of DHN-melanin-free conidia was not further reduced by pyomelanin deficiency, one more clear indication for the inferior role of

pyomelanin in conidia. Interestingly, *pksP* mutant conidia revealed an increased susceptibility to H₂O₂ but not to menadione and diamide, whereas *hppD* mutant hyphae were sensitive to each of the three stress-inducing agents. This observation might be based on the essential diffusion or transportation of diamide and menadione through the cell wall and cell membrane. Germlings are more permeable for diamide and menadione than conidia since their cell wall and membranes are still in the process of synthesis. Furthermore, diamide and menadione have to be transformed intracellularly to achieve a glutathione depletion (Kosower *et al.*, 1972; Thor *et al.*, 1982). H₂O₂, however, is readily converted under iron catalysis to deleterious hydroxyl radicals and is transported by passive diffusion as well as through aquaporins to the site of action (Bienert *et al.*, 2006).

To summarise, both melanins seem to fulfil distinctive roles in the protection of the fungus. DHN-melanin is the pigment which acts on conidia and pyomelanin offers a shield for the protection of germlings and hyphae. Both pigments are independently from each other involved in the oxidative stress response of *A. fumigatus*. This complementary role of the melanins might provide a survival advantage to *A. fumigatus* and demands further investigation in the non-neutropenic mouse model with regard to virulence.

E REFERENCES

- Al-Alawi A, Ryan CF, Flint JD, Muller NL** (2005) *Aspergillus*-related lung disease. *Can Respir J* **12**(7): 377-387
- Amstutz P, Forrer P, Zahnd C, Plückthun A** (2001) *In vitro* display technologies: novel developments and applications. *Curr Opin Biotechnol* **12**(4): 400-405
- Arias-Barrau E, Olivera ER, Luengo JM, Fernández C, Galán B, García JL, Díaz E, Miñambres B** (2004) The homogentisate pathway: a central catabolic pathway involved in the degradation of L-phenylalanine, L-tyrosine, and 3-hydroxyphenylacetate in *Pseudomonas putida*. *J Bacteriol* **186**(15): 5062-5077.
- Asif AR, Oellerich M, Armstrong VW, Riemenschneider B, Monod M, Reichard U** (2006) Proteome of conidial surface associated proteins of *Aspergillus fumigatus* reflecting potential vaccine candidates and allergens. *J Proteome Res* **5**(4): 954-962
- Ballance DJ, Turner G** (1985) Development of a high-frequency transforming vector for *Aspergillus nidulans*. *Gene* **36**(3): 321-331
- Bass S, Greene R, Wells JA** (1990) Hormone phage: an enrichment method for variant proteins with altered binding properties. *Proteins* **8**(4): 309-314
- Behnsen J** (2005) Herstellung eines definiert immunogenen *Aspergillus fumigatus*-Stammes und erste Analyse von dessen Wirtszellinteraktion. Diploma Thesis, Institut für Mikrobiologie, Universität Hannover
- Bentley SD, Chater KF, Cerdeno-Tárraga AM, Challis GL, Thomson NR, James KD, Harris DE, Quail MA, Kieser H, Harper D, Bateman A, Brown S, Chandra G, Chen CW, Collins M, Cronin A, Fraser A, Goble A, Hidalgo J, Hornsby T, Howarth S, Huang CH, Kieser T, Larke L, Murphy L, Oliver K, O'Neil S, Rabinowitsch E, Rajandream MA, Rutherford K, Rutter S, Seeger K, Saunders D, Sharp S, Squares R, Squares S, Taylor K, Warren T, Wietzorrek A, Woodward J, Barrell BG, Parkhill J, Hopwood DA** (2002) Complete genome sequence of the model actinomycete *Streptomyces coelicolor* A3(2). *Nature* **417**(6885): 141-147
- Bienert GP, Schjoerring JK, Jahn TP** (2006) Membrane transport of hydrogen peroxide. *Biochim Biophys Acta* **1758**(8): 994-1003
- Bilinska B** (1996) Progress of infrared investigations of melanin structures. *Spectrochimica Acta Part A: Molecular and Biomolecular Spectroscopy* **52**(9): 1157-1162
- Bok JW, Hoffmeister D, Maggio-Hall LA, Murillo R, Glasner JD, Keller NP** (2006) Genomic mining for *Aspergillus* natural products. *Chem Biol* **13**(1): 31-37
- Brakhage AA** (2005) Systemic fungal infections caused by *Aspergillus* species: epidemiology, infection process and virulence determinants. *Curr Drug Targets* **6**(8): 875-886.
- Brakhage AA, Langfelder K** (2002) Menacing mold: the molecular biology of *Aspergillus fumigatus*. *Annu Rev Microbiol* **56**: 433-455
- Brakhage AA, Schuemann J, Bergmann S, Scherlach K, Schroeckh V, Hertweck C** (2008) Activation of fungal silent gene clusters: a new avenue to drug discovery. *Prog Drug Res* **66**: 1, 3-12.
- Breitling F, Dubel S, Seehaus T, Klewinghaus I, Little M** (1991) A Surface Expression Vector for Antibody Screening. *Gene* **104**(2): 147-153
- Bretagne S** (2003) Molecular diagnostics in clinical parasitology and mycology: limits of the current polymerase chain reaction (PCR) assays and interest of the real-time PCR assays. *Clin Microbiol Infect* **9**(6): 505-511

- Brock M** (2005) Generation and phenotypic characterization of *Aspergillus nidulans* methylisocitrate lyase deletion mutants: Methylisocitrate inhibits growth and conidiation. *Appl Environ Microb* **71**(9): 5465-5475
- Bussolati G, Gugliotta P, Volante M, Pace M, Papotti M** (1997) Retrieved endogenous biotin: a novel marker and a potential pitfall in diagnostic immunohistochemistry. *Histopathology* **31**(5): 400-407
- Cabrita LD, Bottomley SP** (2004) Protein expression and refolding--a practical guide to getting the most out of inclusion bodies. *Biotechnol Annu Rev* **10**: 31-50
- Carreira A, Ferreira LM, Loureiro V** (2001) Brown pigments produced by *Yarrowia lipolytica* result from extracellular accumulation of homogentisic acid. *Appl Environ Microbiol* **67**(8): 3463-3468.
- Chan CM, Woo PCY, Leung ASP, Lau SKP, Che XY, Cao L, Yuen KY** (2002) Detection of antibodies specific to an antigenic cell wall galactomannoprotein for serodiagnosis of *Aspergillus fumigatus* aspergillosis. *Journal of Clinical Microbiology* **40**(6): 2041-2045
- Chazalet V, Debeaupuis JP, Sarfati J, Lortholary J, Ribaud P, Shah P, Cornet M, Vu Thien H, Gluckman E, Brücker G, Latgé JP** (1998) Molecular typing of environmental and patient isolates of *Aspergillus fumigatus* from various hospital settings. *J Clin Microbiol* **36**(6): 1494-1500
- Coon SL, Kotob S, Jarvis BB, Wang S, Fuqua WC, Weiner RM** (1994) Homogentisic acid is the product of MelA, which mediates melanogenesis in the marine bacterium *Shewanella colwelliana* D. *Appl Environ Microbiol* **60**(8): 3006-3010.
- Coppieters K, Dreier T, Silence K, de Haard H, Lauwereys M, Casteels P, Beirnaert E, Jonckheere H, de Wiele CV, Staelens L, Hostens J, Revets H, Remaut E, Elewaut D, Rottiers P** (2006) Formatted anti-tumor necrosis factor alpha VHH proteins derived from camelids show superior potency and targeting to inflamed joints in a murine model of collagen-induced arthritis. *Arthritis Rheum* **54**(6): 1856-1866
- da Silva Ferreira ME, Kress MR, Savoldi M, Goldman MH, Hartl A, Heinekamp T, Brakhage AA, Goldman GH** (2006) The *akuB*(KU80) mutant deficient for nonhomologous end joining is a powerful tool for analyzing pathogenicity in *Aspergillus fumigatus*. *Eukaryot Cell* **5**(1): 207-211.
- da Silva MB, Marques AF, Nosanchuk JD, Casadevall A, Travassos LR, Taborda CP** (2006) Melanin in the dimorphic fungal pathogen *Paracoccidioides brasiliensis*: effects on phagocytosis, intracellular resistance and drug susceptibility. *Microbes Infect* **8**(1): 197-205
- Dadachova E, Bryan RA, Howell RC, Schweitzer AD, Aisen P, Nosanchuk JD, Casadevall A** (2008) The radioprotective properties of fungal melanin are a function of its chemical composition, stable radical presence and spatial arrangement. *Pigment Cell Melanoma Res* **21**(2): 192-199
- Dague E, Alsteens D, Latgé JP, Dufrene YF** (2008) High-resolution cell surface dynamics of germinating *Aspergillus fumigatus* conidia. *Biophys J* **94**(2): 656-660
- David C, Daro A, Szalai E, Atarhouch T, Mergeay M** (1996) Formation of polymeric pigments in the presence of bacteria and comparison with chemical oxidative coupling—II. Catabolism of tyrosine and hydroxyphenylacetic acid by *Alcaligenes eutrophus* CH34 and mutants. *European Polymer Journal* **32**(6): 669-679
- Desmyter A, Transue TR, Ghahroudi MA, Thi MHD, Poortmans F, Hamers R, Muyldermans S, Wyns L** (1996) Crystal structure of a camel single-domain VH antibody fragment in complex with lysozyme. *Nat Struct Biol* **3**(9): 803-811

- Dixon DM, Migliozi J, Cooper CR, Jr., Solis O, Breslin B, Szanislo PJ** (1992) Melanized and non-melanized multicellular form mutants of *Wangiella dermatitidis* in mice: mortality and histopathology studies. *Mycoses* **35**(1-2): 17-21
- Ejzykowicz DE, Cunha MM, Rozental S, Solis NV, Gravelat FN, Sheppard DC, Filler SG** (2009) The *Aspergillus fumigatus* transcription factor Ace2 governs pigment production, conidiation and virulence. *Mol Microbiol* **72**(1): 155-169
- Ellis M** (1999) Therapy of *Aspergillus fumigatus*-Related Diseases. In *Aspergillus fumigatus: Biology, Clinical aspects and molecular approaches to pathogenicity. Contributions to Microbiology*
- Brakhage AA, Jahn B, Schmidt A** (eds), Vol. 2, pp 105-129. Basel: Karger Medical and Scientific Publishers
- Ellis MK, Whitfield AC, Gowans LA, Auton TR, Provan WM, Lock EA, Smith LL** (1995) Inhibition of 4-hydroxyphenylpyruvate dioxygenase by 2-(2-nitro-4-trifluoromethylbenzoyl)-cyclohexane-1,3-dione and 2-(2-chloro-4-methanesulfonylbenzoyl)-cyclohexane-1,3-dione. *Toxicol Appl Pharmacol* **133**(1): 12-19.
- Ewert S, Cambillau C, Conrath K, Plückthun A** (2002) Biophysical properties of camelid VHH domains compared to those of human V(H)3 domains. *Biochemistry-Us* **41**(11): 3628-3636
- Fedorova ND, Khaldi N, Joardar VS, Maiti R, Amedeo P, Anderson MJ, Crabtree J, Silva JC, Badger JH, Albarraq A, Angiuoli S, Bussey H, Bowyer P, Cotty PJ, Dyer PS, Egan A, Galens K, Fraser-Liggett CM, Haas BJ, Inman JM, Kent R, Lemieux S, Malavazi I, Orvis J, Roemer T, Ronning CM, Sundaram JP, Sutton G, Turner G, Venter JC, White OR, Whitty BR, Youngman P, Wolfe KH, Goldman GH, Wortman JR, Jiang B, Denning DW, Nierman WC** (2008) Genomic islands in the pathogenic filamentous fungus *Aspergillus fumigatus*. *PLoS Genet* **4**(4): e1000046
- Feng B, Wang X, Hauser M, Kaufmann S, Jentsch S, Haase G, Becker JM, Szanislo PJ** (2001) Molecular cloning and characterization of WdPKS1, a gene involved in dihydroxynaphthalene melanin biosynthesis and virulence in *Wangiella (Exophiala) dermatitidis*. *Infect Immun* **69**(3): 1781-1794.
- Fernández-Cañón JM, Peñalva MA** (1995a) Fungal metabolic model for human type I hereditary tyrosinaemia. *Proc Natl Acad Sci U S A* **92**(20): 9132-9136.
- Fernández-Cañón JM, Peñalva MA** (1995b) Molecular characterization of a gene encoding a homogentisate dioxygenase from *Aspergillus nidulans* and identification of its human and plant homologues. *J Biol Chem* **270**(36): 21199-21205.
- Fernández-Cañón JM, Peñalva MA** (1997) Spectrophotometric determination of homogentisate using *Aspergillus nidulans* homogentisate dioxygenase. *Anal Biochem* **245**(2): 218-221.
- Fernández-Cañón JM, Peñalva MA** (1998) Characterization of a fungal maleylacetoacetate isomerase gene and identification of its human homologue. *J Biol Chem* **273**(1): 329-337.
- Frases S, Salazar A, Dadachova E, Casadevall A** (2007) *Cryptococcus neoformans* can utilize the bacterial melanin precursor homogentisic acid for fungal melanogenesis. *Appl Environ Microb* **73**(2): 615-621
- Friedrich H** (2007) Untersuchungen zu mikrobiellen Interaktionen von Pilzen der Gattung *Phoma*. Doctoral Thesis, HKI, Friedrich-Schiller-University, Jena
- Galagan JE, Calvo SE, Cuomo C, Ma LJ, Wortman JR, Batzoglou S, Lee SI, Basturkmen M, Spevak CC, Clutterbuck J, Kapitonov V, Jurka J, Sczocchio C, Farman M, Butler J, Purcell S, Harris S, Braus GH, Draht O, Busch S, D'Enfert C, Bouchier C, Goldman GH, Bell-Pedersen D, Griffiths-Jones S, Doonan JH, Yu J, Vienken K, Pain A, Freitag M, Selker EU, Archer DB, Peñalva MA, Oakley BR, Momany M, Tanaka T, Kumagai T, Asai K, Machida M, Nierman WC, Denning DW, Caddick M, Hynes M, Paoletti M, Fischer R, Miller B, Dyer P, Sachs MS,**

- Osmani SA, Birren BW** (2005) Sequencing of *Aspergillus nidulans* and comparative analysis with *A. fumigatus* and *A. oryzae*. *Nature* **438**(7071): 1105-1115
- Ghahroudi MA, Desmyter A, Wyns L, Hamers R, Muyldermans S** (1997) Selection and identification of single domain antibody fragments from camel heavy-chain antibodies. *Febs Lett* **414**(3): 521-526
- Giordano RJ, Cardo-Vila M, Lahdenranta J, Pasqualini R, Arap W** (2001) Biopanning and rapid analysis of selective interactive ligands. *Nat Med* **7**(11): 1249-1253
- Goding JW** (1980) Antibody production by hybridomas. *J Immunol Methods* **39**(4): 285-308
- Gomez BL, Nosanchuk JD, Diez S, Youngchim S, Aisen P, Cano LE, Restrepo A, Casadevall A, Hamilton AJ** (2001) Detection of melanin-like pigments in the dimorphic fungal pathogen *Paracoccidioides brasiliensis* *in vitro* and during infection. *Infect Immun* **69**(9): 5760-5767
- Gressner A** (2007) *Lexikon der Medizinischen Laboratoriumsdiagnostik*, Heidelberg: Springer.
- Haber F, Weiss J** (1934) The Catalytic Decomposition of Hydrogen Peroxide by Iron Salts. *Proceedings of the Royal society of London* **147**: 332-351
- Habicht G, Haupt C, Friedrich RP, Hortschansky P, Sachse C, Meinhardt J, Wieligmann K, Gellermann GP, Brodhun M, Gotz J, Halbhuber KJ, Rocken C, Horn U, Fandrich M** (2007) Directed selection of a conformational antibody domain that prevents mature amyloid fibril formation by stabilizing Abeta protofibrils. *Proc Natl Acad Sci U S A* **104**(49): 19232-19237
- Habicht G, Siegemund M** (2002) Konstruktion einer vollsynthetischen *Camelidae*-VHH-Antikörper-Bibliothek optimierter Qualität und deren Expression in *Escherichia coli*. *Diploma Thesis* Leibniz Institute for Natural Product Research and Infection Biology, Hans-Knöll-Institute, Friedrich-Schiller-Universität, Jena
- Hamers-Casterman C, Atarhouch T, Muyldermans S, Robinson G, Hamers C, Songa EB, Bendahman N, Hamers R** (1993) Naturally occurring antibodies devoid of light chains. *Nature* **363**(6428): 446-448.
- Hanes J, Schaffitzel C, Knappik A, Plückthun A** (2000) Picomolar affinity antibodies from a fully synthetic naive library selected and evolved by ribosome display. *Nat Biotechnol* **18**(12): 1287-1292
- Harmsen MM, De Haard HJ** (2007) Properties, production, and applications of camelid single-domain antibody fragments. *Appl Microbiol Biot* **77**(1): 13-22
- Harmsen MM, Ruuls RC, Nijman IJ, Niewold TA, Frenken LGJ, de Geus B** (2000) Llama heavy-chain V regions consist of at least four distinct subfamilies revealing novel sequence features. *Mol Immunol* **37**(10): 579-590
- Hayden RT, Isotalo PA, Parrett T, Wolk DM, Qian X, Roberts GD, Lloyd RV** (2003) In situ hybridization for the differentiation of *Aspergillus*, *Fusarium*, and *Pseudallescheria* species in tissue section. *Diagn Mol Pathol* **12**(1): 21-26
- Hegedus ZL** (2000) The probable involvement of soluble and deposited melanins, their intermediates and the reactive oxygen side-products in human diseases and aging. *Toxicology* **145**(2-3): 85-101.
- Hermeling S, Crommelin DJA, Schellekens H, Jiskoot W** (2004) Structure-immunogenicity relationships of therapeutic proteins. *Pharm Res* **21**(6): 897-903
- Higuchi R, Krummel B, Saiki RK** (1988) A general method of *in vitro* preparation and specific mutagenesis of DNA fragments: study of protein and DNA interactions. *Nucleic Acids Res* **16**(15): 7351-7367

- Hohl TM, Feldmesser M** (2007) *Aspergillus fumigatus*: principles of pathogenesis and host defense. *Eukaryot Cell* **6**(11): 1953-1963
- Holliger P, Hudson PJ** (2005) Engineered antibody fragments and the rise of single domains. *Nat Biotechnol* **23**(9): 1126-1136
- Horn U, Strittmatter W, Krebber A, Knüpfer U, Kujau M, Wenderoth R, Müller K, Matzku S, Plückthun A, Riesenberger D** (1996) High volumetric yields of functional dimeric miniantibodies in *Escherichia coli*, using an optimized expression vector and high-cell-density fermentation under non-limited growth conditions. *Appl Microbiol Biot* **46**(5-6): 524-532
- Howard RJ, Ferrari MA** (1989) Role of melanin in appressorium function. *Experimental Mycology* **13**(4): 403-418
- Ibrahim-Granet O, Dubourdeau M, Latgé JP, Ave P, Huerre M, Brakhage AA, Brock M** (2008) Methylcitrate synthase from *Aspergillus fumigatus* is essential for manifestation of invasive aspergillosis. *Cell Microbiol* **10**(1): 134-148.
- Jackson JC, Higgins LA, Lin X** (2009) Conidiation color mutants of *Aspergillus fumigatus* are highly pathogenic to the heterologous insect host *Galleria mellonella*. *PLoS One* **4**(1): e4224
- Jacobson ES** (2000) Pathogenic roles for fungal melanins. *Clin Microbiol Rev* **13**(4): 708-717.
- Jacobson ES, Hove E, Emery HS** (1995) Antioxidant function of melanin in black fungi. *Infect Immun* **63**(12): 4944-4945
- Jahn B, Boukhallouk F, Lotz J, Langfelder K, Wanner G, Brakhage AA** (2000) Interaction of human phagocytes with pigmentless *Aspergillus* conidia. *Infect Immun* **68**(6): 3736-3739.
- Jahn B, Koch A, Schmidt A, Wanner G, Gehringer H, Bhakdi S, Brakhage AA** (1997) Isolation and characterization of a pigmentless-conidium mutant of *Aspergillus fumigatus* with altered conidial surface and reduced virulence. *Infect Immun* **65**(12): 5110-5117.
- Jahn B, Langfelder K, Schneider U, Schindel C, Brakhage AA** (2002) PKSP-dependent reduction of phagolysosome fusion and intracellular kill of *Aspergillus fumigatus* conidia by human monocyte-derived macrophages. *Cell Microbiol* **4**(12): 793-803.
- Kehrer JP** (2000) The Haber-Weiss reaction and mechanisms of toxicity. *Toxicology* **149**(1): 43-50.
- Keith KE, Killip L, He P, Moran GR, Valvano MA** (2007) *Burkholderia cenocepacia* C5424 produces a pigment with antioxidant properties using a homogentisate intermediate. *J Bacteriol* **189**(24): 9057-9065. Epub 2007 Oct 9012.
- Keller NP, Hohn TM** (1997) Metabolic Pathway Gene Clusters in Filamentous Fungi. *Fungal Genet Biol* **21**(1): 17-29.
- Kogan TV, Jadoun J, Mittelman L, Hirschberg K, Osherov N** (2004) Involvement of secreted *Aspergillus fumigatus* proteases in disruption of the actin fiber cytoskeleton and loss of focal adhesion sites in infected A549 lung pneumocytes. *J Infect Dis* **189**(11): 1965-1973. Epub 2004 May 1911.
- Köhler G, Milstein C** (1975) Continuous cultures of fused cells secreting antibody of predefined specificity. *Nature* **256**(5517): 495-497
- Kontoyiannis DP, Sumoza D, Tarrand J, Bodey GP, Storey R, Raad II** (2000) Significance of aspergillemia in patients with cancer: A 10-year study. *Clinical Infectious Diseases* **31**(1): 188-189
- Korytowski W, Sarna T** (1990) Bleaching of melanin pigments. Role of copper ions and hydrogen peroxide in autooxidation and photooxidation of synthetic dopa-melanin. *J Biol Chem* **265**(21): 12410-12416

- Kosower EM, Correa W, Kinon BJ, Kosower NS** (1972) Glutathione. VII. Differentiation among substrates by the thiol-oxidizing agent, diamide. *Biochim Biophys Acta* **264**(1): 39-44
- Kotob SI, Coon SL, Quintero EJ, Weiner RM** (1995) Homogentisic acid is the primary precursor of melanin synthesis in *Vibrio cholerae*, a *Hyphomonas* strain, and *Shewanella colwelliana*. *Appl Environ Microbiol* **61**(4): 1620-1622.
- Kouadjo KE, Nishida Y, Cadrin-Girard JF, Yoshioka M, St-Amand J** (2007) Housekeeping and tissue-specific genes in mouse tissues. *BMC Genomics* **8**: 127.
- Krebber A, Bornhauser S, Burmester J, Honegger A, Willuda J, Bosshard HR, Plückthun A** (1997) Reliable cloning of functional antibody variable domains from hybridomas and spleen cell repertoires employing a reengineered phage display system. *J Immunol Methods* **201**(1): 35-55.
- Krumpe LR, Schumacher KM, McMahon JB, Makowski L, Mori T** (2007) Trinucleotide cassettes increase diversity of T7 phage-displayed peptide library. *BMC Biotechnol* **7**: 65
- Kubodera T, Yamashita N, Nishimura A** (2002) Transformation of *Aspergillus* sp. and *Trichoderma reesei* using the pyrithiamine resistance gene (*ptrA*) of *Aspergillus oryzae*. *Biosci Biotechnol Biochem* **66**(2): 404-406.
- Kupfahl C** (2008). Detektion von Gliotoxin in Lungengewebe und Serum bei experimenteller Aspergillose-erste Daten. 42. Wissenschaftliche Tagung der Deutschsprachigen Mykologischen Gesellschaft e.V.; 4.-6. September 2008; Jena.
- Kupfahl C, Heinekamp T, Geginat G, Ruppert T, Härtl A, Hof H, Brakhage AA** (2006) Deletion of the *gliP* gene of *Aspergillus fumigatus* results in loss of gliotoxin production but has no effect on virulence of the fungus in a low-dose mouse infection model. *Mol Microbiol* **62**(1): 292-302. Epub 2006 Aug 2031.
- Kwon-Chung KJ, Sugui JA** (2009) What do we know about the role of gliotoxin in the pathobiology of *Aspergillus fumigatus*? *Med Mycol* **47 Suppl 1**: S97-103
- La Du BN** (2002) Alkaptonuria. In *Connective tissue and its heritable disorders: molecular, genetic, and medical aspects*, Royce PM, Steinmann BU (eds), second edn. Zürich: Wiley-Liss
- Langfelder K, Jahn B, Gehringer H, Schmidt A, Wanner G, Brakhage AA** (1998) Identification of a polyketide synthase gene (*pksP*) of *Aspergillus fumigatus* involved in conidial pigment biosynthesis and virulence. *Med Microbiol Immunol* **187**(2): 79-89.
- Langfelder K, Philippe B, Jahn B, Latgé JP, Brakhage AA** (2001) Differential expression of the *Aspergillus fumigatus pksP* gene detected *in vitro* and *in vivo* with green fluorescent protein. *Infection and Immunity* **69**(10): 6411-6418
- Langfelder K, Streibel M, Jahn B, Haase G, Brakhage AA** (2003) Biosynthesis of fungal melanins and their importance for human pathogenic fungi. *Fungal Genet Biol* **38**(2): 143-158.
- Latgé JP** (1999) *Aspergillus fumigatus* and aspergillosis. *Clin Microbiol Rev* **12**(2): 310-350.
- Latgé JP** (2007) The cell wall: a carbohydrate armour for the fungal cell. *Mol Microbiol* **66**(2): 279-290
- Leenders AC, van Belkum A, Behrendt M, Luijendijk A, Verbrugh HA** (1999) Density and molecular epidemiology of *Aspergillus* in air and relationship to outbreaks of *Aspergillus* infection. *J Clin Microbiol* **37**(6): 1752-1757
- Lessing F, Kniemeyer O, Wozniok I, Loeffler J, Kurzai O, Härtl A, Brakhage AA** (2007) The *Aspergillus fumigatus* transcriptional regulator AfYap1 represents the major regulator for defense against reactive oxygen intermediates but is dispensable for pathogenicity in an intranasal mouse infection model. *Eukaryot Cell* **6**(12): 2290-2302. Epub 2007 Oct 2295.

- Lewis RE, Wiederhold NP, Chi J, Han XY, Komanduri KV, Kontoyiannis DP, Prince RA** (2005) Detection of gliotoxin in experimental and human aspergillosis. *Infect Immun* **73**(1): 635-637
- Liebmann B, Mühleisen TW, Müller M, Hecht M, Weidner G, Braun A, Brock M, Brakhage AA** (2004) Deletion of the *Aspergillus fumigatus* lysine biosynthesis gene *lysF* encoding homoaconitase leads to attenuated virulence in a low-dose mouse infection model of invasive aspergillosis. *Arch Microbiol* **181**(5): 378-383. Epub 2004 Mar 2030.
- Lionakis MS, Lahdenranta J, Sun J, Liu W, Lewis RE, Albert ND, Pasqualini R, Arap W, Kontoyiannis DP** (2005) Development of a ligand-directed approach to study the pathogenesis of invasive aspergillosis. *Infect Immun* **73**(11): 7747-7758
- Luther K, Torosantucci A, Brakhage AA, Heesemann J, Ebel F** (2007) Phagocytosis of *Aspergillus fumigatus* conidia by murine macrophages involves recognition by the dectin-1 beta-glucan receptor and Toll-like receptor 2. *Cell Microbiol* **9**(2): 368-381
- Mantel N** (1966) Evaluation of survival data and two new rank order statistics arising in its consideration. *Cancer chemotherapy reports* **50**(3): 163-170
- Marr KA, Balajee SA, McLaughlin L, Tabouret M, Bentsen C, Walsh TJ** (2004) Detection of galactomannan antigenemia by enzyme immunoassay for the diagnosis of invasive aspergillosis: variables that affect performance. *Journal of Infectious Diseases* **190**(3): 641-649
- Marr KA, Carter RA, Boeckh M, Martin P, Corey L** (2002) Invasive aspergillosis in allogeneic stem cell transplant recipients: changes in epidemiology and risk factors. *Blood* **100**(13): 4358-4366
- Martin CD, Rojas G, Mitchell JN, Vincent KJ, Wu J, McCafferty J, Schofield DJ** (2006) A simple vector system to improve performance and utilisation of recombinant antibodies. *BMC Biotechnol* **6**: 46
- Marvin DA** (1998) Filamentous phage structure, infection and assembly. *Curr Opin Struct Biol* **8**(2): 150-158.
- Maschmeyer G, Haas A, Cornely OA** (2007) Invasive aspergillosis: epidemiology, diagnosis and management in immunocompromised patients. *Drugs* **67**(11): 1567-1601
- Maubon D, Park S, Tanguy M, Huerre M, Schmitt C, Prévost MC, Perlin DS, Latgé JP, Beauvais A** (2006) AGS3, an [alpha](1-3)glucan synthase gene family member of *Aspergillus fumigatus*, modulates mycelium growth in the lung of experimentally infected mice. *Fungal Genetics and Biology* **43**(5): 366-375
- Meletiadiis J, Mouton JW, Meis JF, Bouman BA, Donnelly JP, Verweij PE** (2001) Colorimetric assay for antifungal susceptibility testing of *Aspergillus* species. *J Clin Microbiol* **39**(9): 3402-3408
- Mennink-Kersten MA, Donnelly JP, Verweij PE** (2004) Detection of circulating galactomannan for the diagnosis and management of invasive aspergillosis. *Lancet Infect Dis* **4**(6): 349-357
- Michl D, Heinemann A** (2009) Wirtschaftsdaten von Biopharmazeutika und Therapiefortschritt durch Antikörper. Boston Consulting Group (ed.), *Medizinische Biotechnologie in Deutschland 2009* München
- Miller JH, Albertini AM** (1983) Effects of surrounding sequence on the suppression of nonsense codons. *J Mol Biol* **164**(1): 59-71
- Monod M, Capoccia S, Léchenne B, Zaugg C, Holdom M, Jousson O** (2002) Secreted proteases from pathogenic fungi. *Int J Med Microbiol* **292**(5-6): 405-419.
- Moran GR** (2005) 4-Hydroxyphenylpyruvate dioxygenase. *Arch Biochem Biophys* **433**(1): 117-128.

Muyldermans S (2001) Single domain camel antibodies: current status. *J Biotechnol* **74**(4): 277-302.

Muyldermans S, Atarhouch T, Saldanha J, Barbosa JARG, Hamers R (1994) Sequence and Structure of VH Domain from Naturally-Occurring Camel Heavy-Chain Immunoglobulins Lacking Light-Chains. *Protein Eng* **7**(9): 1129-1135

Neofytos D, Horn D, Anaissie E, Steinbach W, Olyaei A, Fishman J, Pfaller M, Chang C, Webster K, Marr K (2009) Epidemiology and outcome of invasive fungal infection in adult hematopoietic stem cell transplant recipients: analysis of Multicenter Prospective Antifungal Therapy (PATH) Alliance registry. *Clin Infect Dis* **48**(3): 265-273

Neuhoff V, Arold N, Taube D, Ehrhardt W (1988) Improved staining of proteins in polyacrylamide gels including isoelectric focusing gels with clear background at nanogram sensitivity using Coomassie Brilliant Blue G-250 and R-250. *Electrophoresis* **9**(6): 255-262.

Nguyen VK, Hamers R, Wyns L, Muyldermans S (2000) Camel heavy-chain antibodies: diverse germline VHH and specific mechanisms enlarge the antigen-binding repertoire. *Embo J* **19**(5): 921-930

Nierman WC, Pain A, Anderson MJ, Wortman JR, Kim HS, Arroyo J, Berriman M, Abe K, Archer DB, Bermejo C, Bennett J, Bowyer P, Chen D, Collins M, Coulsen R, Davies R, Dyer PS, Farman M, Fedorova N, Fedorova N, Feldblyum TV, Fischer R, Fosker N, Fraser A, García JL, García MJ, Goble A, Goldman GH, Gomi K, Griffith-Jones S, Gwilliam R, Haas B, Haas H, Harris D, Horiuchi H, Huang J, Humphray S, Jimenez J, Keller N, Khouri H, Kitamoto K, Kobayashi T, Konzack S, Kulkarni R, Kumagai T, Lafon A, Latgé JP, Li W, Lord A, Lu C, Majoros WH, May GS, Miller BL, Mohamoud Y, Molina M, Monod M, Mouyna I, Mulligan S, Murphy L, O'Neil S, Paulsen I, Peñalva MA, Perteau M, Price C, Pritchard BL, Quail MA, Rabinowitsch E, Rawlins N, Rajandream MA, Reichard U, Renauld H, Robson GD, Rodriguez de Cordoba S, Rodríguez-Pena JM, Ronning CM, Rutter S, Salzberg SL, Sanchez M, Sánchez-Ferrero JC, Saunders D, Seeger K, Squares R, Squares S, Takeuchi M, Tekaiia F, Turner G, Vazquez de Aldana CR, Weidman J, White O, Woodward J, Yu JH, Fraser C, Galagan JE, Asai K, Machida M, Hall N, Barrell B, Denning DW (2005) Genomic sequence of the pathogenic and allergenic filamentous fungus *Aspergillus fumigatus*. *Nature* **438**(7071): 1151-1156.

Nosanchuk JD, Casadevall A (2003) The contribution of melanin to microbial pathogenesis. *Cell Microbiol* **5**(4): 203-223.

Nosanchuk JD, Gomez BL, Youngchim S, Diez S, Aisen P, Zancope-Oliveira RM, Restrepo A, Casadevall A, Hamilton AJ (2002) *Histoplasma capsulatum* synthesizes melanin-like pigments *in vitro* and during mammalian infection. *Infect Immun* **70**(9): 5124-5131

Nunes LR, Costa de Oliveira R, Leite DB, da Silva VS, dos Reis Marques E, da Silva Ferreira ME, Ribeiro DC, de Souza Bernardes LA, Goldman MH, Puccia R, Travassos LR, Batista WL, Nóbrega MP, Nobrega FG, Yang DY, de Braganca Pereira CA, Goldman GH (2005) Transcriptome analysis of *Paracoccidioides brasiliensis* cells undergoing mycelium-to-yeast transition. *Eukaryot Cell* **4**(12): 2115-2128.

O'Gorman CM, Fuller HT, Dyer PS (2009) Discovery of a sexual cycle in the opportunistic fungal pathogen *Aspergillus fumigatus*. *Nature* **457**(7228): 471-474

Pagano L, Caira M, Nosari A, Van Lint MT, Candoni A, Offidani M, Aloisi T, Irrera G, Bonini A, Picardi M, Caramatti C, Invernizzi R, Mattei D, Melillo L, de Waure C, Reddiconto G, Fianchi L, Valentini CG, Girmenia C, Leone G, Aversa F (2007) Fungal infections in recipients of hematopoietic stem cell transplants: results of the SEIFEM B-2004 study--Sorveglianza Epidemiologica Infezioni Fungine Nelle Emopatie Maligne. *Clin Infect Dis* **45**(9): 1161-1170

- Paris S, Debeaupuis JP, Crameri R, Carey M, Charlès F, Prévost MC, Schmitt C, Philippe B, Latgé JP** (2003) Conidial hydrophobins of *Aspergillus fumigatus*. *Appl Environ Microbiol* **69**(3): 1581-1588
- Peñalva MA** (2001) A fungal perspective on human inborn errors of metabolism: alkaptonuria and beyond. *Fungal Genet Biol* **34**(1): 1-10.
- Plückthun A** (1990) Antibodies from *Escherichia coli*. *Nature* **347**(6292): 497-498.
- Punt PJ, van den Hondel CA** (1992) Transformation of filamentous fungi based on hygromycin B and phleomycin resistance markers. *Methods Enzymol* **216**: 447-457.
- Ramos-Vara JA** (2005) Technical aspects of immunohistochemistry. *Vet Pathol* **42**(4): 405-426
- Reichenberger F, Habicht J, Matt P, Frei R, Soler M, Bolliger CT, Dalquen P, Gratwohl A, Tamm M** (1999) Diagnostic yield of bronchoscopy in histologically proven invasive pulmonary aspergillosis. *Bone Marrow Transpl* **24**(11): 1195-1199
- Riley PA** (1997) Melanin. *Int J Biochem Cell Biol* **29**(11): 1235-1239.
- Rodi DJ, Soares AS, Makowski L** (2002) Quantitative assessment of peptide sequence diversity in M13 combinatorial peptide phage display libraries. *J Mol Biol* **322**(5): 1039-1052
- Rodríguez-Rojas A, Mena A, Martín S, Borrell N, Oliver A, Blázquez J** (2009) Inactivation of the *hmgA* gene of *Pseudomonas aeruginosa* leads to pyomelanin hyperproduction, stress resistance and increased persistence in chronic lung infection. *Microbiology* **155**(Pt 4): 1050-1057
- Romero-Martinez R, Wheeler M, Guerrero-Plata A, Rico G, Torres-Guerrero H** (2000) Biosynthesis and functions of melanin in *Sporothrix schenckii*. *Infect Immun* **68**(6): 3696-3703
- Rosas AL, Nosanchuk JD, Gomez BL, Edens WA, Henson JM, Casadevall A** (2000) Isolation and serological analyses of fungal melanins. *J Immunol Methods* **244**(1-2): 69-80
- Roux KH, Greenberg AS, Greene L, Strelets L, Avila D, McKinney EC, Flajnik MF** (1998) Structural analysis of the nurse shark (new) antigen receptor (NAR): molecular convergence of NAR and unusual mammalian immunoglobulins. *Proc Natl Acad Sci U S A* **95**(20): 11804-11809.
- Ruzafa C, Sanchez-Amat A, Solano F** (1995) Characterization of the melanogenic system in *Vibrio cholerae*, ATCC 14035. *Pigment Cell Res* **8**(3): 147-152.
- Sakagami H, Satoh K, Hakeda Y, Kumegawa M** (2000) Apoptosis-inducing activity of vitamin C and vitamin K. *Cell Mol Biol (Noisy-le-grand)* **46**(1): 129-143
- Salas SD, Bennett JE, Kwon-Chung KJ, Perfect JR, Williamson PR** (1996) Effect of the laccase gene CNLAC1, on virulence of *Cryptococcus neoformans*. *J Exp Med* **184**(2): 377-386
- Sambrook J, Russel DW** (2001) *Molecular Cloning: A Laboratory Manual*, third edn. Cold Spring Harbor: Cold Spring Harbor Laboratory Press.
- Schierle CF, Berkmen M, Huber D, Kumamoto C, Boyd D, Beckwith J** (2003) The DsbA signal sequence directs efficient, cotranslational export of passenger proteins to the *Escherichia coli* periplasm via the signal recognition particle pathway. *J Bacteriol* **185**(19): 5706-5713
- Schumann J, Hertweck C** (2006) Advances in cloning, functional analysis and heterologous expression of fungal polyketide synthase genes. *J Biotechnol* **124**(4): 690-703
- Scott CR** (2006) The genetic tyrosinemias. *Am J Med Genet C Semin Med Genet* **142C**(2): 121-126
- Seegmiller JE, Zannoni VG, Laster L, La Du BN** (1961) An enzymatic spectrophotometric method for the determination of homogentisic acid in plasma and urine. *J Biol Chem* **236**: 774-777.

- Sergeeva A, Kolonin MG, Molldrem JJ, Pasqualini R, Arap W** (2006) Display technologies: Application for the discovery of drug and gene delivery agents. *Adv Drug Deliver Rev* **58**(15): 1622-1654
- Shen R, Su ZZ, Olsson CA, Goldstein NI, Fisher PB** (1994) Surface-epitope masking: a strategy for the development of monoclonal antibodies specific for molecules expressed on the cell surface. *J Natl Cancer Inst* **86**(2): 91-98
- Shevchenko A, Wilm M, Vorm O, Mann M** (1996) Mass spectrometric sequencing of proteins silver-stained polyacrylamide gels. *Anal Chem* **68**(5): 850-858.
- Skerra A** (1993) Bacterial expression of immunoglobulin fragments. *Curr Opin Immunol* **5**(2): 256-262
- Skerra A, Plückthun A** (1988) Assembly of a functional immunoglobulin Fv fragment in *Escherichia coli*. *Science* **240**(4855): 1038-1041
- Smith GP** (1985) Filamentous Fusion Phage - Novel Expression Vectors That Display Cloned Antigens on the Virion Surface. *Science* **228**(4705): 1315-1317
- Spellig T, Bottin A, Kahmann R** (1996) Green fluorescent protein (GFP) as a new vital marker in the phytopathogenic fungus *Ustilago maydis*. *Mol Gen Genet* **252**(5): 503-509
- Steinert M, Flügel M, Schuppler M, Helbig JH, Supriyono A, Proksch P, Lück PC** (2001) The Lly protein is essential for p-hydroxyphenylpyruvate dioxygenase activity in *Legionella pneumophila*. *FEMS Microbiol Lett* **203**(1): 41-47.
- Straus W** (1979) Peroxidase procedures. Technical problems encountered during their application. *J Histochem Cytochem* **27**(10): 1349-1351
- Subirà M, Martino R, Rovira M, Vazquez L, Serrano D, De la Cámara R** (2003) Clinical applicability of the new EORTC/MSG classification for invasive pulmonary aspergillosis in patients with hematological malignancies and autopsy-confirmed invasive aspergillosis. *Ann Hematol* **82**(2): 80-82
- Sugareva V** (2006) Analysis of the melanin biosynthesis in *Aspergillus fumigatus*. Thesis Leibniz-Institute for Natural Product Research and Infection Biology, Friedrich-Schiller-University, Jena
- Sugareva V, Härtl A, Brock M, Hubner K, Rohde M, Heinekamp T, Brakhage AA** (2006) Characterisation of the laccase-encoding gene *abr2* of the dihydroxynaphthalene-like melanin gene cluster of *Aspergillus fumigatus*. *Arch Microbiol* **186**(5): 345-355. Epub 2006 Sep 2019.
- Tarrand JJ, Lichterfeld M, Warraich I, Luna M, Han XY, May GS, Kontoyiannis DP** (2003) Diagnosis of invasive septate mold infections - A correlation of microbiological culture and histologic or cytologic examination. *Am J Clin Pathol* **119**(6): 854-858
- Tekaia F, Latgé JP** (2005) *Aspergillus fumigatus*: saprophyte or pathogen? *Curr Opin Microbiol* **8**(4): 385-392
- Teutschbein J, Albrecht D, Pötsch M, Guthke R, Brakhage AA, Kniemeyer O.** (2009) Two-dimensional reference map of conidial proteins from the human pathogen *Aspergillus fumigatus*. Jena. *in preparation*
- Thie H, Schirrmann T, Paschke M, Dübel S, Hust M** (2008) SRP and Sec pathway leader peptides for antibody phage display and antibody fragment production in *E. coli*. *N Biotechnol* **25**(1): 49-54
- Thor H, Smith MT, Hartzell P, Bellomo G, Jewell SA, Orrenius S** (1982) The metabolism of menadione (2-methyl-1,4-naphthoquinone) by isolated hepatocytes. A study of the implications of oxidative stress in intact cells. *J Biol Chem* **257**(20): 12419-12425

- Tijssen P** (1985a) Competitive, solid-phase enzyme immunoassay. In *Practice and Theory of Enzyme Immunoassays*, Burdon RH, van Knippenberg PH (eds), Vol. 15, Chapter 2: Outline of the strategies for enzyme immunoassays, p 19. Québec: Elsevier
- Tijssen P** (1985b) Physicochemical basis of antibody-antigen interaction. In *Practice and Theory of Enzyme Immunoassays*, Burdon RH, van Knippenberg PH (eds), Vol. 15, Chapter 8: Kinetics and nature of antibody-antigen Interactions, p 123. Québec: Elsevier
- Tsai HF, Chang YC, Washburn RG, Wheeler MH, Kwon-Chung KJ** (1998) The developmentally regulated *alb1* gene of *Aspergillus fumigatus*: its role in modulation of conidial morphology and virulence. *J Bacteriol* **180**(12): 3031-3038.
- Tsai HF, Fujii I, Watanabe A, Wheeler MH, Chang YC, Yasuoka Y, Ebizuka Y, Kwon-Chung KJ** (2001) Pentaketide melanin biosynthesis in *Aspergillus fumigatus* requires chain-length shortening of a heptaketide precursor. *J Biol Chem* **276**(31): 29292-29298
- Tsai HF, Washburn RG, Chang YC, Kwon-Chung KJ** (1997) *Aspergillus fumigatus arp1* modulates conidial pigmentation and complement deposition. *Mol Microbiol* **26**(1): 175-183
- Tsai HF, Wheeler MH, Chang YC, Kwon-Chung KJ** (1999) A developmentally regulated gene cluster involved in conidial pigment biosynthesis in *Aspergillus fumigatus*. *J Bacteriol* **181**(20): 6469-6477.
- Turick CE, Tisa LS, Caccavo F, Jr.** (2002) Melanin production and use as a soluble electron shuttle for Fe(III) oxide reduction and as a terminal electron acceptor by *Shewanella algae* BrY. *Appl Environ Microbiol* **68**(5): 2436-2444.
- van der Linden RHJ, Frenken LGJ, de Geus B, Harmsen MM, Ruuls RC, Stok W, de Ron L, Wilson S, Davis P, Verrips CT** (1999) Comparison of physical chemical properties of llama VHH antibody fragments and mouse monoclonal antibodies. *Bba-Protein Struct M* **1431**(1): 37-46
- Wahner-Roedler DL, Kyle RA** (2005) Heavy chain diseases. *Best Pract Res Clin Haematol* **18**(4): 729-746.
- Wang Y, Aisen P, Casadevall A** (1995) *Cryptococcus neoformans* melanin and virulence: mechanism of action. *Infect Immun* **63**(8): 3131-3136.
- Wang Y, Aisen P, Casadevall A** (1996) Melanin, melanin "ghosts," and melanin composition in *Cryptococcus neoformans*. *Infect Immun* **64**(7): 2420-2424
- Ward ES, Gussow D, Griffiths AD, Jones PT, Winter G** (1989) Binding Activities of a Repertoire of Single Immunoglobulin Variable Domains Secreted from *Escherichia Coli*. *Nature* **341**(6242): 544-546
- Wartenberg D** (2008) Identifizierung und Charakterisierung der sekretierten Proteine des humanpathogenen Pilzes *Aspergillus fumigatus*. *Diploma Thesis* Leibniz-Institut für Naturstoff-Forschung und Infektionsbiologie, HKI, Friedrich-Schiller-Universität Jena
- Weidner G, d'Enfert C, Koch A, Mol PC, Brakhage AA** (1998) Development of a homologous transformation system for the human pathogenic fungus *Aspergillus fumigatus* based on the *pyrG* gene encoding orotidine 5'-monophosphate decarboxylase. *Curr Genet* **33**(5): 378-385.
- Weigert MG, Cesari IM, Yonkovich SJ, Cohn M** (1970) Variability in the lambda light chain sequences of mouse antibody. *Nature* **228**(5276): 1045-1047.
- Wels W, Harwerth IM, Zwickl M, Hardman N, Groner B, Hynes NE** (1992) Construction, bacterial expression and characterization of a bifunctional single-chain antibody-phosphatase fusion protein targeted to the human erbB-2 receptor. *Biotechnology (N Y)* **10**(10): 1128-1132
- Wheeler MH, Bell AA** (1988) Melanins and their importance in pathogenic fungi. *Curr Top Med Mycol* **2**: 338-387.

- Wolke SM** (2007) Proteom- und molekulargenetische Analyse von *Aspergillus fumigatus* und *A. nidulans*. *Diploma Thesis* Leibniz-Institut für Naturstoff-Forschung und Infektionsbiologie, HKI, Friedrich-Schiller-Universität Jena
- Yabuuchi E, Ohyama A** (1972) Characterization of "Pyomelanin"-Producing Strains of *Pseudomonas aeruginosa*. *International Journal of Systematic Bacteriology* **22**(2): 53-64
- Yang H, Wang L, Xie Z, Tian Y, Liu G, Tan H** (2007) The tyrosine degradation gene *hppD* is transcriptionally activated by HpdA and repressed by HpdR in *Streptomyces coelicolor*, while *hpdA* is negatively autoregulated and repressed by HpdR. *Mol Microbiol* **65**(4): 1064-1077
- Yeghen T, Kibbler CC, Prentice HG, Berger LA, Wallesby RK, McWhinney PHM, Lampe FC, Gillespie S** (2000) Management of invasive pulmonary aspergillosis in hematology patients: A review of 87 consecutive cases at a single institution. *Clinical Infectious Diseases* **31**(4): 859-868
- Youngchim S, Morris-Jones R, Hay RJ, Hamilton AJ** (2004) Production of melanin by *Aspergillus fumigatus*. *J Med Microbiol* **53**(3): 175-181
- Yu JH, Keller N** (2005) Regulation of secondary metabolism in filamentous fungi. *Annu Rev Phytopathol* **43**: 437-458
- Zielinska-Jankiewicz K, Kozajda A, Piotrowska M, Szadkowska-Stanczyk I** (2008) Microbiological contamination with moulds in work environment in libraries and archive storage facilities. *Ann Agric Environ Med* **15**(1): 71-78

ABBREVIATIONS

Ab	antibody
AMM	<i>Aspergillus</i> minimal medium
bp	base pairs
BSA	bovine serum albumin
c	complementation
cDNA	DNA complementary to mRNA
CDR	complementarity-determining region
Cm ^R	chloramphenicol resistance
CV	column volume
Δ	deletion
DHN	dihydroxynaphthalene
DNA	deoxyribonucleic acid
DOPA	dihydroxyphenylalanine
2-D	two-dimensional
DTT	dithiothreitol
EC50	half maximal effective concentration
EDTA	ethylenediaminetetraacetic acid
e.g.	for example
ELISA	enzyme-linked immunosorbent assay
FPLC	fast protein liquid chromatography
FR	framework region
FTIR	Fourier transform infrared
Fv	association of VH with VL
gDNA	genomic DNA
Gene ID	the systematic gene identifier
<i>gfp</i>	green fluorescent protein
Glc	glucose
HCAb	heavy-chain antibody, Ab naturally lacking a light chain
HE	haematoxylin-eosin
HGA	homogentisic acid
HPLC	high performance liquid chromatography
HRP	horseradish peroxidase
HS-PB	high salt panning buffer
HT-1	hereditary tyrosinaemia type 1
Hyg ^R	hygromycin resistance
IA	invasive aspergillosis
i.e.	that is
IgG	immunoglobuline G
IMAC	immobilized metal ion affinity chromatography
IPTG	isopropyl β-D-1-thiogalactopyranoside

LB	lysogeny broth
MALDI-TOF/TOF	matrix-assisted laser desorption ionisation – tandem time of flight
mRNA	messenger ribonucleic acid
MW	molecular mass
NTBC	2-[2-nitro-4-(trifluoromethyl)benzoyl]cyclohexane-1,3-dione
OD	optical density
PAGE	polyacrylamide gel electrophoresis
PAS	periodic acid - Schiff
PB	panning buffer
PBS	phosphate buffered saline
PCR	polymerase chain reaction
PEG	poly(ethylene glycol)
PNPP	<i>p</i> -nitrophenyl phosphate
PtrA ^R	pyrithiamine resistance
REM	raster electron microscopy
RT	room temperature
scFv	single-chain Fv
SD	standard deviation
SDS	sodium dodecyl sulfate
spp.	species
ssDNA	single-stranded DNA
Tet ^R	tetracyclin resistance
TFA	trifluoroacetic acid
THN	tetrahydroxynaphthalene
UV	ultra violet
VH	variable region of IgG heavy chain
VHH	VH of a heavy-chain Ab
VL	variable region of IgG light chain
WT	wild type
XTT	2,3-bis(2-methoxy-4-nitro-5-sulfophenyl)-2H-tetrazolium-5-carboxanilide

FIGURES

Fig. 1. Electron micrograph of <i>A. fumigatus</i> conidiophores.	1
Fig. 2. Biosynthesis of DHN-melanin in <i>A. fumigatus</i>	6
Fig. 3. L-tyrosine degradation pathway via homogentisate	8
Fig. 4. Schematic presentation of conventional and heavy-chain antibodies and antigen binding fragments thereof.....	10
Fig. 5. Phage ELISA and variable domains of the enriched antibody	40
Fig. 6. Sequence of the engineered antibody and optimisation of antibody production	42
Fig. 7. SDS-PAGE of MelPhoA purification procedure and corresponding alkaline phosphatase activity assay.....	44
Fig. 8. ELISA studies with MelPhoA	46
Fig. 9. Immunofluorescence for the detection of melanin with MelPhoA	49
Fig. 10. Target identification of MelPhoA by 2-D gel electrophoresis of conidial extracts....	51
Fig. 11. Characterisation of <i>arp2</i> deletion and the corresponding complemented strain	55
Fig. 12. Susceptibility of <i>arp2</i> mutant strains to H ₂ O ₂ , diamide and menadione	56
Fig. 13. Virulence of the <i>apr2</i> mutant strains in the mouse infection model	57
Fig. 14. Organisation of the genes in the tyrosine degradation cluster	58
Fig. 15. Deletion and complementation strategy of <i>hppD</i> and <i>hmgA</i> genes and corresponding Southern blot analysis.....	61
Fig. 16. Characterisation of growth and pigmentation of pyomelanin mutant strains.....	63
Fig. 17. Scanning electron microscopy of pyomelanin mutant strains.....	66
Fig. 18. FTIR analysis of pyomelanins	68
Fig. 19. Pigment formation, HGA synthesis and L-tyrosine consumption in pyomelanin mutant strains.....	69
Fig. 20. Semiquantitative transcript analysis of <i>hmgA</i> and <i>hppd</i> in <i>A. fumigatus</i> liquid cultures	71
Fig. 21. HmgA activity assay dependent on the addition of L-tyrosine.....	72
Fig. 22. Transcript analysis of <i>hmgA</i> and <i>hppD</i> in the infected mouse lung.....	73
Fig. 23. Analysis of <i>hppD</i> and <i>pksP</i> gene expression by fluorescence microscopy	75
Fig. 24. Susceptibility of pyomelanin mutant strains to H ₂ O ₂ , diamide and menadione.....	77
Fig. 25. Virulence of pyomelanin mutant strains in the mouse infection model.....	79
Fig. 26. Histopathology of infected and non-infected mouse lungs.	80

TABLES

Table 1. Examples of human pathogenic fungi with a virulence associated to melanin.....	5
Table 2. <i>Escherichia coli</i> strains and phages used	15
Table 3. Fungal strains used.....	15
Table 4. Oligonucleotides used	17
Table 5. Summary of the conditions in each panning cycle.....	28
Table 6. Fluorescence microscopy data.....	37
Table 7. Titers after panning cycles	39
Table 8. Proteins identified in Western blot analysis with MelPhoA after 2-D gel electrophoresis of conidial extracts	51
Table 9. Putative homologs of <i>arp2</i> in fungi closely related to <i>A. fumigatus</i>	52
Table 10. Radial growth rates of the $\Delta arp2$ strain	56
Table 11. Comparison of the <i>A. fumigatus</i> homogentisate cluster with that in the <i>A. nidulans</i> genome.....	59
Table 12. Radial growth rates of pyomelanin mutant strains.....	67
Table 13. Inhibition of growth by H ₂ O ₂ in the XTT assay.....	79
Table 14. Differences in lethality of the strains.....	79

PUBLIKATIONSLISTE

Teile dieser Arbeit wurden in folgenden Publikationen veröffentlicht:

Behnsen J, Hartmann A, Schmaler J, Gehrke A, Brakhage AA, Zipfel PF (2008) The opportunistic human pathogenic fungus *Aspergillus fumigatus* evades the host complement system. *Infect Immun* **76**:820-7.

Schmaler-Ripcke J, Sugareva V, Gebhardt P, et al. (2009) Production of pyomelanin, a second type of melanin, via the tyrosine degradation pathway in *Aspergillus fumigatus* (2009) *Appl Environ Microbiol* **75**(2):493-503.

Schmaler-Ripcke J, Habicht G, Brakhage A A, Horn U A novel method to generate camelid antibodies against conidial structures. *in Bearbeitung*

Teile dieser Arbeit wurden auf folgenden wissenschaftlichen Konferenzen präsentiert:

Schmaler-Ripcke J, Sugareva V, Keller S, Macheleidt J, Heinekamp T and Brakhage A A (2009) The human pathogenic fungus *Aspergillus fumigatus* produces pyomelanin via the tyrosine degradation pathway. *Posterpräsentation auf dem FEMS meeting- "Human Fungal Pathogens: Molecular Mechanisms of Host-Pathogen Interactions and Virulence" in La Colle sur Loup, Frankreich*

Schmaler J, Habicht G, Horn U and Brakhage A A (2008) Generation and Characterisation of Camelid Antibodies against Fungal Melanin. *Posterpräsentation auf der "9th European Conference of Fungal Genetics" in Edinburgh*

Schmaler J, Habicht G, Horn U and Brakhage A A (2008) Generation and Characterisation of Camelid Antibodies against Fungal Melanin. *Posterpräsentation auf der Tagung der „Deutschsprachigen Mykologischen Gesellschaft“ in Jena*

Schmaler J, Habicht G, Horn U and Brakhage A A (2007) Generation and Characterisation of Camelid Antibodies against Fungal Melanin. *Posterpräsentation auf der „Jahrestagung der Vereinigung für Allgemeine und Angewandte Mikrobiologie“ in Osnabrück*

DANKSAGUNGEN

Die praktischen Arbeiten zu der vorliegenden Dissertation wurden im Zeitraum von Oktober 2005 bis November 2008 am Leibniz-Institut für Naturstoff-Forschung und Infektionsbiologie in der Abteilung für Molekulare und Angewandte Mikrobiologie durchgeführt. Bei all denen, die mich bei der Anfertigung dieser Arbeit unterstützt haben, möchte ich mich sehr herzlich bedanken.

Mein Dank gilt insbesondere Herrn **Prof. Dr. Axel Brakhage** für die Überlassung des anspruchsvollen Themas und für die ideenvolle Unterstützung bei der Umsetzung der Arbeit.

Ferner gilt mein Dank Herrn **Dr. Uwe Horn** und seiner Arbeitsgruppe für die wissenschaftliche Betreuung und technische Unterstützung bei der Herstellung und Reinigung des Kamelantikörpers.

Ebenso bedanke ich mich bei Frau **Dr. Ilse Jacobsen** und ihren Assistentinnen für die Durchführung der Mausinfektionsversuche und die histochemische Analyse der infizierten Mauslungen.

Der Arbeitsgruppe von Herrn **PD Dr. Martin Westermann** danke ich für die Unterstützung bei den elektronenmikroskopischen Aufnahmen der *A. fumigatus* -Mutanten.

Ferner danke ich Frau **Dr. Venelina Sugareva** für die Vorarbeiten zum Pyomelaninprojekt, Herrn **Dr. Robert Winkler** für die Hilfestellungen bei den HPLC- Messungen, Herrn **Dr. Peter Gebhardt** für die FTIR Aufnahmen der Pigmente und Frau **Dr. Janka Teutschbein** für die Anwendung des Antikörpers zur Detektion nach 2-D gel electrophoresis.

Meinen Kollegen **Dr. Alexander Gehrke, Dr. Thorsten Heinekamp, Dr. Olaf Kniemeyer, Dr. Matthias Brock, Dipl.-Biol. André Schmidt** und Frau **Dr. Petra Spröte** danke ich für kritische Diskussionen und die damit verbundenen Anregungen.

Den technischen Mitarbeiterinnen **Frau Sylke Fricke, Frau Silke Steinbach** und ganz besonders Frau **Nancy Hannwacker** danke ich für die Unterstützung bei vielen technischen Details.

Vielen Dank an die ganze Abteilung MAM für die sehr angenehme Arbeitsatmosphäre.

Besonderer Dank gebührt nicht zuletzt meiner **Familie** für die immerwährende Hilfe und Unterstützung, besonders in der Zeit der Schwangerschaft und nach der Geburt meines Sohnes.

LEBENS LAUF

Persönliche Daten

Name: Jeannette Schmalzer-Ripcke
geboren am: 23.11.1979 in Hoyerswerda
Familienstand: verheiratet

Schul- und Ausbildungsdaten

Schulabschlüsse: 07/97 Scottish Certification of Higher Education, Wick – Highschool, U.K.
06/99 Abitur, Max-Steenbeck-Gymnasium, Cottbus

Hochschulausbildung: 09/99-10/03 Studium der Pharmazie, FSU Jena

Praktische Ausbildung zum Apotheker: 11/03-04/04 Pharmaziepraktikant, Flora-Apotheke in Jena
05/04-10/04 Pharmaziepraktikant, Université Paris Sud, Diplomarbeit: „Preparation, characterisation and optimisation of Poly (lactic-co-glycolic acid) Microspheres containing Phosphorothioate Oligodeoxynucleotides for the antisense therapy of vitreoretinal diseases.“
05/04-10/04 Stipendiatin des DAAD
10/04-12/04 Fortführung der Diplomarbeit, FSU Jena

Berufsabschluss: 12/04 3. Pharmazeutische Staatsprüfung
01/05 Approbation zur Apothekerin
11/05 Diplom der Pharmazie, FSU Jena

Berufliche Tätigkeit

01/05-12/08 Wissenschaftliche Mitarbeiterin am Leibniz-Institut für Naturstoff-Forschung und Infektionsbiologie in Jena
seit 12/08 Elternzeit

München, 10. August 2009

EHRENWÖRTLICHE ERKLÄRUNG

Hiermit versichere ich, dass

- mir die geltende Promotionsordnung der Biologisch-Pharmazeutischen Fakultät der FSU Jena bekannt ist,
- ich die vorliegende Dissertation selbst angefertigt habe und alle von mir benutzten Hilfsmittel, persönliche Mitteilungen und Quellen der Arbeit angegeben habe,
- ich weder die Hilfe eines Promotionsberaters in Anspruch genommen habe noch Dritten unmittelbare oder mittelbare geldwerte Leistungen für Arbeiten erbracht habe, die im Zusammenhang mit dem Inhalt der Dissertation stehen,
- ich die vorliegende Dissertation noch nicht als Prüfungsarbeit für eine staatliche oder andere wissenschaftliche Prüfung eingereicht habe,
- ich die vorliegende Dissertation oder eine in wesentlichen Teilen ähnliche Abhandlung oder eine andere Arbeit nicht als Dissertation in einer anderen Hochschule eingereicht habe,
- mir außer den in der Danksagung genannten Personen niemand sonst Unterstützung bei der Auswahl und Auswertung des Materials sowie bei der Herstellung des Manuskripts gewährt hat. Personen, die bei der Anfertigung der Publikationen beteiligt waren, sind in der Publikationsliste angegeben.

München, den 19.06.2009

Jeannette Schmalzer-Ripcke